

Contents

18 Heavy electrons	<i>page 2</i>
18.1 Kondo lattice and Doniach Phase Diagram	2
18.2 The Coqblin-Schrieffer Model	8
18.2.1 Construction of the model	8
18.2.2 Enhancement of the Kondo temperature	11
18.3 Large N Expansion for the Kondo Lattice: Preliminaries	13
18.4 The Read Newns Path Integral	15
18.4.1 The Effective Action	18
18.5 Mean-field theory of the Kondo impurity	22
18.5.1 The impurity effective action	22
18.5.2 Minimization of Free energy	25
18.6 Mean-field theory of the Kondo Lattice	28
18.6.1 Diagonalization of the Hamiltonian	28
18.6.2 Mean Field Free Energy and Saddle point	30
18.6.3 Kondo Lattice Green's Function	33
18.7 The composite nature of the f-electron	35
18.7.1 A Thought experiment: a Kondo lattice of nuclear spins	35
18.7.2 Cooper pair analogy	35
18.8 Tunneling into Heavy Electron Fluids	40
18.8.1 The Cotunneling Hamiltonian	40
18.8.2 Tunneling conductance and the "Fano Lattice"	42
18.9 Optical Conductivity of Heavy Electrons	45
18.9.1 Heuristic Discussion	45
18.9.2 Calculation of the optical conductivity, including interband term	46
18.10 Gauge invariance and the charge of the f-electron	50
18.11 Mixed Valence and the Slave Boson	54
18.11.1 Path integrals with Slave Bosons	56
18.12 Kondo and Topological Kondo Insulators	60
18.13 Summary	60
Exercises	61
<i>References</i>	63

Although the single impurity Kondo problem was essentially solved by the early seventies, it took a further decade before the physics community was ready to accept the notion that the same phenomenon could occur in a dense “Kondo lattice” of local moments, forming quasiparticles with greatly enhanced masses that we now call “heavy electrons”. The early resistance to change was rooted in a number of misconceptions about spin physics and the Kondo effect. Some of the first heavy electron systems to be discovered are superconductors, yet it was well known that small concentrations of magnetic ions, typically a few percent, suppress conventional superconductivity, so the appearance of superconductivity in a dense magnetic system appeared at first sight, to be impossible. Indeed, the observation of superconductivity in UPb_{13} in 1973 [1] was dismissed as an artifact, and ten more years passed before it was revisited and acclaimed as a heavy fermion superconductor, in which the Kondo effect quenches the local moments to form a new kind of “heavy fermion metal”[2, 3]. In this chapter, we will study some of the key physics of Kondo lattices that makes this possible.

18.1 Kondo lattice and Doniach Phase Diagram

Local moment metals normally develop antiferromagnetic order at low temperatures. A magnetic moment induces a cloud of Friedel oscillations in spin density of a metal with a magnetization profile given by

$$\langle \vec{M}(\mathbf{x}) \rangle = -J \int d^3x' \chi(\mathbf{x} - \mathbf{x}') \langle \vec{S}(\mathbf{x}') \rangle, \quad (18.1)$$

where J is the strength of the Kondo coupling and

$$\begin{aligned} \chi(\mathbf{x}) &= \int_{\mathbf{q}} \chi(\mathbf{q}) e^{i\mathbf{q}\cdot\mathbf{x}}, \\ \chi(\mathbf{q}) &= 2 \int_{\mathbf{k}} \frac{f(\epsilon_{\mathbf{k}}) - f(\epsilon_{\mathbf{k}+\mathbf{q}})}{\epsilon_{\mathbf{k}+\mathbf{q}} - \epsilon_{\mathbf{k}}} \end{aligned} \quad (18.2)$$

is the the non-local susceptibility of the metal. If a second local moment is introduced at location \mathbf{x} , then it couples to $\langle \vec{M}(\mathbf{x}) \rangle$, shifting the energy by an amount $J \vec{S}(\mathbf{x}) \cdot \langle \vec{M}(\mathbf{x}) \rangle$, giving rise to a long-range magnetic interaction called the “RKKY” interaction, (named after Ruderman, Kittel, Kasuya and Yosida[4])

$$H_{RKKY} = \frac{1}{2} \sum_{\mathbf{x}, \mathbf{x}'} \overbrace{-J^2 \chi(\mathbf{x} - \mathbf{x}') \vec{S}(\mathbf{x}) \cdot \vec{S}(\mathbf{x}')}_{J_{RKKY}(\mathbf{x}-\mathbf{x}')}, \quad (18.3)$$

where the factor of $\frac{1}{2}$ arises because of the summation over \mathbf{x} and \mathbf{x}' . The sharp discontinuity in electron occupancy at the Fermi surface manifests itself as $q = 2k_F$ Friedel oscillations in the RKKY interaction (see

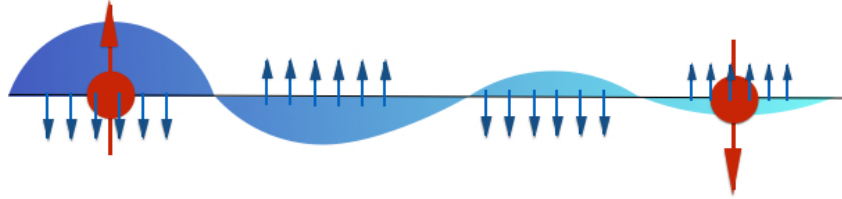


Fig. 18.1 Illustrating how the polarization of spin around a magnetic impurity gives rise to Friedel oscillations, inducing an RKKY interaction between the spins

example 16.1),

$$J_{RKKY}(r) \sim J^2 \rho \frac{\cos 2k_F r}{|r|^3}. \quad (18.4)$$

where r is the distance from the impurity and ρ the conduction electron density of states per spin. The oscillatory nature of this magnetic interaction tends to frustrate the interaction between spins, so that in alloys containing a dilute concentration of magnetic transition metal ions, the RKKY interaction gives rise to a frustrated, glassy magnetic state known as a spin glass, but in dense systems, it the RKKY interaction typically gives rise to an ordered antiferromagnet with a Néel temperature $T_N \sim J^2 \rho$.

The first heavy electron materials to be discovered are now called “Kondo insulators”. In the late sixties, Menth, Buehler and Geballe at AT&T Bell Laboratories[5], discovered an unusual metal SmB_6 containing magnetic Sm^{3+} ions. While apparently magnetic metals, with a Curie Weiss susceptibility at room temperature, on cooling SmB_6 transforms continuously into a paramagnetic insulator with a tiny 10meV gap. The subsequent discovery of similar behavior in SmS under pressure, led Brian Maple and Deiter Wohlleben[6], working at the University of California, San Diego, to propose that quantum-mechanically coherent valence fluctuations in rare earth ions destabilize magnetism, allowing the f-spin to delocalize into the conduction sea. SmS and SmB_6 are a special case, where the additional heavy f-quasiparticles dope the metal to form a highly correlated insulator. More typically however, this process gives rise to a heavy fermion metal.

The first heavy fermion metal, CeAl_3 was discovered by Andres, Graebner and Ott in 1976 [3]. Like many other heavy fermion metals, this metal displays:

- A Curie-Weiss susceptibility $\chi \sim (T + \theta)^{-1}$ at high temperatures.
- A paramagnetic spin susceptibility $\chi \sim \text{const}$ at low temperatures, in this case, below 1K.
- A dramatically enhanced linear specific heat $C_V = \gamma T$ at low temperatures, where in CeAl_3 $\gamma \sim 1600 \text{mJ/mol/K}^2$ is about 1600 times larger than in copper.
- A quadratic temperature dependence of the low temperature resistivity $\rho = \rho_o + AT^2$

Andres, Graebner and Ott proposed that the ground-state excitations of CeAl_3 were those of a Landau Fermi liquid, in which the effective mass of the quasiparticles is about 1000 bare electron masses. The Landau Fermi liquid expressions for the magnetic susceptibility χ and the linear specific heat coefficient γ are

$$\begin{aligned} \chi &= (\mu_B)^2 \frac{N^*(0)}{1 + F_o^a} \\ \gamma &= \frac{\pi^2 k_B^2}{3} N^*(0) \end{aligned} \quad (18.5)$$

where $N^*(0) = \frac{m^*}{m} N(0)$ is the renormalized density of states and F_0^a is the spin-dependent part of the s-wave interaction between quasiparticles. What could be the origin of this huge mass renormalization? Like other Cerium heavy fermion materials, the Cerium atoms in this metal are in a $Ce^{3+}(4f^1)$ configuration, and because they are spin-orbit coupled, they form huge local moments with a spin of $J = 5/2$. In their paper, Andres, Ott and Graebner suggested that a lattice version of the Kondo effect is responsible.

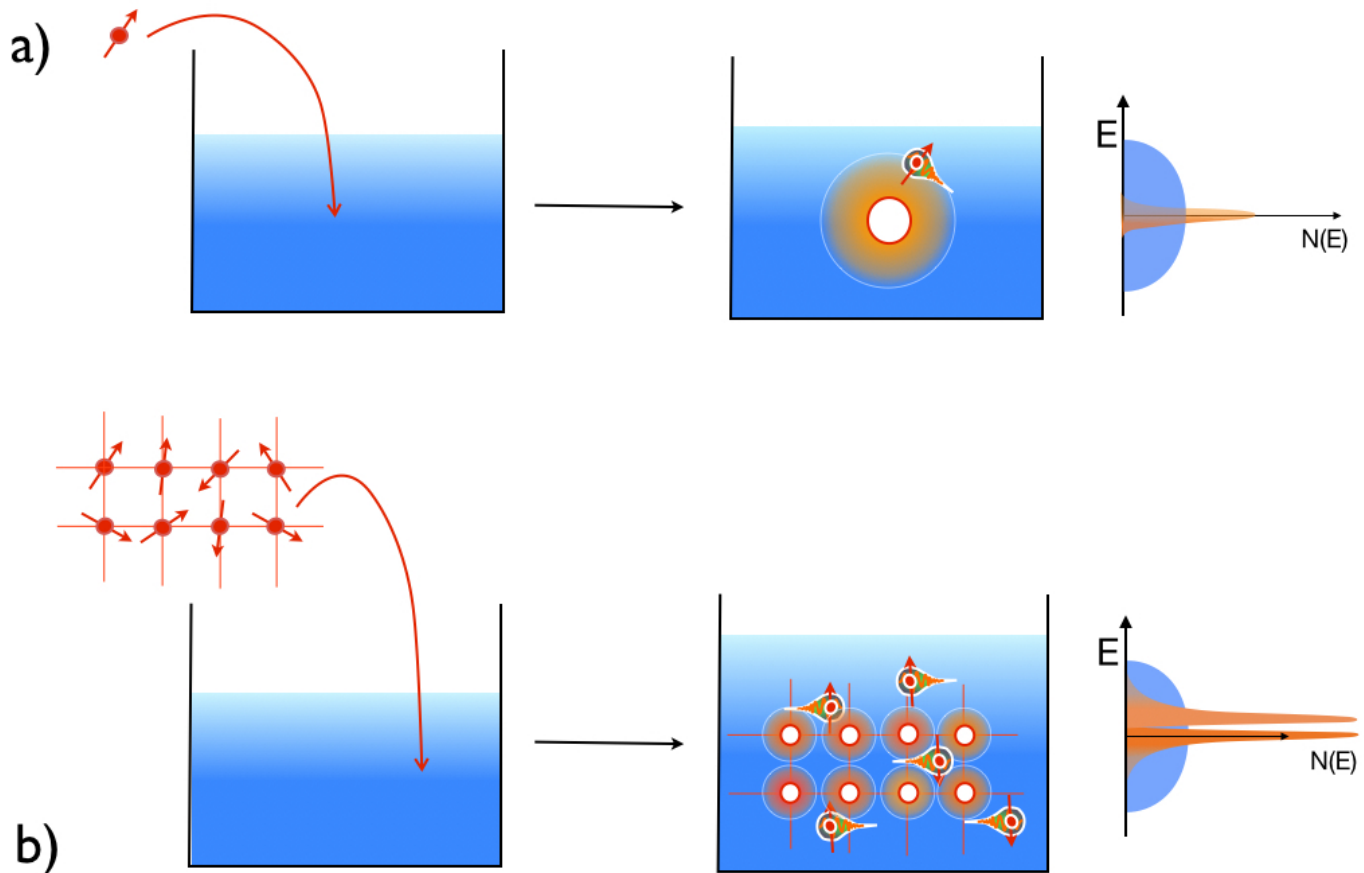


Fig. 18.2 Schematic illustration of the Kondo effect. (a) Single spin in a conduction sea “ionizes” into a Kondo singlet and a heavy fermion orbiting in the vicinity of the Kondo singlet, forming a Kondo resonance at the Fermi surface. (b) Immersion of a lattice of spins in a conduction sea injects a resonance at each site in the lattice, giving rise to a new band of delocalized heavy fermions with a hybridization gap. The density of carriers is increased in the Kondo lattice.

These discoveries prompted Neville Mott[7] and Sebastian Doniach[8] to propose that heavy electron systems should be modelled as a “Kondo-lattice”, where a dense array of local moments interact with the

conduction sea via an antiferromagnetic interaction J . The simplest Kondo lattice Hamiltonian[9] is

$$H = \sum_{\mathbf{k}\sigma} \epsilon_{\mathbf{k}} c_{\mathbf{k}\sigma}^{\dagger} c_{\mathbf{k}\sigma} + J \sum_j \vec{S}_j \cdot c_{j\alpha}^{\dagger} \vec{\sigma}_{\alpha\beta} c_{j\beta}, \quad (18.6)$$

where

$$c_{j\alpha}^{\dagger} = \frac{1}{\sqrt{N_s}} \sum_{\mathbf{k}} c_{\mathbf{k}\alpha}^{\dagger} e^{i\mathbf{k}\cdot\mathbf{R}_j} \quad (18.7)$$

creates an electron at site j . Mott and Doniach pointed out that there are two energy scales in the Kondo lattice: the Kondo temperature T_K and the RKKY scale E_{RKKY} ,

$$\begin{aligned} T_K &= D e^{-1/(2J\rho)} \\ E_{RKKY} &= J^2 \rho \end{aligned} \quad (18.8)$$

For small $J\rho$, $E_{RKKY} \gg T_K$ leading to an antiferromagnetic ground-state, but when $J\rho$ is large, $T_K \gg$

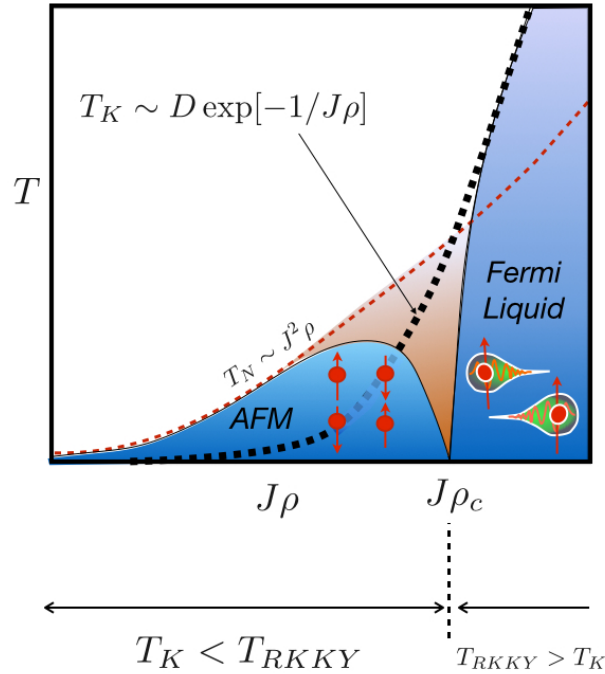


Fig. 18.3

Doniach phase diagram for the Kondo lattice, illustrating the antiferromagnetic regime and the heavy fermion regime, for $T_K < T_{RKKY}$ and $T_K > T_{RKKY}$ respectively. The transition between these two regimes is usually a continuous quantum phase transition. The effective Fermi temperature of the heavy Fermi liquid is indicated as a solid line. Experimental evidence suggests that in many heavy fermion materials this scale drops to zero at the antiferromagnetic quantum critical point.

E_{RKKY} , stabilizing a ground-state in which every site in the lattice resonantly scatters electrons. Doniach predicted[8] that the transition between the antiferromagnet and the dense Kondo state would be a continuous

quantum phase transition. In the Kondo lattice ground state which ensues, Bloch's theorem insures that the resonant elastic scattering at each site will generate a renormalized f- band, of width $\sim T_K$. In contrast with the impurity Kondo effect, here elastic scattering at each site acts coherently. For this reason, as the heavy electron metal develops at low temperatures, its resistivity drops towards zero.

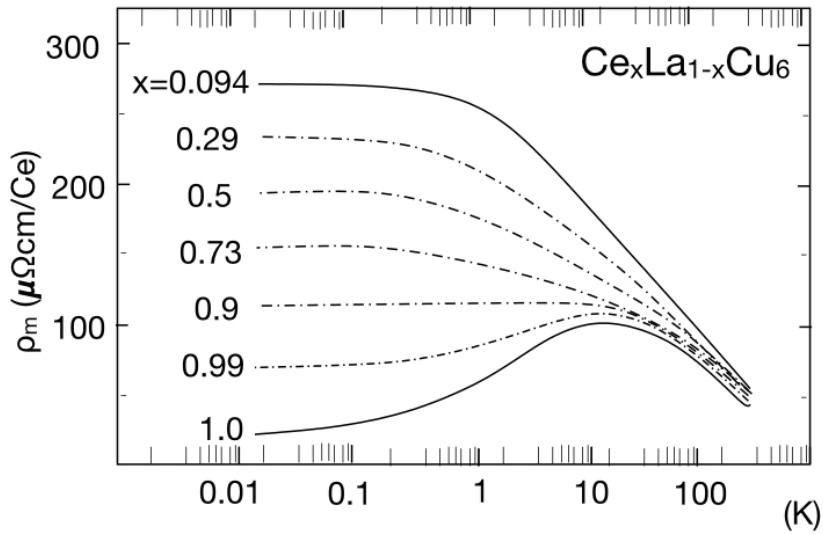


Fig. 18.4 Development of coherence in heavy fermion systems. Resistance in $\text{Ce}_{1-x}\text{La}_x\text{Cu}_6$ after Onuki and Komatsubara[10]

One of the fascinating aspects of the Kondo lattice concerns the Luttinger sum rule. Martin[11], working at Xerox Palo Alto research, pointed out that both the Kondo impurity and lattice models can be regarded as the result of adiabatically increasing the interaction strength U in a corresponding Anderson model, whilst preserving the valence of the magnetic ion. During this process, the conservation of charge gives rise to “node counting” sum rules. In the last chapter we saw that for an impurity, the scattering phase shift at the Fermi energy counts the number of localized electrons, according to the Friedel sum rule

$$\sum_{\sigma} \frac{\delta_{\sigma}}{\pi} = n_f = 1$$

This sum rule survives to large U , and reappears as the constraint on the scattering phase shift created by the Abrikosov Suhl resonance. In the lattice, the corresponding sum rule is the “Luttinger sum rule”, which states that the Fermi surface volume counts the number of electrons, which at small U is just the number of localized (4f, 5f or 3d) and conduction electrons. When U becomes large, the number of localized electrons is now the number of spins, so that

$$2 \frac{\mathcal{V}_{FS}}{(2\pi)^3} = n_e + n_{\text{spins}} \quad (18.9)$$

Although this sum rule is derived by Martin's adiabatic argument, it is an independent property of the Kondo lattice, and it holds independently of the origin of the localized moments. In other words, we could imagine

a Kondo lattice of nuclear spins, provided the Kondo temperature were large enough to guarantee a paramagnetic state. Physically, we can regard the conduction sea as a magnetically polar fluid which magnetically solvates the localized moments, causing them to dissolve into the conduction sea where they become mobile heavy electrons. A more detailed derivation of Martin's original proposal has been provided by Oshikawa, at the Institute for Solid State Physics, in Tokyo[12].

Experimentally, there is a great deal of support for the above picture. It is possible, for example, to follow the effect of progressively increasing the concentration of Ce in the non-magnetic host LaCu₆.(18.4) At dilute concentrations, the resistivity rises to a maximum at low temperatures. At dense concentrations, the resistivity shows the same high temperature behavior, but at low temperatures coherence between the sites leads to a dramatic drop in the resistivity. The thermodynamics of the dense and dilute system are essentially identical, but the transport properties display the effects of coherence.

The most direct evidence that the Fermi surface of f-electron systems counts the f-electrons derives from Quantum Oscillation (de Haas van Alphen and Shubnikov de Haas oscillation) measurements of the Fermi surface[13, 14]. Typically, in the heavy Fermi liquid, the measured de Haas van Alphen orbits are consistent with band-structure calculations in which the f-electrons are assumed to be delocalized. By contrast, the measured masses of the heavy electrons often exceed the band-structure calculated masses of the narrow f-band by an order of magnitude or more. Perhaps the most remarkable discovery of recent years, is the observation that the volume of the f-electron Fermi surface appears to "jump" to a much smaller value when the f-electrons anti-ferro magnetically order, indicating that once the Kondo effect is interrupted by magnetism, the heavy f-electrons re-localize[15].

Example 18.1: The RKKY interaction between two moments in a Fermi liquid is given by

$$J_{RKKY}(\mathbf{x}) = -J^2 \int \frac{d^3q}{(2\pi)^3} e^{i\mathbf{q}\cdot\mathbf{x}} \chi(\mathbf{q}) \quad (18.10)$$

where as shown in Chapter 8, $\chi(\mathbf{q}) = 2\rho F[q/2k_F]$ is the static magnetic susceptibility and

$$F(x) = \frac{1}{2} + \frac{1-x^2}{4x} \ln \left| \frac{1+x}{1-x} \right| \quad (18.11)$$

is the Lindhardt function. Use the Fourier transform

$$\int_0^\infty dy \sin(\alpha y) \ln \left| \frac{1+y}{1-y} \right| = \pi \frac{\sin \alpha}{\alpha} \quad (18.12)$$

to show that the real-space RKKY interaction between local moments is given by

$$J_{RKKY}(r) = J^2 \rho \frac{1}{2\pi^2 r^3} \left[\cos 2k_F r - \frac{\sin 2k_F r}{2k_F r} \right]. \quad (18.13)$$

where r is measured in lattice units.

Solution:

We begin by using the isotropy of $\chi(\mathbf{q}) = \chi(q)$ to carry out the angular integral in the Fourier transform:

$$\begin{aligned} \chi(\mathbf{x}) &= \int_{\mathbf{q}} e^{i\mathbf{q}\cdot\mathbf{x}} \chi(\mathbf{q}) = \int_0^\infty \frac{4\pi q^2 dq}{(2\pi)^3} \int \frac{d\Omega}{4\pi} e^{i\mathbf{q}\cdot\mathbf{x}} \chi(q) = \frac{1}{2\pi^2 r} \int_0^\infty dq q \sin(qr) \chi(q) \\ &= \frac{2\rho}{2\pi^2 r} \int_0^\infty dq q \sin(qr) F \left[\frac{q}{2k_F} \right]. \end{aligned} \quad (18.14)$$

If we change variable to $y = q/(2k_F)$, so that $dq = (2k_F)^2 dy$, we obtain

$$\chi(r) = \frac{\rho}{\pi^2 r} (2k_F)^2 \int_0^\infty dy \sin(2k_F r y) F[y] = \frac{\rho}{\pi^2 r} (2k_F)^2 G[2k_F r] \quad (18.15)$$

where

$$G[\alpha] = \int_0^\infty dy \sin(\alpha y) \left(\frac{y}{2} + \frac{(1-y^2)}{4} \ln \left| \frac{1+y}{1-y} \right| \right). \quad (18.16)$$

Notice that near $y \sim 1$, the singular part of the integrand goes as $dy(y-1) \ln(y-1)$, and since the singular part of the integral has dimension $[y^2] \equiv [\alpha^{-2}]$, we expect this integral to have a $1/\alpha^2 \sim 1/(k_F r)^2$ dependence. To Fourier transform the last two terms in (18.16) we use the result

$$\int_0^\infty dy \sin(\alpha y) \ln \left| \frac{1+y}{1-y} \right| = \pi \frac{\sin \alpha}{\alpha}. \quad (18.17)$$

(This result is obtained as the inverse Fourier transform of $\sin \alpha / \alpha$). By differentiating both sides twice with respect to α we then obtain

$$\int_0^\infty dy \sin(\alpha y) (1-y^2) \ln \left| \frac{1+y}{1-y} \right| = \pi \left(1 + \frac{d^2}{d\alpha^2} \right) \frac{\sin \alpha}{\alpha} = -2\pi \left(\frac{\cos \alpha}{\alpha^2} - \frac{\sin \alpha}{\alpha^3} \right), \quad (18.18)$$

with the expected $1/\alpha^2$ dependence. To complete the job we need to Fourier transform the first term in (18.16). If we differentiate $\int_{-\infty}^\infty dx \cos \alpha y = 2\pi \delta(\alpha)$ with respect to α we obtain

$$\int_0^\infty dy y \sin \alpha y = -\pi \delta'(\alpha). \quad (18.19)$$

Combining (18.18) and (18.19), we obtain

$$G[\alpha] = \frac{\pi}{2} \left[\frac{\sin \alpha}{\alpha^3} - \frac{\cos \alpha}{\alpha^2} - \delta'(\alpha) \right]. \quad (18.20)$$

When inserted into (18.15) we finally obtain

$$J_{RKKY}(r) = -J^2 \chi(r) = \frac{J^2 \rho}{2\pi r^3} \left[\cos 2k_F r - \frac{\sin 2k_F r}{2k_F r} \right] \quad (18.21)$$

where we have dropped the $\delta'(2k_F r)$ term. Notice that at small distances, $J_{RKKY}(r) < 0$ is a ferromagnetic interaction.

18.2 The Coqblin-Schrieffer Model

18.2.1 Construction of the model

The stabilization of the heavy fermion state in f-electron materials owes its origins to the strong spin-orbit coupling, which locks the spin and orbital angular momentum into a large half-integer moment that is unquenched by crystal fields. For example, in Ce^{3+} ions, the $4f^1$ electron is spin-orbit coupled into a state with $j = 3 - 1/2 = 5/2$, giving a spin degeneracy of $N = 2j + 1 = 6$. Ytterbium heavy fermion materials involve the $\text{Yb}:4f^{13}$ configuration, which is most readily understood as a single hole in the filled $4f^{14}$ f-shell, giving with one hole in the upper spin-orbit multiplet with angular momentum $j = 3 + 1/2 = 7/2$, or $N = 8$. The

large spin degeneracy $N = 2j + 1$ of the local moments has the effect of enhancing the Kondo temperature to a point where the zero-point spin fluctuations destroy magnetism.

The presence of large spin-orbit coupling requires a generalization of the Kondo model developed by Coqblin and Schrieffer[16]: they considered a spin-orbit coupled version of the infinite U Anderson model in which the z component of the electron angular momentum, $M \in [-j, j]$, runs from $-j$ to j ,

$$H = \sum_{k,M} \epsilon_k c_{\mathbf{k}M}^\dagger c_{\mathbf{k}M} + E_f \sum_M |f^1 : M\rangle \langle f^1 : M| + \sum_{k,M} V [c_{\mathbf{k}M}^\dagger |f^0\rangle \langle f^1 : M| + \text{H.c.}]. \quad (18.22)$$

In this model, both the f - and conduction electrons carry spin indices M that run from $-j$ to j . This strange feature is a consequence of rotational invariance, which causes total angular momentum \vec{J} to be conserved by hybridization process: this means that the hybridization is diagonal in a basis where partial-wave states of the conduction sea are written in states of definite j . In this basis, spin-orbit coupled f states hybridize diagonally with partial wave states of the conduction electrons in the same spin-orbit coupled j states as the f -electron. Suppose $|\mathbf{k}\sigma\rangle$ represents a plane wave of momentum \mathbf{k} , then one can construct a state of definite orbital angular momentum l by integrating the plane wave with a spherical harmonic, as follows:

$$|klm\sigma\rangle = \int \frac{d\Omega}{4\pi} |\mathbf{k}\sigma\rangle Y_{lm}(\hat{\mathbf{k}}) \quad (18.23)$$

When spin orbit interactions are strong, one must work with a partial wave of definite j , obtained by combining these states in the following linear combinations.

$$|kM\rangle = \sum_{\sigma=\pm\frac{1}{2}} |klM - \sigma, \sigma\rangle \left(lM - \sigma, \frac{1}{2}\sigma \middle| jM \right) \quad (18.24)$$

where $\left(lm, \frac{1}{2}\sigma \middle| jM \right)$ is the Clebsch Gordan coefficient between the spin-orbit coupled state $|jM\rangle$ and the l -s coupled state $|lm, \sigma\rangle$. These coefficients can be explicitly evaluated as

$$\left(lM - \sigma, \frac{1}{2}\sigma \middle| jM \right) = \begin{cases} \sqrt{\frac{1}{2} + \frac{2M\sigma}{2l+1}}, & j = l + \frac{1}{2} \\ \text{sgn}\sigma \sqrt{\frac{1}{2} - \frac{2M\sigma}{2l+1}}, & j = l - \frac{1}{2} \end{cases} \quad (M \in [-j, j], \sigma = \pm 1/2) \quad (18.25)$$

Putting this all together, a partial wave state of definite j, M can then be written as

$$c_{\mathbf{k}M}^\dagger = \sum_{\sigma=\pm\frac{1}{2}} \int \frac{d\Omega}{4\pi} c_{\mathbf{k},\sigma}^\dagger \mathcal{Y}_{\sigma,M}(\hat{\mathbf{k}}) \quad (18.26)$$

where

$$\mathcal{Y}_{\sigma,M}(\mathbf{k}) = \left(l, M - \sigma ; \frac{1}{2}\sigma \middle| jM \right) Y_{l,M-\sigma}(\hat{\mathbf{k}}) \quad (18.27)$$

is a spin-orbit coupled spherical Harmonic. Note that the spin-orbit coupled partial wave states form a complete basis for an impurity model involving a single spherically symmetric magnetic site. This is no longer the case in a lattice, where the set of partial waves at different sites is overcomplete, and an electron which sets off in one partial wave state at one site, can arrive in another partial wave state at another site.

When $E_f \ll 0$, the valence of the ion approaches unity ($n_f \rightarrow 1$) and one can integrate out the virtual fluctuations $f^1 \rightleftharpoons f^0 + e^-$ via a Schrieffer Wolff transformation to obtain the Coqblin Schrieffer model

$$H_{CS} = \sum_{kM} \epsilon_k c_{\mathbf{k}M}^\dagger c_{\mathbf{k}M} - J \sum_{k,k',M,M'} (f_{M'}^\dagger c_{k'M}) (c_{\mathbf{k}M}^\dagger f_M), \quad (M, M' \in [-j, j]). \quad (18.28)$$

where $J = V^2/|E_f|$ is the amplitude for the virtual process. The second term describes a virtual fluctuation in which an f-electron with $j_z = M'$ jumps out into the conduction sea, creating a state with excitation energy of order $|E_f|$, only to be subsequently replaced by an electron with $j_z = M$. Notice how the f-charge $Q = n_f$ of the impurity is conserved by the spin-exchange interaction, $[H, n_f] = 0$, so that the interaction in the Coqblin Schrieffer model only involves the spin degrees of freedom. It is sometimes useful to rewrite the Coqblin Schrieffer model in the form

$$H_{CS} = \sum_{kM} \epsilon_k c_{kM}^\dagger c_{kM} + J \sum_{k,k',M,M'} c_{kM}^\dagger c_{k'M'} \overbrace{\left(f_{M'}^\dagger f_M - \frac{1}{N} n_f \delta_{M,M'} \right)}^{S_{M'M}} + \hat{V} \quad (M, M' \in [-j, j]). \quad (18.29)$$

where $S_{M'M}$ is the SU(N) generalization of a traceless Pauli spin operator. This form of the model emphasizes that the interaction is a pure spin exchange process. In writing this expression, we have omitted the elastic scattering term $\hat{V} = J \left(\frac{n_f}{N} \right) \sum_{k,k',M} (c_{kM}^\dagger c_{k'M} - \delta_{k,k'})$ which results from the rearrangement of the operators. This term does not renormalize, and into a phase shift of the conduction electrons (for the impurity) or a shift of the chemical potential (in the lattice).

Example 18.2: In a certain tetragonal crystalline environment, the low-lying ground-state of a Cerium Ce^{3+} ion is a $|j = 5/2, M_j = \pm \frac{3}{2}\rangle$ state. The hybridization of this state with Bloch-waves of momentum $|\mathbf{k}| = k$ is described by the Hamiltonian

$$H_{\text{mv}} = V \sum_{M=\pm \frac{3}{2}} \int \frac{k^2 dk}{2\pi^2} [c_{kM}^\dagger f_M + \text{H.c.}] \quad (18.30)$$

where V is the strength of hybridization near the Fermi energy and c_{kM}^\dagger creates a conduction electron in an $l = 3, j = 5/2, M_j = \pm \frac{3}{2}$ partial wave state of wavevector k .

- Recast H_{mv} using a plane wave basis for the conduction electrons.
- Show that the hybridization vanishes along the z-axis of momentum space. Why does this happen?

Solution:

- We begin by rewriting the partial wave states as plane waves, using (18.26), we have

$$c_{kM}^\dagger = \sum_{\sigma=\pm \frac{1}{2}} \int \frac{d\Omega}{4\pi} c_{\mathbf{k},\sigma}^\dagger \mathcal{Y}_{\sigma M}(\mathbf{k}) \quad (18.31)$$

where

$$\begin{aligned} \mathcal{Y}_{\sigma M}(\mathbf{k}) &= \left(3, M - \sigma; \frac{1}{2}\sigma \middle| \frac{5}{2}M \right) Y_{3, M-\sigma}(\hat{\mathbf{k}}) \\ &= \text{sgn}\sigma \sqrt{\frac{1}{2} - \frac{\text{sgn}(M\sigma)}{14}} Y_{3, M-\sigma}(\hat{\mathbf{k}}). \quad (\sigma = \pm \frac{1}{2}, M = \pm \frac{3}{2}) \end{aligned} \quad (18.32)$$

The hybridization Hamiltonian is then written

$$H_{\text{mv}} = V \sum_{\mathbf{k}, \sigma, M} [c_{\mathbf{k},\sigma}^\dagger \mathcal{Y}_{\sigma M}(\hat{\mathbf{k}}) f_M + \text{H.c.}] \quad (18.33)$$

- Now the Clebsch Gordon coefficients are either $\pm \sqrt{3/7}$ or $\pm \sqrt{4/7}$ so that

$$\mathcal{Y}_{\sigma M}(\mathbf{k}) = \begin{pmatrix} \mathcal{Y}_{\frac{1}{2} \frac{3}{2}}(\hat{\mathbf{k}}) & \mathcal{Y}_{\frac{1}{2} -\frac{3}{2}}(\hat{\mathbf{k}}) \\ \mathcal{Y}_{-\frac{1}{2} \frac{3}{2}}(\hat{\mathbf{k}}) & \mathcal{Y}_{-\frac{1}{2} -\frac{3}{2}}(\hat{\mathbf{k}}) \end{pmatrix} = \begin{pmatrix} \sqrt{\frac{3}{7}} Y_{3,1}(\hat{\mathbf{k}}) & \sqrt{\frac{4}{7}} Y_{3,-2}(\hat{\mathbf{k}}) \\ -\sqrt{\frac{4}{7}} Y_{3,2}(\hat{\mathbf{k}}) & -\sqrt{\frac{3}{7}} Y_{3,-1}(\hat{\mathbf{k}}) \end{pmatrix} \quad (18.34)$$

The spherical harmonics are given by (Mathematica: SphericalHarmonicY),

$$\begin{aligned} Y_{3,\pm 1}(\hat{\mathbf{k}}) &= \mp \sqrt{\frac{21}{64\pi}} (\hat{k}_x \pm i\hat{k}_y)(4\hat{k}_z^2 - 1) \propto \mp (\hat{k}_x \pm i\hat{k}_y) \\ Y_{3,0}(\hat{\mathbf{k}}) &= \sqrt{\frac{105}{32\pi}} (\hat{k}_x \pm i\hat{k}_y)\hat{k}_z \propto \mp (\hat{k}_x \pm i\hat{k}_y)^2. \end{aligned} \quad (18.35)$$

We see that near the z-axis of momentum space the off-diagonal components of \mathcal{Y} vanish quadratically with k , whereas the diagonal components vanish linearly, so that

$$\mathcal{Y}(\hat{\mathbf{k}}) \sim \begin{pmatrix} \hat{k}_x + i\hat{k}_y & 0 \\ \hat{0} & (\hat{k}_x - i\hat{k}_y) \end{pmatrix}, \quad (18.36)$$

which vanishes linearly with (\hat{k}_x, \hat{k}_y) along the z-axis. This mismatch occurs because plane waves travelling along the z-axis carry $\pm \frac{1}{2}$ units of angular momentum in their direction of motion, and can therefore not hybridize with the high-spin $M_J = \pm \frac{3}{2}$ f-states, giving rise to a vorticity in the hybridization. This phenomenon is believed to be important for the semi-metallic behavior in the compounds CeNiSn and CeRhSb[17], sometimes called ‘‘failed Kondo insulators’’.

18.2.2 Enhancement of the Kondo temperature

To get an idea of how the Kondo effect is modified by the large degeneracy, consider the first-order renormalization of the interaction, which is given by the diagrams

$$\begin{aligned} J_{eff}(D') &= \text{Diagram 1} + \text{Diagram 2} \\ &= J + NJ^2\rho \ln\left(\frac{D}{D'}\right) \end{aligned} \quad (18.37)$$

(where the cross on the intermediate conduction electron state indicates that all states in the energy window $|\epsilon_k| \in [D', D]$ are integrated out). The important point to notice here, is that the rate of renormalization has been enhanced by a factor of N , due to the multiplicity of intermediate hole states. We can immediately see that the second term is comparable with the first at a scale $D' \equiv T_K = D \exp\left[-\frac{1}{NJ\rho}\right]$, with an N -fold enhancement of the coupling constant. More precisely, we see that the beta function $\beta(g) = \partial g(D')/\partial \ln D' = -g^2$, where $g(D') = N\rho J_{eff}(D')$. A more extensive calculation shows that the beta function to third order takes the form

$$\beta(g) = \frac{dg}{d \ln D'} = -g^2 + \frac{g^3}{N}. \quad (18.38)$$

The beta function describes a family of Kondo models with different cut-offs D' but the same low energy physics. We can determine T_K as the temperature where the coupling constant becomes of order unity, $g \sim 1$. If we integrate out the conduction electrons with energy greater than T_K , we find

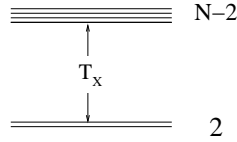
$$\int_{T_K}^D d \ln D' = \ln\left(\frac{D}{T_K}\right) = \int_1^{NJ\rho} \frac{dg}{-g^2 + g^3/N} \approx \int_1^{NJ\rho} dg \left[-\frac{1}{g^2} - \frac{1}{Ng}\right] = \frac{1}{NJ\rho} - 1 - \frac{1}{N} \ln(NJ\rho), \quad (18.39)$$

which leads to the Kondo temperature

$$T_K = De(NJ\rho)^{\frac{1}{N}} \exp\left[-\frac{1}{NJ\rho}\right] \quad (18.40)$$

so that large degeneracy enhances the Kondo temperature in the exponential factor. By contrast, the RKKY interaction strength is given by $T_{RKKY} \sim J^2\rho$, and it does not involve any N fold enhancement factors, thus in systems with large spin degeneracy, the enhancement of the Kondo temperature favors the formation of the heavy fermion ground-state.

In practice, rare-earth ions are exposed to the crystal fields of their host, which splits the $N = 2j + 1$ fold degeneracy into many multiplets. Even in this case, the large degeneracy is helpful, because the crystal field splitting is small compared with the band-width. At energies D' large compared with the crystal field splitting T_X , $D' \gg T_X$, the physics is that of an N fold degenerate ion, whereas at energies D' small compared with the crystal field splitting, the physics is typically that of a Kramers doublet, i.e.



$$\frac{\partial g}{\partial \ln D} = \begin{cases} -g^2 & (D \gg T_X) \\ -\frac{2}{N}g^2 & (D \ll T_X) \end{cases} \quad (18.41)$$

from which we see that at low energy scales, the leading order renormalization of g is given by

$$\frac{1}{g(D')} = \frac{1}{NJ\rho} - \ln\left(\frac{D}{T_X}\right) - \frac{2}{N} \ln\left(\frac{T_X}{D'}\right)$$

where the first logarithm describes the high energy screening with spin degeneracy N , and the second logarithm describes the low-energy screening, with spin degeneracy 2. This expression is ~ 0 when $D' \sim T_K^*$, the Kondo temperature, so that

$$0 = \frac{1}{NJ\rho} - \ln\left(\frac{D}{T_X}\right) - \frac{2}{N} \ln\left(\frac{T_X}{T_K^*}\right)$$

from which we deduce that the renormalized Kondo temperature has the form[18]

$$T_K^* = D \exp\left(-\frac{1}{2J_o\rho}\right) \left(\frac{D}{T_X}\right)^{\frac{N}{2}-1}.$$

Here the first term is the expression for the Kondo temperature of a spin 1/2 Kondo model. The second term captures the enhancement of the Kondo temperature derived from the renormalization on scales larger than the crystal field splitting. For $T_X \sim 100K$, $D \sim 1000K$ and $N = 6$, the enhancement factor is order $10^{6/2-1} = 100$. In short, spin-orbit coupling substantially enhances the Kondo temperature even in the presence of crystal fields, and this is an important source of stabilization for the Kondo lattice in local moment rare earth and actinide materials. The absence of this effect in transition metal systems means that they are much more prone to the formation of spin-glasses, rather than heavy fermion metals¹.

¹ To obtain heavy fermion behavior in transition metal systems one needs magnetic frustration. A good example of such behavior is provided by the pyrochlore transition metal heavy fermion system, LiV_2O_3 , see [19].

18.3 Large N Expansion for the Kondo Lattice: Preliminaries

We shall now solve the Kondo lattice and impurity model, in the large N limit. In the early eighties, Anderson[20] pointed out that the large spin degeneracy $N = 2j + 1$ furnishes a small parameter $1/N$ which might be used to develop a controlled expansion about the limit $N \rightarrow \infty$. Anderson's observation opened up a new approach to the heavy fermion problem: the "large N expansion"[21].

In 1983, two groups, the current author working with Philip W. Anderson at Princeton[22] and Dennis Newns and Nicholas Read at Imperial College, London, working with Sebastian Doniach at Stanford University[23], realized that in the large N limit, the $RKKY$ interaction in the Kondo model could be ignored relative to the Kondo effect. Building on this idea, and taking advantage of Edward Witten's large N approach to the Gross-Neveu problem[21] and earlier path-integral formulations of the Kondo problem[24, 25], Nicholas Read and Dennis Newns formulated a large- N path integral approach for the Kondo lattice[23, 26, 27], work later extended by Assa Auerbach and Kathryn Levin at the University of Chicago[28]. We shall later examine how this method can be extended to include valence fluctuations in the infinite Anderson model using "slave bosons" [29, 26, 27, 30, 31].

The basic idea is to take a limit where every term in the Hamiltonian grows extensively with N . In the path integral for the partition function, the corresponding action then grows extensively with N , so that

$$Z = \int \mathcal{D}[\psi] e^{-NS} = \int \mathcal{D}\psi \exp\left[-\frac{S}{1/N}\right] \equiv \int \mathcal{D}[\psi] \exp\left[-\frac{S}{\hbar_{eff}}\right]. \quad (18.42)$$

Here

$$\frac{1}{N} \sim \hbar_{eff}$$

behaves as an effective Planck's constant for the theory, focussing the path integral into a non-trivial "semi-classical" or "mean field" solution as $\hbar_{eff} \rightarrow 0$. As $N \rightarrow \infty$, the quantum fluctuations of intensive variables \hat{a} , such as the electron density per spin, become smaller and smaller, scaling as $\langle \delta a^2 \rangle / \langle a^2 \rangle \sim 1/N$. In this way, one can obtain new results by expanding around the solvable large N limit in powers of $\frac{1}{N}$. For the Kondo model, we are lucky, because much of the important physics of is already captured by the large N limit (Fig. 18.5).

For simplicity, we shall consider a "toy" Kondo lattice, in which all electrons have a spin degeneracy $N = 2j + 1$, interacting with the local moment at each site via a Coqblin Schrieffer interaction,

$$H = \sum_{\mathbf{k}\alpha} \epsilon_{\mathbf{k}} c_{\mathbf{k}\alpha}^\dagger c_{\mathbf{k}\alpha} + \frac{J}{N} \sum_{j,\alpha\beta} c_{j\alpha}^\dagger c_{j\beta} S_{\alpha\beta}(j). \quad (18.43)$$

where $c_{j\alpha}^\dagger = \frac{1}{\sqrt{N_s}} \sum_{\mathbf{k}} c_{\mathbf{k}\alpha}^\dagger e^{-i\mathbf{k}\cdot\mathbf{R}_j}$ creates an electron localized at site j and the spin of the local moment at position \mathbf{R}_j is represented by pseudo-fermions

$$S_{\alpha\beta}(j) = f_{j\alpha}^\dagger f_{j\beta} - \frac{n_f(j)}{N} \delta_{\alpha\beta}. \quad (18.44)$$

This representation requires that we set a value for the conserved f occupancy $n_f(j)$ at each site. In preparation for a path integral approach we rewrite the interaction in the factorized form encountered in (18.28), so that now

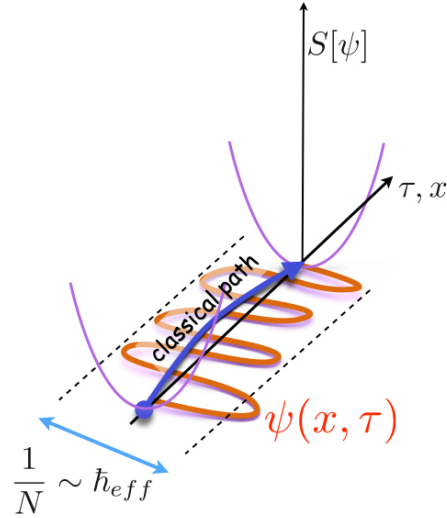


Fig. 18.5

Schematic diagram illustrating the convergence of a quantum path integral about a semi-classical trajectory in the large N limit.

$$H = \sum_{\mathbf{k}\alpha} \epsilon_{\mathbf{k}} c_{\mathbf{k}\alpha}^\dagger c_{\mathbf{k}\alpha} - \frac{J}{N} \sum_{j,\alpha\beta} : (c_{j\beta}^\dagger f_{j\beta}) (f_{j\alpha}^\dagger c_{j\alpha}) : \quad (18.45)$$

Read Newns model for the Kondo lattice

where the potential scattering terms resulting from the rearrangement of the f -operators have been absorbed into a shift of the chemical potential. Notice that:

- in this factorized form, the antiferromagnetic Kondo interaction is “attractive”.
- the coupling constant has been scaled to vary as J/N , to ensure that the interaction grows extensively with N . The interaction involves the product of two terms that scale as $O(N)$, scaling as $J/N \times O(N^2) \sim O(N)$.
- the model has a global $SU(N)$ symmetry associated with the conservation of the total magnetization.
- the Coqblin Schrieffer model also has a **local gauge invariance**: the absence of f -charge fluctuations allows us to change the phase of the f -electrons *independently* at each site

$$f_{j\sigma} \rightarrow e^{i\phi_j} f_{j\sigma}. \quad (18.46)$$

The appearance of local gauge symmetries in a strongly correlated electron problem is actually a general phenomenon. Here, the incompressible nature of the f -electrons gives rise to a constraint on the Hilbert space, which manifests itself as a gauge field.

Finally, before we continue, we need to decide what value to give the conserved charge $n_f = Q$. Most times, in the physical models of interest, $n_f = 1$ at each site, so one might be inclined to explicitly maintain this condition. However, the large N expansion requires that the action is extensive in N , and this forces us to consider more general classes of solution where $n_f = Q$ also scales with N so that the f -filling factor $q = Q/N$

is finite as $N \rightarrow \infty$. With this device, even if we only impose the constraint $\langle n_f \rangle = Q$ on the average, the RMS fluctuations $\sqrt{\langle \delta n_f^2 \rangle} \sim O(\sqrt{N})$ can be neglected relative to $Q \sim O(N)$. Thus if we're interested in a Kramer's doublet Kondo model, we take the half-filled case $q = 1/2$, $Q = N/2$, but if we want to understand a $j = 7/2$ Yb³⁺ atom without crystal fields, then in the physical system $N = 2j + 1 = 8$, and we should fix $q = Q/N = 1/8$.

18.4 The Read Newns Path Integral

To construct the path integral, we need to first take care of the constraint $n_f = Q$. We want to write the partition function as a trace

$$Z = \text{Tr} \left[e^{-\beta H} \prod_j P_Q(j) \right] \quad (18.47)$$

where $P_Q(j)$ projects out the states with $n_f(j) = Q$ at site j . The constraints $P_Q(j)$ commute with the Hamiltonian and can be rewritten as a Fourier transform

$$P_Q(j) = \delta_{n_{fj}, Q} = \int_0^{2\pi} \frac{d\alpha_j}{2\pi} \exp[-i\alpha_j(n_{fj} - Q)] = \int_0^{2\pi i T} \frac{d\lambda_j}{2\pi i T} \exp[-\beta\lambda_j(n_{fj} - Q)], \quad (18.48)$$

where $\lambda_j = i\alpha_j T$ plays the role of a local chemical potential, integrated between $\lambda_j = 0$ and $\lambda_j = 2\pi i T$ along the imaginary axis. Substituting this expression for $P_Q(j)$ in the partition function, we obtain

$$Z = \int \mathcal{D}[\lambda] \text{Tr} \left[e^{-\beta H[\lambda]} \right] \quad (18.49)$$

where now

$$H[\lambda] = \sum_{\mathbf{k}\alpha} \epsilon_{\mathbf{k}} c_{\mathbf{k}\alpha}^\dagger c_{\mathbf{k}\alpha} - \frac{J}{N} \sum_{j,\alpha\beta} : (c_{j\beta}^\dagger f_{j\beta}) (f_{j\alpha}^\dagger c_{j\alpha}) : + \sum_j \lambda_j (n_{fj} - Q). \quad (18.50)$$

and formally $\mathcal{D}[\lambda] = \prod_j \frac{d\lambda_j}{2\pi i T}$. Now, following the lines of Chapter 12, we rewrite the trace as a path integral

$$Z = \int \mathcal{D}[\psi^\dagger, \psi, \lambda] \exp \left[- \int_0^\beta d\tau \overbrace{(\psi^\dagger \partial_\tau \psi + H[\bar{\psi}, \psi, \lambda])}^{L[\psi^\dagger, \psi, \lambda]} \right] \quad (18.51)$$

where $\psi^\dagger \equiv (\{c^\dagger\}, \{f^\dagger\})$ schematically represent the conduction and f-electron fields, while ψ is its conjugate. Inside the path integral we shall use ψ^\dagger and ψ to represent the Grassman co-ordinates of the path integral, with the understanding that when used outside the path integral, these symbols represents the corresponding field operators. Written in full, the Lagrangian is

$$L[\psi^\dagger, \psi, \lambda] = \sum_{\mathbf{k},\sigma} c_{\mathbf{k}\sigma}^\dagger (\partial_\tau + \epsilon_{\mathbf{k}}) c_{\mathbf{k}\sigma} + \sum_j f_{j\sigma}^\dagger (\partial_\tau + \lambda_j) f_{j\sigma} - \frac{J}{N} \sum_{j,\alpha\beta} (c_{j\beta}^\dagger f_{j\beta}) (f_{j\alpha}^\dagger c_{j\alpha}) - \sum_j \lambda_j Q. \quad (18.52)$$

The next step is to carry out a Hubbard Stratonovich transformation on the interaction,

$$- \frac{J}{N} \sum_{\alpha\beta} (c_{j\beta}^\dagger f_{j\beta}) (f_{j\alpha}^\dagger c_{j\alpha}) \rightarrow \sum_\alpha [\bar{V}_j (c_{j\alpha}^\dagger f_{j\alpha}) + (f_{j\alpha}^\dagger c_{j\alpha}) V_j] + N \frac{\bar{V}_j V_j}{J}. \quad (18.53)$$

In the original Kondo model, we started out with an interaction between electrons and spins. Now, by carrying out the Hubbard Stratonovich transformation, we have formulated the interaction as the exchange of a charged boson

$$-\frac{J}{N} \sum_{\mathbf{k}, \mathbf{k}', \alpha, \beta} (c^\dagger_{\beta} f_{\beta})(f^\dagger_{\alpha} c_{\alpha}) \quad (18.54)$$

where the solid lines represent the conduction electron propagators, and the dashed lines represent the f-electron operators. Notice how the bare amplitude associated with the exchange boson is frequency independent, i.e the interaction is instantaneous. Physically, we may interpret this exchange process as due an intermediate valence fluctuation.

The path integral now involves an additional integration over the hybridization fields V and \bar{V} ,

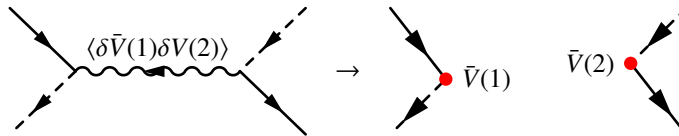
$$Z = \int \mathcal{D}[\bar{V}, V, \lambda] \int \mathcal{D}[\psi^\dagger, \psi] \exp \left[- \int_0^\beta (\psi^\dagger \partial_\tau \psi + H[\bar{V}, V, \lambda]) \right]$$

$$H[\bar{V}, V, \lambda] = \sum_{\mathbf{k}} \epsilon_{\mathbf{k}} c^\dagger_{\mathbf{k}\sigma} c_{\mathbf{k}\sigma} + \sum_j \left[\bar{V}_j (c^\dagger_{j\sigma} f_{j\sigma}) + (f^\dagger_{j\sigma} c_{j\sigma}) V_j + \lambda_j (n_{fj} - Q) + N \frac{\bar{V}_j V_j}{J} \right], \quad (18.55)$$

Read Newns path integral for the Kondo lattice.

where we have suppressed summation signs for repeated spin indices (summation convention).

The importance of the Read Newns path integral, is that it allows us to develop a mean-field description of the many body Kondo scattering processes that captures the physics and is asymptotically exact as $N \rightarrow \infty$. In this approach, the condensation of the hybridization field describes the formation of bound-states between spins and electrons that can not be dealt with in perturbation theory. Bound-states induce long range temporal correlations in scattering and indeed, once the hybridization condenses, the interaction lines break-up into independent anomalous scattering events, denoted by



The hybridization V in the Read Newns action carries the local $U(1)$ gauge charge of the f-electrons, giving rise to an important local gauge invariance:

$$f_{j\sigma} \rightarrow e^{i\phi_j} f_{j\sigma}, \quad V_j \rightarrow e^{i\phi_j} V_j, \quad \lambda_j \rightarrow \lambda_j - i\dot{\phi}_j(\tau). \quad (18.56)$$

Read Newns gauge transformation.

It is often useful to use this invariance to choose a gauge in which V_j is real and gauge neutral. We do this by absorbing the phase of the hybridization $V_j = |V_j|e^{i\phi_j}$ into the f-electron. Let us examine how the action at site j transforms when we redefine the f-electrons to absorb this phase:

$$\begin{aligned} S_K(j) &= \int_0^\beta d\tau \left[f_{j\sigma}^\dagger (\partial_\tau + \lambda_j) f_{j\sigma} + \overbrace{(|V_j|e^{-i\phi_j} c_{j\sigma}^\dagger f_{j\sigma} + |V_j|e^{i\phi_j} f_{j\sigma}^\dagger c_{j\sigma})}^{V_j} + N \frac{|V_j|^2}{J_K} - \lambda_j Q \right] \\ &\xrightarrow{f_j \rightarrow e^{i\phi_j} f_j} \int_0^\beta d\tau \left[f_{j\sigma}^\dagger (\partial_\tau + \lambda_j + i\dot{\phi}_j) f_{j\sigma} + |V_j| (c_{j\sigma}^\dagger f_{j\sigma} + f_{j\sigma}^\dagger c_{j\sigma}) + N \frac{|V_j|^2}{J_K} - \lambda_j Q \right]. \end{aligned} \quad (18.57)$$

In our starting model, the constraint field was constant, but in this “radial gauge”, it has acquired a time dependence derived from the precession of phase ϕ . If we define the dynamical variable $\lambda_j(\tau) = \lambda_j + i\dot{\phi}_j$, this becomes

$$S_K(j) = \int_0^\beta d\tau \left[f_{j\sigma}^\dagger [\partial_\tau + \lambda_j(\tau)] f_{j\sigma} + |V_j| (c_{j\sigma}^\dagger f_{j\sigma} + f_{j\sigma}^\dagger c_{j\sigma}) + N \frac{|V_j|^2}{J_K} - \lambda_j(\tau) Q \right] + \overbrace{iQ \int_0^\beta d\tau \dot{\phi}_j}^{iQ\Delta\phi_j = i2\pi Qn}. \quad (18.58)$$

The remainder term comes from making the change of variables in the constraint term $\lambda_j = \lambda_j(\tau) - i\dot{\phi}_j$. Fortunately, this term is an exact integral, and since the change in the phase of the hybridization is an integral multiple of 2π it adds an overall phase $e^{i2\pi n Q} = 1$ to the path integral, and can hence be dropped. In this radial gauge, the Newn’s Read path integral becomes

$$\begin{aligned} Z &= \int \mathcal{D}[|V|, \lambda] \int \mathcal{D}[\psi^\dagger, \psi] \exp \left[- \int_0^\beta (\psi^\dagger \partial_\tau \psi + H[|V|, \lambda]) \right] \\ H[|V|, \lambda] &= \sum_{\mathbf{k}} \epsilon_{\mathbf{k}} c_{\mathbf{k}\sigma}^\dagger c_{\mathbf{k}\sigma} + \sum_j \left[|V_j| (c_{j\sigma}^\dagger f_{j\sigma} + f_{j\sigma}^\dagger c_{j\sigma}) + \lambda_j (n_{fj} - Q) + N \frac{|V_j|^2}{J} \right], \end{aligned} \quad (18.59)$$

Read Newns path integral: “radial gauge”.

By absorbing the phase, the constraint field becomes a dynamical potential field, integrated along the entire imaginary axis (see example 18.2 for details). Subsequently, when we use the radial gauge, we will drop the moduli sign. The interesting feature about this Hamiltonian, is that with the real hybridization, the conduction and f-electrons now transform under a single global $U(1)$ gauge transformation, i.e the f-electrons have become *charged*. We will return to this issue in a later section.

18.4.1 The Effective Action

We now develop the large N expansion by calculating the effective action. We'll begin without fixing the gauge. The interior fermion integral in the path integral (18.59) defines an effective action $S_E[\bar{V}, V, \lambda]$ by the relation

$$\exp[-NS_E[\bar{V}, V, \lambda]] \equiv Z_E[\bar{V}, V, \lambda] = \int \mathcal{D}[\psi^\dagger, \psi] \exp[-S[\bar{V}, V, \lambda, \psi^\dagger, \psi]], \quad (18.60)$$

where we have defined $Z_E = e^{-NS_E}$ and using (18.55),

$$S = \int_0^\beta d\tau \left[\sum_{\mathbf{k}} c_{\mathbf{k}\sigma}^\dagger (\partial_\tau + \epsilon_{\mathbf{k}}) c_{\mathbf{k}\sigma} + \sum_j \left(f_{j\sigma}^\dagger (\partial_\tau + \lambda_j) f_{j\sigma} + (\bar{V}_j c_{j\sigma}^\dagger f_{j\sigma} + V_j f_{j\sigma}^\dagger c_{j\sigma}) + N \frac{\bar{V}_j V_j}{J} - \lambda_j Q \right) \right] \quad (18.61)$$

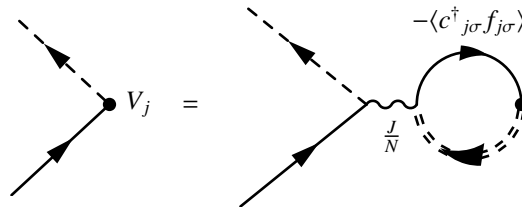
The extensive growth of the effective action with N means that at large N , the integration in (18.55) is dominated by its stationary points:

$$Z = \int \mathcal{D}[\lambda, \bar{V}, V] \exp[-NS_E[\bar{V}, V, \lambda]] \approx \exp[-NS_E[\bar{V}, V, \lambda]] \Big|_{\text{Saddle Point}} \quad (18.62)$$

If we identify $NS_E = -\ln Z_E$, so that $N\delta S_E = -\delta Z_E/Z_E$, then differentiating (18.60) with respect to \bar{V}_j and λ_j , we see that the saddle point conditions impose the self-consistent relations

$$\begin{aligned} \frac{\delta NS_E}{\delta \bar{V}_j(\tau)} &= \frac{1}{Z_E} \int \mathcal{D}[\psi^\dagger, \psi] \overbrace{\left(c_{j\sigma}^\dagger(\tau) f_{j\sigma}(\tau) + \frac{NV_j(\tau)}{J} \right)}^{\delta S / \delta \bar{V}_j(\tau)} e^{-S} = \langle c_{j\sigma}^\dagger f_{j\sigma} \rangle(\tau) + \frac{N}{J} V_j(\tau) = 0 \\ \frac{\delta NS_E}{\delta \lambda_j(\tau)} &= \frac{1}{Z_E} \int \mathcal{D}[\psi^\dagger, \psi] (n_f(j, \tau) - Q) e^{-S} = \langle n_f(j, \tau) \rangle - Q = 0, \end{aligned} \quad (18.63)$$

where repeated spin indices imply summation. The second equation in (18.63) is the satisfaction of the constraint, on the average. The first relation, which can be written $V_j = -\frac{J}{N} \langle c_{j\sigma}^\dagger f_{j\sigma} \rangle$, is recognized as the mean-field self-consistency associated with the Hubbard-Stratonovich factorization. We can denote this self-consistency by the Feynman diagram,



indicating that the condensation of the boson V is self-consistently induced by an anomalous hybridization. Fortunately, we will not have to solve these equations by explicitly calculating the expectation values, instead as we found in previous chapters (see section 14.3) they are implicitly imposed by finding the stationary point of the action.

In practice, we shall seek static solutions, using the radial gauge to absorb the phase of the hybridization, so that $\bar{V}_j(\tau) = V_j(\tau) = |V_j|$, $\lambda_j(\tau) = \lambda_j$. In this case the saddle point partition function $Z_E[V, \lambda]$ is simply the partition function of the static mean-field Hamiltonian $H_{MF} = H[V, \lambda]$, $Z_E = \text{Tr} e^{-\beta H_{MF}}$. Now we may write

the action in the form

$$S = \int_0^\beta d\tau \left[\sum_\sigma \psi_\sigma^\dagger (\partial_\tau + \underline{h}) \psi_\sigma + \sum_j \left(N \frac{V_j^2}{J} - \lambda_j \mathcal{Q} \right) \right]. \quad (18.64)$$

where the matrix $\underline{h}[V, \lambda]$ is a mean-field Hamiltonian, read off from (18.55). For instance, in a tight-binding representation,

$$H[V, \lambda] = \sum_{i,j,\sigma} (c_{i\sigma}^\dagger, f_{i\sigma}^\dagger) \overbrace{\begin{bmatrix} (t_{ij} - \mu\delta_{ij}) & \bar{V}_j\delta_{ij} \\ V_j\delta_{ij} & \lambda_j\delta_{ij} \end{bmatrix}}^{\underline{h}[V,\lambda]} \begin{pmatrix} c_{j\sigma} \\ f_{j\sigma} \end{pmatrix} + \sum_j \left(N \frac{|V_j|^2}{J} - \lambda_j \mathcal{Q} \right) \quad (18.65)$$

where the t_{ij} are the hopping matrix elements obtained by Fourier transforming $\epsilon_{\mathbf{k}} = \sum_{\mathbf{R}_{ij}} (t(\mathbf{R}_{ij}) - \mu\delta_{ij}) e^{-i\mathbf{k}\cdot\mathbf{R}_{ij}}$.

Since the action is Gaussian in the Fermi fields, the Fermi integral can be carried out using formula (??) in terms of the determinant of the action:

$$\begin{aligned} \int \mathcal{D}[\psi^\dagger, \psi] \exp \left[- \int_0^\beta d\tau \sum_\sigma \psi_\sigma^\dagger (\partial_\tau + \underline{h}) \psi_\sigma \right] &= (\det[\partial_\tau + \underline{h}])^N = \exp \left[N \ln \det[\partial_\tau + \underline{h}] \right] \\ &= \exp \left[N \text{Tr} \ln[\partial_\tau + \underline{h}] \right] \end{aligned} \quad (18.66)$$

where the power N derives from the N identical integrals over each spin component of ψ_σ . In the last line, we have replaced $\ln \det \rightarrow \text{Tr} \ln$. Thus

$$NS_E[V, \lambda] = N \left[-\text{Tr} \ln(\partial_\tau + \underline{h}) + \sum_j \int_0^\beta d\tau \left(\frac{|V_j|^2}{J} - \lambda_j \mathcal{Q} \right) \right]. \quad (18.67)$$

Since $Z_E = e^{-\beta F_{MF}} = e^{-NS_E}$, where F_{MF} is the mean field free energy, it follows that

$$F_{MF}[V, \lambda] = \frac{1}{\beta} S_E[V, \lambda] = -\frac{N}{\beta} \text{Tr} \ln(\partial_\tau + \underline{h}[V, \lambda]) + \sum_j \left(\frac{N|V_j|^2}{J} - \lambda_j \mathcal{Q} \right). \quad (18.68)$$

If we switch to the frequency domain, replacing $\partial_\tau \rightarrow -i\omega_n$ by a Matsubara frequency, we may also write

$$\begin{aligned} F_{MF} &= -NT \sum_{i\omega_n} \text{Tr} \ln \left[-\mathcal{G}^{-1}(i\omega_n) \right] + \sum_j \left(\frac{N|V_j|^2}{J} - \lambda_j \mathcal{Q} \right) \\ \mathcal{G}^{-1} &= (i\omega_n - \underline{h}[V, \lambda]). \end{aligned} \quad (18.69)$$

where we have identified $\mathcal{G}^{-1} = (i\omega_n - \underline{h}[V, \lambda])$ with the inverse Green's function. Sometimes, it's convenient to re-express S_E in terms of the eigenvalues E_ζ of the Hamiltonian. If we diagonalize the Hamiltonian, so that $\underline{h} \rightarrow E_\zeta \delta_{\zeta\zeta'}$, then $\text{Tr} \ln(-i\omega_n + \underline{h}) = \sum_\zeta \ln(E_\zeta - i\omega_n)$. We can also do the Matsubara sum, under which $-T \sum_{i\omega_n} \ln(E_\zeta - i\omega_n) \rightarrow -T \ln(1 + e^{-\beta E_\zeta})$, so that the free energy can also be written

$$F_E[V, \lambda] = -NT \sum_\zeta \ln(1 + e^{-\beta E_\zeta}) + \sum_j \left(\frac{N|V_j|^2}{J} - \lambda_j \mathcal{Q} \right). \quad (18.70)$$

(18.69) and (18.70) are complimentary: the former reflects the path-integral approach while the latter, a more conventional mean-field approach. Let us now apply them to the Kondo impurity and lattice models.

Example 18.3: This example shows in detail, how to derive the measure of the Read-Newn's path integral. The initial Kondo lattice path integral involves static constraint fields λ_j , integrated over a finite range of the imaginary axis: $\lambda_j \in [0, i2\pi T]$, as follows:

$$Z = \prod_j \int_0^{2\pi iT} \frac{d\lambda_j}{2\pi iT} \int \mathcal{D}[V, \psi] \exp \left[- \int_0^\beta (\bar{\psi} \partial_\tau \psi + H[V, \lambda]) \right]. \quad (18.71)$$

By inserting the identity $\int \mathcal{D}[g_j] = 1$, into the Kondo path integral, where $\mathcal{D}[g_j]$ denotes the integration over the entire orbit of gauge transformations $g_j(\tau) = e^{i\phi_j(\tau)}$, show that λ_j is promoted to a dynamical variable $\lambda'_j(\tau) = \lambda_j + i\dot{\phi}_j(\tau)$, integrated over the entire imaginary axis.

Solution:

If we insert the identity $\prod_j \int \mathcal{D}[g_j] = 1$ into the path integral, it becomes

$$Z = \int \mathcal{D}[\lambda, g, V, \psi] e^{-S[\lambda, V, \psi]}. \quad (18.72)$$

At this point, g is just a dummy variable. We need to (i) carry out a gauge transformation to absorb g into the fields (ii) rewrite the measure of integration in terms of the transformed fields.

i) **Change of variables.**

The first step is to show that the action is unchanged by the gauge transformation,

$$f_j(\tau) = e^{i\phi_j(\tau)} f'_j(\tau), \quad V_j(\tau) = e^{i\phi_j(\tau)} V'_j(\tau), \quad (18.73)$$

Under this transformation, the Hamiltonian is unchanged but the f-Berry phase term acquires an additional $i\dot{\phi}_j$ term from to the time-dependence of $g_j(\tau) = e^{i\phi_j(\tau)}$,

$$f^\dagger (\partial_j + \lambda_j) f \rightarrow f'^\dagger e^{-i\dot{\phi}_j} (\partial_\tau + \lambda_j) e^{i\dot{\phi}_j} f' = f'^\dagger (\partial_j + \lambda_j + i\dot{\phi}_j) f'. \quad (18.74)$$

To absorb this term we must also transform the λ_j field, introducing the dynamic variable $\lambda'_j(\tau) = \lambda_j + i\dot{\phi}_j(\tau)$. Subtly, under the transformation, the constraint term adds a phase shift to the action:

$$\begin{aligned} S[V, \lambda, \psi] &= \int_0^\beta d\tau \sum_j [f_j^\dagger (\partial_\tau + \lambda'_j) f'_j - (\lambda'_j - i\dot{\phi}_j) Q] + \dots \\ &= S[V', \lambda', \psi'] + iQ \sum_j \int_0^\beta d\tau \dot{\phi}_j. \end{aligned} \quad (18.75)$$

Now $Q \int_0^\beta d\tau \dot{\phi}_j = Q\Delta\phi_j$ is determined by the change in ϕ_j between $\tau = 0$ and $\tau = \beta$. Since $g_j = e^{i\phi_j}$ is periodic in time, $\Delta\phi_j$ is an integer multiple M_j of 2π and since Q is an integer, the phase shift is multiple of 2π , leaving e^{-S} invariant:

$$\exp(-S[V, \lambda, \psi]) = \exp \left(-S[V', \lambda', \psi'] - 2\pi i \sum_j (QM_j) \right) = \exp(-S[V', \lambda', \psi']). \quad (18.76)$$

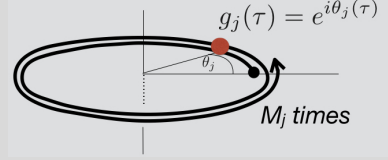
ii) **Change of measure.**

Since the gauge transformation is unitary, the measure for the hybridization and f-electron fields is unchanged (phase factors cancel),

$$\prod_\tau d\bar{V}_j(\tau) dV_j(\tau) = \prod_\tau d\bar{V}'_j(\tau) dV'_j(\tau), \quad \prod_\tau df^\dagger_j(\tau) df_j(\tau) = \prod_\tau df'^\dagger_j(\tau) df'_j(\tau). \quad (18.77)$$

Next, we show that the remaining measure $\mathcal{D}[\lambda, g] = \mathcal{D}[\lambda']$, with a flat measure of integration over

the dynamical variable $\lambda'_j(\tau) = \lambda_j + i\dot{\phi}_j$. Since $\phi_j(\beta) = \phi_j(0) + 2\pi M_j$ is periodic up to a multiple of 2π , we may write



$$\phi_j(\tau) = 2\pi T M_j \tau + \tilde{\theta}_j(\tau) \quad (18.78)$$

which describes a path for $g_j(\tau) = e^{i\phi_j(\tau)}$ that wraps M_j times around the origin. The second term is a periodic function of τ that can be decomposed into its Matsubara Fourier components, $\tilde{\theta}_j(\tau) = \sum_n \tilde{\theta}_n(j) e^{-i\nu_n \tau}$. The original measure for integrating over the static λ_j and g_j is

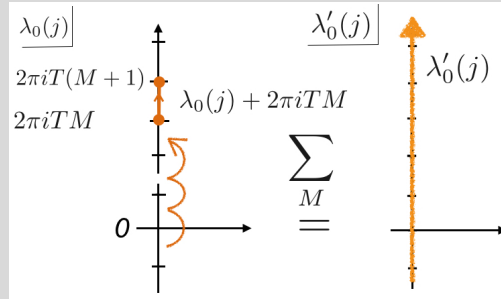
$$\begin{aligned} \mathcal{D}[\lambda_j, g_j] &= \sum_{M_j} \int_0^{2\pi iT} d\lambda_j \prod_{\tau} d\tilde{\phi}_j(\tau) \\ &= \sum_{M_j} \int_0^{2\pi iT} d\lambda_j \prod_n d\tilde{\phi}_n(j) \end{aligned} \quad (18.79)$$

where, in the last line, the measure for the integration over $\tilde{\phi}_j$ has been replaced by the integration over its Matsubara Fourier components.

Now the dynamic variable $\lambda'_j(\tau) = \lambda_j + i\dot{\theta}_j = \lambda_j + 2\pi i T M_j + i\dot{\tilde{\theta}}_j(\tau)$ has a Fourier series

$$\lambda'_j(\tau) = \sum_n \lambda'_n(j) e^{-i\nu_n \tau} \quad (18.80)$$

where $\lambda'_0(j) = \lambda_j + 2\pi i T M_j$ and $\lambda'_n(j) = i(-i\nu_n) \tilde{\theta}_n(j) = \nu_n \tilde{\phi}_n(j)$.



When we integrate over λ_j , the range of the $\lambda'_0(j) = \lambda_j + 2\pi i T M_j$ runs from $2\pi i T M_j$ to $2\pi i T (M_j + 1)$ along the imaginary axis, so that when we sum over all M_j $\lambda'_0(j)$ runs over the entire imaginary axis (See figure on left.). It follows that the combination

$$\sum_{M_j} \int_{2\pi i T M_j}^{2\pi i T (M_j + 1)} d\lambda'_0(j) \equiv \int_{-i\infty}^{i\infty} d\lambda'_0(j). \quad (18.81)$$

gives an unconstrained integral over the static part $\lambda'_0(j)$ of $\lambda'_j(\tau)$.

For $n \neq 0$, the Fourier coefficients $\lambda'_n(j) = \nu_n \tilde{\theta}_n(j)$ are directly proportional so up to a normalization, their measures are equal

$$\prod_{n \neq 0} d\lambda'_n(j) = \mathcal{N} \prod_{n \neq 0} d\tilde{\theta}_n(j)$$

where we have dropped the normalization factor $\prod_n = \prod_{n \neq 0} \nu_n$. Thus by integrating over all possible $\tilde{\phi}_j$, we integrate over all finite frequency Fourier components of $\lambda'_j(\tau)$. Combining the static and dynamic part of the measure, it follows that

$$\mathcal{D}[\lambda_j, g_j] \equiv \mathcal{D}[\lambda'_j] = \prod_n d\lambda'_n(j),$$

and since $\mathcal{D}[V, \psi] = \mathcal{D}[V', \psi']$,

$$\mathcal{D}[g, \lambda, V, \psi] = \mathcal{D}[\lambda', V', \psi'] \quad (18.82)$$

where the measure for the dynamical field λ' is flat.

18.5 Mean-field theory of the Kondo impurity

18.5.1 The impurity effective action

The large N mean-field theory of the Kondo effect maps the original Hamiltonian onto a self-consistently determined resonant level model, which we will write in the form

$$H_{MF} = \sum_{\sigma} \left(\cdot \cdot c^{\dagger}_{\mathbf{k}\sigma} \cdot \cdot, f^{\dagger}_{\sigma} \right) \left(\begin{array}{c|c} \epsilon_{\mathbf{k}} \delta_{\mathbf{k},\mathbf{k}'} & \bar{V} \\ \hline V & \lambda \end{array} \right) \begin{pmatrix} \vdots \\ c_{\mathbf{k}'\sigma} \\ \vdots \\ f_{\sigma} \end{pmatrix} + \frac{NV^2}{J} - \lambda Q \quad (18.83)$$

In chapter 17 (section ??), we learned that the single resonance described by this model is located at an energy λ , with a hybridization width $\Delta = \pi\rho V^2$ (Eq. ??). By minimizing the Free energy of this system, we need to figure out how λ and Δ are related to the Kondo coupling constant. Let us first evaluate the Free energy of the resonance. We can read off \underline{h} from (18.83), so from 18.69, the mean-field free energy is then given by

$$F_{MF} = -TN \sum_n \ln \det \left(\begin{array}{c|c} (\epsilon_{\mathbf{k}} - i\omega_n) \delta_{\mathbf{k},\mathbf{k}'} & \bar{V} \\ \hline V & \lambda - i\omega_n \end{array} \right) + \left(\frac{NV^2}{J} - \lambda Q \right) \quad (18.84)$$

Using the result $\det \begin{pmatrix} D & C \\ B & A \end{pmatrix} = \det D \det [A - BD^{-1}C]$, we can “integrate out” the conduction electrons to write

$$F_{MF} = -TN \sum_n \ln \left[-i\omega_n + \lambda + \sum_{\mathbf{k}} \frac{|V|^2}{i\omega_n - \epsilon_{\mathbf{k}}} \right] + \left(\frac{NV^2}{J} - \lambda Q \right) + F_C \quad (18.85)$$

where $F_C = -TN \sum_{\mathbf{k},n} \ln(\epsilon_{\mathbf{k}} - i\omega_n)$ is the conduction electron Free energy. Using the large band-width approximation $\sum_{\mathbf{k}} \frac{|V|^2}{i\omega_n - \epsilon_{\mathbf{k}}} = -i\Delta \text{sgn}(\omega_n) \equiv \Delta_n$ (see Eq. ??), this becomes

$$F_{MF}[V, \lambda] = -\frac{N}{\beta} \sum_n \ln \left[-i\omega_n + \lambda + i\Delta_n \right] e^{i\omega_n 0^+} + N \left(\frac{|V|^2}{J_K} - \lambda Q \right) + F_C \quad (18.86)$$

If we carry out the Matsubara summation by the standard methods, replacing $-T \sum_n F(i\omega_n) \rightarrow \oint \frac{dz}{2\pi i} f(z) F[z]$, where the contour runs anticlockwise around the poles in the Fermi function (Fig. 18.6a). Now the logarithm contains a branch-cut along the real axis, where $\Delta_n = \Delta \text{sgn}(\text{Im}z)$ jumps from $i\Delta$ below the real axis to $-i\Delta$ above it. If we introduce a finite bandwidth D , this branch-cut runs from $z = -D$ to $z = +D$.

Distorting the contour to run clockwise around this branch-cut (Fig. 18.6 (b)) we obtain

$$\begin{aligned} F_{MF}[V, \lambda] &= N \int_{-D}^D \frac{d\omega}{2\pi i} f(\omega) (\ln[-\omega + \lambda - i\Delta] - \ln[-\omega + \lambda + i\Delta]) + N \left(\frac{|V|^2}{J_K} - \lambda Q \right) + F_C \\ &= -N \int_{-D}^D d\omega f(\omega) \overbrace{\left(\frac{1}{\pi} \text{Im} \ln[\lambda + i\Delta - \omega] \right)}^{\delta_f(\omega)/\pi} + N \left(\frac{|V|^2}{J_K} - \lambda Q \right) + F_C \end{aligned} \quad (18.87)$$

where we have made the identification $\delta(\omega) = \text{Im} \ln[\lambda + i\Delta - \omega] = \tan^{-1} \left(\frac{\Delta}{\lambda - \omega} \right)$ as the scattering phase shift

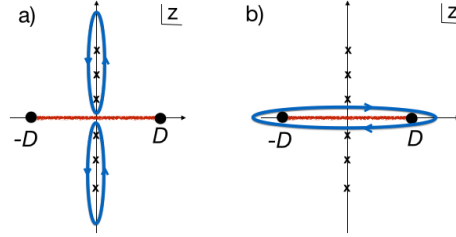


Fig. 18.6 Contour used in evaluating Free energy. (a) undistorted contour (b) contour distorted to run around branch-cut in the f-electron Green's function.

of the impurity (see eq. 17.33). We then obtain

$$F_{MF}[V, \lambda] = -N \int_{-D}^D d\omega \left(\frac{\delta_f(\omega)}{\pi} \right) f(\omega) + N \left(\frac{|V|^2}{J_K} - \lambda Q \right) + F_C \quad (18.88)$$

We can give this result a simple interpretation: the effect of the resonant phase shift changes the allowed momenta of the radial partial-wave states, which in turn causes the one-particle eigenstates of the continuum to move by a fraction δ_f/π of the energy level spacing $\Delta\epsilon$ according to the relation (see (??)) $\tilde{\epsilon}_k = \epsilon_k - \frac{\delta(\epsilon_k)}{\pi} \Delta\epsilon$, where k labels the eigenstates. The corresponding change in the Free energy of the continuum is then

$$\Delta F = \sum_k \frac{\partial}{\partial \epsilon_k} \left(-T \ln [1 + e^{-\beta \epsilon_k}] \right) \left[-\frac{\delta_f(\epsilon_k)}{\pi} \Delta\epsilon \right] = - \sum_k f(\epsilon_k) \frac{\delta(\epsilon_k)}{\pi} \Delta\epsilon \equiv - \int d\epsilon \frac{\delta_f(\epsilon)}{\pi} f(\epsilon) \quad (18.89)$$

where we have replaced the discrete summation by an integral. The first term in (18.88) is precisely this shift in the continuum Free energy.

Example 18.4:

- a) Diagonalize the impurity resonant level Hamiltonian

$$H_{MF} = \sum_{k\sigma} \epsilon_k c_{k\sigma}^\dagger c_{k\sigma} + \sum_{k\sigma} V [c_{k\sigma}^\dagger f_\sigma + f_\sigma^\dagger c_{k\sigma}] + \lambda \sum_\sigma n_{f\sigma}. \quad (18.90)$$

and compute the scattering phase shift of the resonant level.

- b) Show that injection of an f-state into the continuum induces a resonant correction to the total the density of states,

$$\rho \rightarrow \rho^*(E) = \rho + \frac{1}{\pi} \frac{\Delta}{(E - \lambda)^2 + \Delta^2}. \quad (18.91)$$

Solution:

- a) To diagonalize the Hamiltonian, we write it in the form

$$H = \sum_{\gamma\sigma} E_\gamma a_{\gamma\sigma}^\dagger a_{\gamma\sigma} \quad (18.92)$$

where the quasiparticle operators a_γ are related to the original operators via the one-particle eigenstates, $a_{\gamma\sigma}^\dagger = \sum_k c_{k\sigma}^\dagger \langle k|\gamma\rangle + f_\sigma^\dagger \langle f|\gamma\rangle \equiv \sum_k \alpha_k c_{k\sigma}^\dagger + \beta f_\sigma^\dagger$. Now if we denote the amplitudes of the one-particle eigenstates $|\gamma\rangle$ by $\langle \eta|\gamma\rangle \equiv (\dots \langle k'|\gamma\rangle \dots \langle f|\gamma\rangle)$, then since $h_{\eta\eta'} \langle \eta'|\gamma\rangle = \langle \eta|H|\gamma\rangle = E_\gamma \langle \eta|\gamma\rangle$, it follows that the amplitudes $\langle \eta|\gamma\rangle$ must satisfy the eigenvalue equation

$$\underline{h} \cdot \begin{pmatrix} \vdots \\ \alpha_{\mathbf{k}} \\ \vdots \\ \beta \end{pmatrix} = \left(\begin{array}{c|c} \epsilon_{\mathbf{k}} \delta_{\mathbf{k},\mathbf{k}'} & \bar{V} \\ \hline -V & \lambda \end{array} \right) \begin{pmatrix} \vdots \\ \alpha_{\mathbf{k}'} \\ \vdots \\ \beta \end{pmatrix} = E_\gamma \begin{pmatrix} \vdots \\ \alpha_{\mathbf{k}} \\ \vdots \\ \beta \end{pmatrix} \quad (18.93)$$

or

$$\begin{aligned} \epsilon_k \alpha_k + V\beta &= E_\gamma \alpha_k \\ V \sum_{k'} \alpha_{k'} + \lambda\beta &= E_\gamma \beta. \end{aligned} \quad (18.94)$$

(If you like, you can rederive this by expanding the quasiparticle operators on both sides of (18.92) in terms of the conduction and f- electron fields, carrying out the commutator and then comparing coefficients of $c_{k\sigma}^\dagger$ and f_σ^\dagger (see Ex. 15.3.) Solving for α_k using the first equation, and substituting into the second, we obtain

$$E_\gamma - \lambda - \sum_k \frac{V^2}{E_\gamma - \epsilon_k} = 0 \quad (18.95)$$

We can recognize this solution as a pole of the f-Green function, $G_f(E_\gamma)^{-1} = 0$, (see Eq. ?? and Eq. ??).

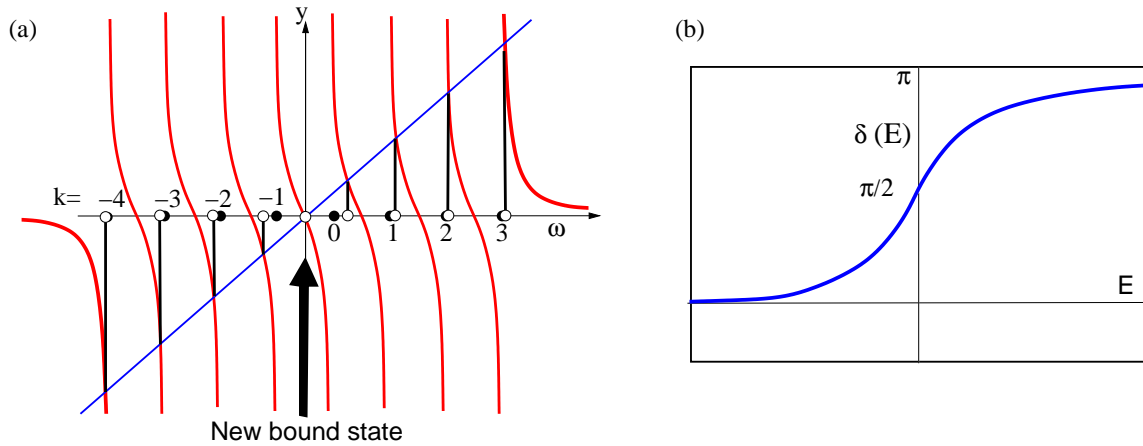


Fig. 18.7

(a) Graphical solution of the equation $y = \lambda + \sum_k \frac{V^2}{y - \epsilon_k}$, for eight equally spaced conduction electron energies for a resonance located at $\lambda = 0$ (arrow). Notice how the injection of a bound-state at $y = 0$ displaces electron band-states away from the Fermi surface, increasing the number of eigenstates by one. (b) Energy dependence of the scattering phase shift.

The solutions of eigenvalue equation (18.95) are illustrated graphically in Fig. (18.7). Suppose the energies of the conduction sea are given by the $2M$ discrete values

$$\epsilon_k = \left(k + \frac{1}{2}\right)\Delta\epsilon, \quad k \in \{-M, \dots, M-1\} \quad (18.96)$$

distributed symmetrically above and below the Fermi energy. Consider the particle-hole case when the f-state is exactly half filled, i.e. when $\lambda = 0$. From the diagram, we see that one solution to the eigenvalue equation corresponds to $E_\gamma = 0$, i.e. the original $2M$ band-electron energies have been displaced to both lower and higher energies, forming a band of $2M + 1$ eigenvalues: the resonance has injected one new eigenstate into the band. Each new eigenvalue is shifted infinitesimally relative to the original

conduction electron energies, according to

$$E_\gamma = \epsilon_\gamma - \Delta\epsilon \frac{\delta(E_\gamma)}{\pi} \quad (18.97)$$

where $\delta(E_\gamma) \in [0, \pi]$ is the resonant scattering phase shift.

Let us now determine the dependence of $\delta[E]$ on the conduction electron energy. Substituting the phase shift into the eigenvalue equation (18.95), we obtain

$$E_\gamma = \lambda + \sum_{n=\gamma+1-M}^{\gamma+M} \frac{V^2}{\Delta\epsilon(n - \frac{\delta_\gamma}{\pi})} \rightarrow \lambda + \frac{\Delta}{\pi} \sum_{n=-\infty}^{\infty} \frac{1}{(n - \frac{\delta_\gamma}{\pi})}. \quad (18.98)$$

Here we have identified $\rho \equiv \frac{1}{\Delta\epsilon}$ as the conduction electron density of states, writing $\Delta = \pi V^2 / \Delta\epsilon = \pi V^2 \rho$ as the resonance level width. We have also taken the liberty extending the bounds of the summation to infinity. Using contour integration methods, recognizing that $\cot z$ has poles at $z = \pi n$ of strength one,

$$\begin{aligned} \sum_{n=-\infty}^{\infty} \frac{\pi}{(\pi n - \delta_\gamma)} &= \sum_n \oint_{\text{poles } z = \pi n} \frac{dz}{2\pi i} \frac{\pi \cot z}{z - \delta_\gamma} \\ &= - \oint_{\text{pole at } z = \delta_\gamma} \frac{dz}{2\pi i} \frac{\pi \cot z}{z - \delta_\gamma} = -\pi \cot \delta(E_\gamma). \end{aligned} \quad (18.99)$$

Using this result, (18.98) becomes

$$E_\gamma = \lambda - \Delta \cot \delta[E_\gamma] \Rightarrow \tan \delta[E_\gamma] = \frac{\Delta}{\lambda - E_\gamma}. \quad (18.100)$$

b) From (18.97) we deduce that

$$\begin{aligned} \frac{d\epsilon}{dE} &= 1 + \frac{\Delta\epsilon}{\pi} \frac{d\delta(E)}{dE} \\ &= 1 + \frac{1}{\pi\rho} \frac{d\delta(E)}{dE} \end{aligned} \quad (18.101)$$

where $\rho = 1/\Delta\epsilon$ is the density of states in the continuum. The new density of states $\rho^*(E)$ is given by $\rho^*(E)dE = \rho d\epsilon$, so that

$$\rho^*(E) = \rho(0) \frac{d\epsilon}{dE} = \rho + \rho_i(E) \quad (18.102)$$

where

$$\rho_i(E) = \frac{1}{\pi} \frac{d\delta(E)}{dE} = \frac{1}{\pi} \frac{\Delta^2}{(E - \lambda)^2 + \Delta^2} \quad (18.103)$$

corresponds to the enhancement of the conduction electron density of states due to injection of resonant bound-state.

18.5.2 Minimization of Free energy

With these results, let us now calculate the Free energy and minimize it to self-consistently evaluate λ and Δ . From the last section. The shift in the Free energy due to the Kondo effect is then

$$\Delta F = -N \int_{-D}^D \frac{d\epsilon}{\pi} f(\epsilon) \text{Im} \ln[\xi - \epsilon] - \lambda Q + \frac{N\Delta}{\pi J\rho} \quad (18.104)$$

where we have introduced the complex number $\xi = \lambda + i\Delta$ whose real and imaginary parts represents the position and width of the resonant level, respectively. This integral can be done at finite temperature, but for

simplicity, let us carry it out at $T = 0$, when the Fermi function becomes a step function, $f(x) = \theta(-x)$. This gives

$$\begin{aligned}\Delta E &= \frac{N}{\pi} \text{Im} \left[(\xi - \epsilon) \ln \left[\frac{\xi - \epsilon}{e} \right] \right]_{\epsilon=-D}^{\epsilon=0} - \lambda Q + \frac{N\Delta}{\pi J\rho} \\ &= \frac{N}{\pi} \text{Im} \left[\xi \ln \left[\frac{\xi}{eD} \right] - D \ln \left[\frac{D}{e} \right] \right] - \lambda Q + \frac{N\Delta}{\pi J\rho}\end{aligned}\quad (18.105)$$

where we have expanded $(\xi + D) \ln \left[\frac{D+\xi}{e} \right] \rightarrow D \ln \left[\frac{D}{e} \right] + \xi \ln D$ to obtain the second line. We can further simplify this expression by noting that

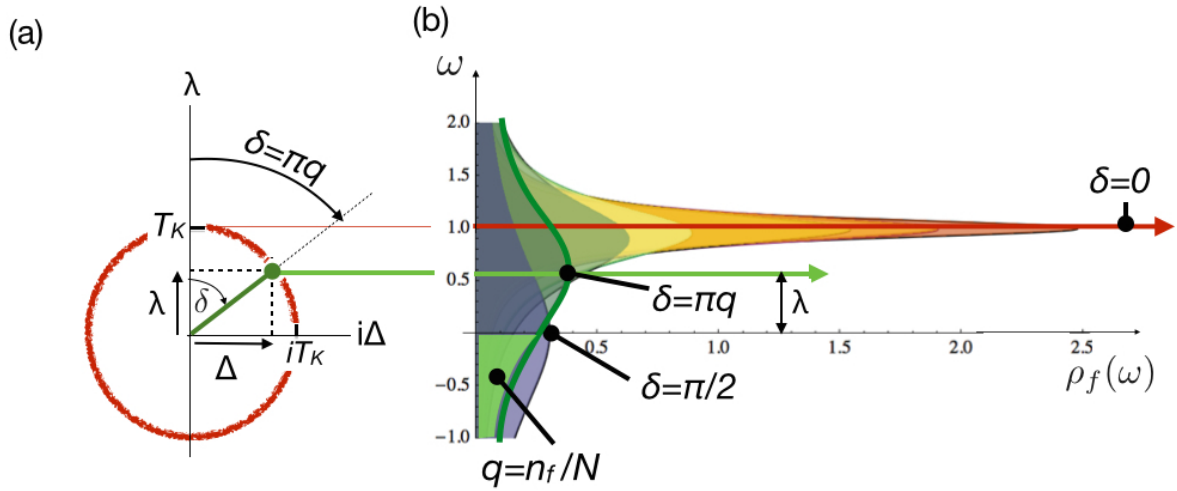
$$-\lambda Q + \frac{N\Delta}{\pi J\rho} = -\frac{N}{\pi} \text{Im} \left[\xi \ln \left[e^{-\frac{1}{\rho} + i\pi q} \right] \right]\quad (18.106)$$

where $q = Q/N$, so that

$$\Delta E = \frac{N}{\pi} \text{Im} \left[\xi \ln \left[\frac{\xi}{e T_K e^{i\pi q}} \right] \right]\quad (18.107)$$

where we have dropped the constant term and introduced the Kondo temperature $T_K = D e^{-\frac{1}{\rho}}$. The stationary point $\partial E / \partial \xi = 0$ is given by

$$\xi = \lambda + i\Delta = T_K e^{i\pi q} \quad \begin{cases} T_K = \sqrt{\lambda^2 + \Delta^2} \\ \tan(\pi q) = \frac{\Delta}{\lambda} \end{cases}$$



$$\xi = \lambda + i\Delta = T_K e^{i\delta}$$

Fig. 18.8

Illustrating the mean-field solution to the impurity Kondo model. (a) Showing how the real and imaginary parts of the resonant level position $\xi = \lambda + i\Delta$ lie on a circle of radius T_K , with a phase shift $\delta = \pi q = \pi n_f/N$. (b) Showing corresponding f density of states $\rho_f(\omega)$ for a range of different occupancies

Notice that

- The phase shift $\delta = \pi q$ is the same in each spin scattering channel, reflecting the singlet nature of the ground state. The relationship between the filling of the resonance and the phase shift $Q = \sum_{\sigma} \frac{\delta_{\sigma}}{\pi} = N \frac{\delta}{\pi}$ is Friedel's sum rule.
- The energy is stationary with respect to small variations in λ and Δ . It is only a local minimum once the condition $\partial E / \partial \lambda = 0 \equiv (\langle \hat{n}_f \rangle - Q)$, is imposed, which gives $\lambda = \Delta \cot(\pi q)$ and hence

$$\Delta E = \frac{N}{\pi} \left[\Delta \ln \left[\frac{\Delta}{e T_K \sin \pi q} \right] \right] \quad (18.108)$$

Plotted as a function of V , this is the classic ‘‘Mexican Hat’’ potential, with a minimum where $\partial E / \partial V = 0$ at $\Delta = \pi \rho |V|^2 = T_K \sin \pi q$. (Fig. 18.11)

- According to (18.102), the enhancement of the density of states at the Fermi energy is

$$\begin{aligned} \rho^*(0) &= \rho + \frac{\Delta}{\pi(\Delta^2 + \lambda^2)} \\ &= \rho + \frac{\sin^2(\pi q)}{\pi T_K} \end{aligned} \quad (18.109)$$

per spin channel. When the temperature is changed or a magnetic field introduced, one can neglect changes in Δ and λ , since the Free energy is stationary. This implies that in the large N limit, the susceptibility and linear specific heat are those of a non-interacting resonance of width Δ . The change in linear specific heat $\Delta C_V = \Delta \gamma T$ and the change in the paramagnetic susceptibility $\Delta \chi$ are given by

$$\begin{aligned} \Delta \gamma &= \left[\frac{N \pi^2 k_B^2}{3} \right] \rho_i(0) = \left[\frac{N \pi^2 k_B^2}{3} \right] \frac{\sin^2(\pi q)}{\pi T_K} \\ \Delta \chi &= \left[N \frac{j(j+1)(g\mu_B)^2}{3} \right] \rho_i(0) = \left[N \frac{j(j+1)(g\mu_B)^2}{3} \right] \frac{\sin^2(\pi q)}{\pi T_K} \end{aligned} \quad (18.110)$$

Notice how it is the Kondo temperature that determines the size of these two quantities. The dimensionless ‘‘Wilson’’ ratio of these two quantities is

$$W = \left[\frac{(\pi k_B)^2}{(g\mu_B)^2 j(j+1)} \right] \frac{\Delta \chi}{\Delta \gamma} = 1$$

At finite N , fluctuations in the mean-field theory can no longer be ignored. These fluctuations induce interactions amongst the quasiparticles, and the Wilson ratio becomes

$$W = \frac{1}{1 - \frac{1}{N}}.$$

The dimensionless Wilson ratio of a large variety of heavy electron materials lies remarkably close to this value.

18.6 Mean-field theory of the Kondo Lattice

18.6.1 Diagonalization of the Hamiltonian

We can now make the jump from the single impurity problem to the lattice. The virtue of the large N method is that while approximate, it can be readily scaled up to the lattice. We'll now recompute the effective action for the lattice, using equation 18.69. Let us assume that the hybridization and constraint fields at the saddle point are uniform, with $V_j = V$ and $\lambda_j = \lambda$ at every site. Infact, even if we start with a $V_j = Ve^{-i\phi_j}$ with a different phase at each site, we can always use the Read Newns gauge transformation (18.56) to absorb the additional phase onto the f -electron field. We then have a translationally invariant mean-field Hamiltonian. We begin by rewriting the mean field Hamiltonian in momentum space as follows

$$\begin{aligned} H_{MFT} &= \sum_{\mathbf{k}\sigma} (c^\dagger_{\mathbf{k}\sigma}, f^\dagger_{\mathbf{k}\sigma}) \overbrace{\begin{pmatrix} \epsilon_{\mathbf{k}} & V \\ \bar{V} & \lambda \end{pmatrix}}^{\underline{h}(\mathbf{k})} \begin{pmatrix} c_{\mathbf{k}\sigma} \\ f_{\mathbf{k}\sigma} \end{pmatrix} + NN_s \left(\frac{|V|^2}{J} - \lambda q \right) \\ &= \sum_{\mathbf{k}\sigma} \psi^\dagger_{\mathbf{k}\sigma} \underline{h}(\mathbf{k}) \psi_{\mathbf{k}\sigma} + NN_s \left(\frac{|V|^2}{J} - \lambda q \right). \end{aligned} \quad (18.111)$$

Here, $f^\dagger_{\mathbf{k}\sigma} = \frac{1}{\sqrt{N_s}} \sum_j f^\dagger_{j\sigma} e^{i\mathbf{k}\cdot\mathbf{R}_j}$ is the Fourier transform of the f -electron field and we have introduced the two component notation

$$\psi_{\mathbf{k}\sigma} = \begin{pmatrix} c_{\mathbf{k}\sigma} \\ f_{\mathbf{k}\sigma} \end{pmatrix}, \quad \psi^\dagger_{\mathbf{k}\sigma} = (c^\dagger_{\mathbf{k}\sigma}, f^\dagger_{\mathbf{k}\sigma}), \quad \underline{h}(\mathbf{k}) = \begin{pmatrix} \epsilon_{\mathbf{k}} & V \\ \bar{V} & \lambda \end{pmatrix}. \quad (18.112)$$

We should think about H_{MFT} as a renormalized Hamiltonian, describing the low energy quasiparticles, moving through a self-consistently determined array of resonant scattering centers. Later, we will see that the f -electron operators are composite objects, formed as bound-states between spins and conduction electrons.

The mean-field Hamiltonian can be diagonalized in the form

$$H_{MFT} = \sum_{\mathbf{k}\sigma} (a^\dagger_{\mathbf{k}\sigma}, b^\dagger_{\mathbf{k}\sigma}) \begin{pmatrix} E_{\mathbf{k}^+} & 0 \\ 0 & E_{\mathbf{k}^-} \end{pmatrix} \begin{pmatrix} a_{\mathbf{k}\sigma} \\ b_{\mathbf{k}\sigma} \end{pmatrix} + Nn \left(\frac{\bar{V}V}{J} - \lambda q \right). \quad (18.113)$$

Here $a^\dagger_{\mathbf{k}\sigma} = u_{\mathbf{k}} c^\dagger_{\mathbf{k}\sigma} + v_{\mathbf{k}} f^\dagger_{\mathbf{k}\sigma}$ and $b^\dagger_{\mathbf{k}\sigma} = -v_{\mathbf{k}} c^\dagger_{\mathbf{k}\sigma} + u_{\mathbf{k}} f^\dagger_{\mathbf{k}\sigma}$ are linear combinations of $c^\dagger_{\mathbf{k}\sigma}$ and $f^\dagger_{\mathbf{k}\sigma}$, playing the role of “quasiparticle operators” with corresponding energy eigenvalues

$$\text{Det} \left[E_{\mathbf{k}\pm} \mathbb{1} - \begin{pmatrix} \epsilon_{\mathbf{k}} & V \\ \bar{V} & \lambda \end{pmatrix} \right] = (E_{\mathbf{k}\pm} - \epsilon_{\mathbf{k}})(E_{\mathbf{k}\pm} - \lambda) - |V|^2 = 0, \quad (18.114)$$

or

$$E_{\mathbf{k}\pm} = \frac{\epsilon_{\mathbf{k}} + \lambda}{2} \pm \left[\left(\frac{\epsilon_{\mathbf{k}} - \lambda}{2} \right)^2 + |V|^2 \right]^{\frac{1}{2}}, \quad (18.115)$$

and eigenvectors taking the BCS form

$$\begin{Bmatrix} u_{\mathbf{k}} \\ v_{\mathbf{k}} \end{Bmatrix} = \left[\frac{1}{2} \pm \frac{(\epsilon_{\mathbf{k}} - \lambda)/2}{2 \sqrt{\left(\frac{\epsilon_{\mathbf{k}} - \lambda}{2} \right)^2 + |V|^2}} \right]^{\frac{1}{2}}. \quad (18.116)$$

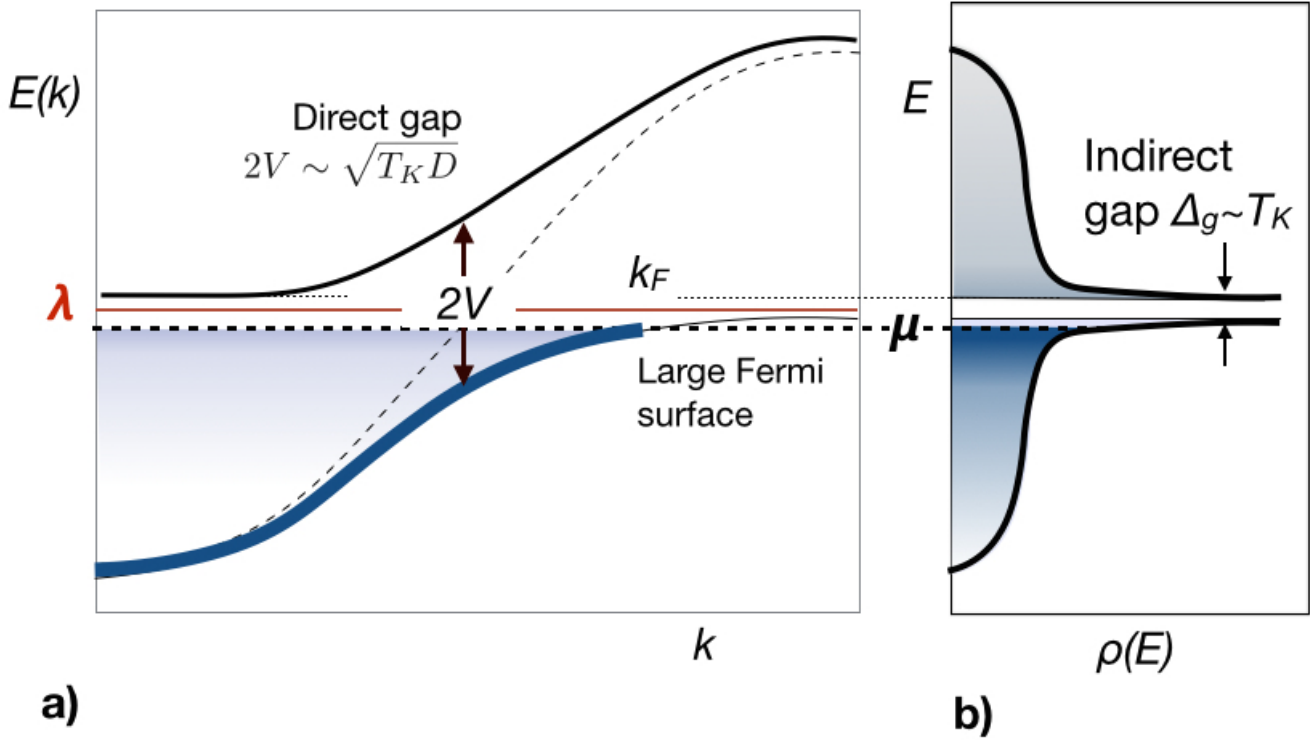


Fig. 18.9 (a) Dispersion for the Kondo lattice mean field theory. (b) Renormalized density of states, showing “hybridization gap” (Δ_g).

The hybridized dispersion described by these energies is shown in Fig. 18.9.

Note that:

- Hybridization builds an upper and lower band, separated by a direct “hybridization gap” of size $2V$ and a much smaller indirect gap. If we put $\epsilon_{\mathbf{k}} = \pm D$, we see that the upper and lower edges of the gap are given by

$$E^{\pm} = \frac{\mp D + \lambda}{2} \pm \sqrt{\left(\frac{\mp D - \lambda}{2}\right)^2 + V^2} \approx \lambda \pm \frac{V^2}{D}, \quad (D \gg \lambda) \quad (18.117)$$

so the indirect gap has a size $\Delta_g \sim 2V^2/D$, where D is the half-bandwidth. From our mean-field solution to the Kondo impurity problem, we can anticipate $V^2/D \sim V^2\rho \sim T_K$, so that $\Delta_g \sim T_K$, the single ion Kondo temperature, which implies that $V \sim \sqrt{T_K D}$.

- In the special case when the chemical potential lies in the gap, a Kondo insulator is formed.
- The effective mass of the Fermi surface is opposite to the conduction sea, so a conduction sea of electrons is transformed into a heavy Fermion sea of holes.
- The Fermi surface volume expands in response to the formation of heavy electrons (see Fig. 18.10). The

enlarged Fermi surface volume now counts the total number of occupied quasiparticle states

$$N_{tot} = \left\langle \sum_{k\lambda\sigma} n_{k\lambda\sigma} \right\rangle = \langle \hat{n}_f + \hat{n}_c \rangle \quad (18.118)$$

where $n_{k\lambda\sigma} = a_{k\lambda\sigma}^\dagger a_{k\lambda\sigma}$ is the number operator for the quasiparticles and n_c is the total number of conduction electrons. This means

$$N_{tot} = N \frac{V_{FS} a^3}{(2\pi)^3} = Q + n_c, \quad (18.119)$$

where a^3 is the volume of the unit cell. This is rather remarkable, for the expansion of the Fermi surface implies an increased charge density in the Fermi sea. Since charge is conserved, we are forced to conclude there is a compensating $+Q|e|$ charge density per unit cell provided by the Kondo singlets formed at each site, as illustrated in Fig. 18.10.

- We can construct the mean-field ground-state from the quasiparticle operators as follows:

$$|MF\rangle = \prod_{|\mathbf{k}| < k_F \sigma} b_{\mathbf{k}\sigma}^\dagger |0\rangle = \prod_{|\mathbf{k}| < k_F \sigma} (-v_{\mathbf{k}} c_{\mathbf{k}\sigma} + u_{\mathbf{k}} f_{\mathbf{k}\sigma}^\dagger) |0\rangle. \quad (18.120)$$

However, this state only satisfies the constraint on the average. We can improve it by imposing the constraint, forming a ‘‘Gutzwiller’’ wavefunction[?, ?, ?]

$$|GW\rangle = P_Q \prod_{|\mathbf{k}| < k_F \sigma} (-v_{\mathbf{k}} c_{\mathbf{k}\sigma} + u_{\mathbf{k}} f_{\mathbf{k}\sigma}^\dagger) |0\rangle, \quad (18.121)$$

where, using (18.48)

$$P_Q = \prod_j P_Q(j) = \int_0^{2\pi} \prod_j \frac{d\alpha_j}{2\pi} e^{i \sum_j \alpha_j (\hat{n}_{fj} - Q)}. \quad (18.122)$$

The action of the constraint gives rise to a highly incompressible Fermi liquid, in which the compressibility is far smaller than the density of states.

18.6.2 Mean Field Free Energy and Saddle point

Let us now use the results of the last section to calculate the mean-field free energy F_{MFT} and determine, self-consistently the parameters λ and V which set the scales of the Kondo lattice. Using 18.69 we obtain

$$F_{MF} = -NT \sum_{\mathbf{k}, i\omega_r} \text{Tr} \ln \left[\overbrace{-i\omega_r + \begin{pmatrix} \epsilon_{\mathbf{k}} & V \\ V & \lambda \end{pmatrix}}^{-\mathcal{G}_{\mathbf{k}}^{-1}(i\omega_r)} \right] + \mathcal{N}_s \left(\frac{N|V|^2}{J} - \lambda Q \right), \quad (18.123)$$

where \mathcal{N}_s is the number of sites in the lattice. Note that translational invariance means that momentum is conserved and the Green’s function is diagonal in momentum, so we can re-write the trace over the momentum as a sum over \mathbf{k} . Let us remind ourselves of the steps taken between (18.69) and (18.70). We begin by re-writing the trace of the logarithm as a determinant, which we then factorize in terms of the energy eigenvalues,

$$\begin{aligned} \text{Tr} \ln \left[-i\omega_r \underline{1} + \begin{pmatrix} \epsilon_{\mathbf{k}} & V \\ V & \lambda \end{pmatrix} \right] &= \ln \det \left[-z \underline{1} + \begin{pmatrix} \epsilon_{\mathbf{k}} & V \\ V & \lambda \end{pmatrix} \right] = \ln \left[\overbrace{(\epsilon_{\mathbf{k}} - i\omega_r)(\lambda - i\omega_r) - V^2}^{(E_{\mathbf{k}+} - i\omega_r)(E_{\mathbf{k}-} - i\omega_r)} \right] \\ &= \sum_{n=\pm} \ln(E_{\mathbf{k}n} - i\omega_r). \end{aligned} \quad (18.124)$$

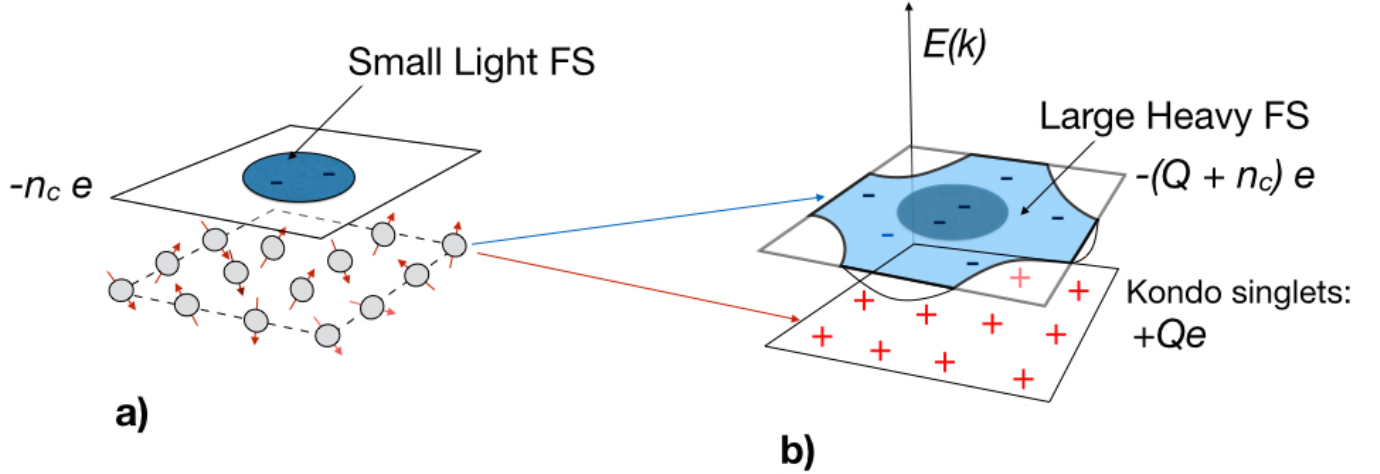


Fig. 18.10 (a) High temperature state: small Fermi surface with a background of spins; (b) Low temperature state where large Fermi surface develops against a background of positive charge. Each spin “ionizes” into Q heavy electrons, leaving behind a background of Kondo singlets, each with charge $+Qe$.

Next, by carrying out the summation over Matsubara frequencies, using the result $-T \sum_{i\omega_r} \ln(E_{k\mathbf{n}} - i\omega_r) = -T \ln(1 + e^{-\beta E_{k\mathbf{n}}})$, we obtain

$$\frac{F}{N} = -T \sum_{\mathbf{k}, \pm} \ln \left[1 + e^{-\beta E_{\mathbf{k}\pm}} \right] + N_s \left(\frac{V^2}{J} - \lambda q \right). \quad (18.125)$$

Let us discuss the ground-state, in which only the lower-band contributes to the Free energy. As $T \rightarrow 0$, we can replace $-T \ln(1 + e^{-\beta E_{\mathbf{k}}}) \rightarrow \theta(-E_{\mathbf{k}})E_{\mathbf{k}}$, so the ground-state energy $E_0 = F(T = 0)$ involves an integral over the occupied states of the lower band:

$$\frac{E_0}{NN_s} = \int_{-\infty}^0 dE \rho^*(E) E + \left(\frac{V^2}{J} - \lambda q \right) \quad (18.126)$$

where we have introduced the density of heavy electron states $\rho^*(E) = \sum_{\mathbf{k}, \pm} \delta(E - E_{\mathbf{k}}^{(\pm)})$. Now by (18.114) the relationship between the energy E of the heavy electrons and the energy ϵ of the conduction electrons is

$$E = \epsilon + \frac{V^2}{E - \lambda}.$$

As we sum over momenta \mathbf{k} within a given energy shell, there is a one-to-one correspondence between each conduction electron state and each quasiparticle state, so we can write $\rho^*(E)dE = \rho(\epsilon)d\epsilon$, where the density of heavy electron states

$$\rho^*(E) = \rho \frac{d\epsilon}{dE} = \rho \left(1 + \frac{V^2}{(E - \lambda)^2} \right). \quad (18.127)$$

Here we have approximated the underlying conduction electron density of states by a constant $\rho = 1/(2D)$. The originally flat conduction electron density of states is now replaced by a “hybridization gap”, flanked by

two sharp peaks of width approximately $\pi\rho V^2 \sim T_K$ (Fig. 18.9). Note that the lower band-width is lowered by an amount $-V^2/D$. With this information, we can carry out the integral over the energies, to obtain

$$\frac{E_o}{NN_s} = \rho \int_{-D-V^2/D}^0 dE E \left(1 + \frac{V^2}{(E-\lambda)^2} \right) + \left(\frac{V^2}{J} - \lambda q \right) \quad (18.128)$$

where we have assumed that the upper band is empty, and the lower band is partially filled. Carrying out the integral we obtain

$$\begin{aligned} \frac{E_o}{NN_s} &= -\frac{\rho}{2} \left(D + \frac{V^2}{D} \right)^2 + \frac{\Delta}{\pi} \int_{-D}^0 dE \left(\frac{1}{E-\lambda} + \frac{\lambda}{(E-\lambda)^2} \right) + \left(\frac{V^2}{J} - \lambda q \right) \\ &= -\frac{D^2\rho}{2} + \frac{\Delta}{\pi} \ln \left(\frac{\lambda}{D} \right) + \left(\frac{V^2}{J} - \lambda q \right) \end{aligned} \quad (18.129)$$

where we have replaced $\Delta = \pi\rho V^2$ and have dropped terms of order $O(\Delta^2/D)$. We can rearrange this expression, absorbing the band-width D and Kondo coupling constant into a single Kondo temperature $T_K = De^{-\frac{1}{\rho}}$ as follows

$$\begin{aligned} \frac{E_o}{NN_s} &= -\frac{D^2\rho}{2} + \frac{\Delta}{\pi} \ln \left(\frac{\lambda}{D} \right) + \left(\frac{\pi\rho V^2}{\pi\rho J} - \lambda q \right) \\ &= -\frac{D^2\rho}{2} + \frac{\Delta}{\pi} \ln \left(\frac{\lambda}{D} \right) + \left(\frac{\Delta}{\pi\rho J} - \lambda q \right) \\ &= -\frac{D^2\rho}{2} + \frac{\Delta}{\pi} \ln \left(\frac{\lambda}{De^{-\frac{1}{\rho}}} \right) - \lambda q \\ &= -\frac{D^2\rho}{2} + \frac{\Delta}{\pi} \ln \left(\frac{\lambda}{T_K} \right) - \lambda q. \end{aligned} \quad (18.130)$$

This describes the energy of a whole scaling trajectory of Kondo lattice models with different $J(D)$ and cutoff D , but fixed Kondo temperature. If we impose the constraint $\frac{\partial E_o}{\partial \lambda} = \langle n_f \rangle - Q = 0$ we obtain $\frac{\Delta}{\pi\lambda} - q = 0$, so

$$\frac{E_o(V)}{NN_s} = \frac{\Delta}{\pi} \ln \left(\frac{\Delta}{\pi q e T_K} \right) - \frac{D^2\rho}{2}, \quad (\Delta = \pi\rho|V|^2) \quad (18.131)$$

Let us pause for a moment to consider this energy functional qualitatively. There are two points to be made

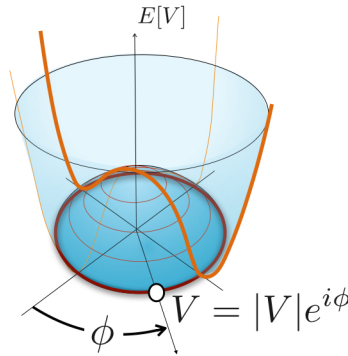


Fig. 18.11 Mexican hat potential for the Kondo Lattice, evaluated at constant $\langle n_f \rangle = Q$ as a function of a complex hybridization $V = |V|e^{i\phi}$

- The energy surface $E_0(V)$ is actually independent of the phase of $V = |V|e^{i\phi}$ (see Fig. 18.11), and has the form of “Mexican Hat” at low temperatures. The minimum of this functional will then determine a family of saddle point values $V = |V_o|e^{i\phi}$, where ϕ can have any value. If we differentiate the ground-state energy with respect to Δ , we obtain

$$0 = \frac{1}{\pi} \ln \left(\frac{\Delta}{\pi q T_K} \right)$$

or

$$\Delta = \pi q T_K$$

confirming that $\Delta \sim T_K$.

- The mean-field value of the constraint field λ is determined relative to the Fermi energy μ . Were we to introduce a slowly varying external potential field to the conduction electron sea, then the chemical potential becomes locally shifted so that $\mu \rightarrow \mu + e\phi(t)$. So long as the field $\phi(t)$ is varied at a rate slowly compared with the Kondo temperature, the constraint field will always track with the chemical potential, and since the constraint field is pinned to the chemical potential, $\lambda \rightarrow \lambda + e\phi(t)$. In the process, the constraint term will become

$$\lambda(\hat{n}_f(j) - Q) \rightarrow \lambda(\hat{n}_f(j) - Q) + e\phi(t)(\hat{n}_f(j) - Q). \quad (18.132)$$

Since the f-electrons now couple to the external potential $e\phi$ we have to ascribe a physical charge $e = -|e|$ to them. By contrast, the $-Q$ term in the constraint must be interpreted as a “background positive charge” $|e|Q \equiv |e|$ per site. These lines of reasoning indicate that we should think of the Kondo effect as an **many-body ionization phenomenon** in which the neutral local moment splits up into a negatively charged heavy electron and a stationary positive background charge we can associate with the formation of a Kondo singlet.

18.6.3 Kondo Lattice Green’s Function

Lets now take a look at the matrix Green’s function, given by

$$\mathcal{G}_{\mathbf{k}}(\tau) = -\langle \psi_{\mathbf{k}\sigma}(\tau) \psi_{\mathbf{k}\sigma}^\dagger(0) \rangle \equiv \begin{bmatrix} G_c(\mathbf{k}, \tau) & G_{cf}(\mathbf{k}, \tau) \\ G_{fc}(\mathbf{k}, \tau) & G_f(\mathbf{k}, \tau) \end{bmatrix} \quad (18.133)$$

where $G_c(\mathbf{k}, \tau) = -\langle c_{\mathbf{k}}(\tau) c_{\mathbf{k}\sigma}^\dagger(0) \rangle$, $G_{cf}(\mathbf{k}, \tau) = -\langle c_{\mathbf{k}}(\tau) f_{\mathbf{k}\sigma}^\dagger(\tau) \rangle$ and so on. The anomalous off-diagonal members of this Green’s function remind us of the Gork’ov functions in BCS theory, and develop with the coherent hybridization. Using the two component notation (18.112), and the results of Chapter 13.4.3, this Green’s function can be written

$$\mathcal{G}_{\mathbf{k}}(\tau) = -(\partial_\tau + \underline{h}_{\mathbf{k}})^{-1} \xrightarrow{\text{F.T.}} \mathcal{G}_{\mathbf{k}}(z) = (z - \underline{h}_{\mathbf{k}})^{-1} \quad (18.134)$$

or more explicitly,

$$\begin{aligned} \mathcal{G}_{\mathbf{k}}(z) = (z - \underline{h}_{\mathbf{k}})^{-1} &= \begin{pmatrix} z - \epsilon_{\mathbf{k}} & -V \\ -V & z - \lambda \end{pmatrix}^{-1} = \begin{pmatrix} G_c(\mathbf{k}, z) & G_{cf}(\mathbf{k}, z) \\ G_{fc}(\mathbf{k}, z) & G_f(\mathbf{k}, z) \end{pmatrix} \\ &= \frac{1}{(z - \epsilon_{\mathbf{k}})(z - \lambda) - V^2} \begin{pmatrix} z - \lambda & V \\ V & z - \epsilon_{\mathbf{k}} \end{pmatrix}, \end{aligned} \quad (18.135)$$

where we have taken the liberty of analytically extending $i\omega_r \rightarrow z$ into the complex plane. Now we can read off the Green's functions. In particular, the "hybridized" conduction electron Green's function is

$$G_c(\mathbf{k}, z) = \text{---} \blacktriangleright \text{---} = \frac{z - \lambda}{(z - \epsilon_{\mathbf{k}})(z - \lambda) - V^2}$$

$$= \frac{1}{z - \epsilon_{\mathbf{k}} - \frac{V^2}{z - \lambda}} \equiv \frac{1}{z - \epsilon_{\mathbf{k}} - \Sigma_c(z)} \quad (18.136)$$

which we can interpret physically as conduction electrons scattering off resonant f-states at each site, giving rise to a momentum-conserving self energy

$$\Sigma_c(z) = \text{---} \bullet \text{---} \text{---} \blacktriangleright \text{---} \bullet \text{---} = \frac{V^2}{z - \lambda}, \quad (18.137)$$

$O(1)$

We can this process as a pole at energy $z = \lambda$ in the conduction t-matrix. We shall argue later that this pole represents the formation of a composite fermion. A similar process occurs in the impurity Kondo model, but in that case the scattering is local, and connects all wavevectors, whereas in the lattice, coherence implies momentum is conserved. Notice that the denominator in each of the Green's functions involves the same quasiparticle poles, since $(z - \epsilon_{\mathbf{k}})(z - \lambda) - V^2 = (z - E_{\mathbf{k}}^+)(z - E_{\mathbf{k}}^-)$, and hence near the Fermi surface, at $E_{\mathbf{k}_F} = 0$ conduction Green's function can be written

$$G_c(z \sim E_{\mathbf{k}}) = \frac{Z_{\mathbf{k}}}{z - E_{\mathbf{k}}} \quad (18.138)$$

where

$$Z_{\mathbf{k}} = (1 - \partial_z \Sigma_c(z))^{-1} |_{z=0} = \frac{1}{1 + \frac{V^2}{\lambda^2}} \sim \frac{T_K}{D} \sim \frac{m}{m^*} \ll 1 \quad (18.139)$$

where we have identified the scales $V^2/D \sim T_K$ (hence $V^2 \sim DT_K$) and $\lambda \sim T_K$ with the single ion Kondo temperature. We see that the strength of the quasiparticle pole in the conduction electrons, related to the mass renormalization, is very small.

Similarly, the f-Green's function is

$$G_f(\mathbf{k}, z) = \text{===} \blacktriangleright \text{===} = \frac{z - \epsilon_{\mathbf{k}}}{(z - \epsilon_{\mathbf{k}})(z - \lambda) - V^2} = \frac{1}{i\omega_r - \lambda - \frac{V^2}{z - \epsilon_{\mathbf{k}}}}. \quad (18.140)$$

Finally, the "anomalous" Green's functions are given by

$$G_{cf}(\mathbf{k}, z) = \text{===} \blacktriangleright \bullet \text{---} = \frac{1}{z - \epsilon_{\mathbf{k}}} V G_f(\mathbf{k}, i\omega_n) = \frac{V}{(z - \epsilon_{\mathbf{k}})(z - \lambda) - V^2}, \quad (18.141)$$

which we can interpret as the result of hybridization. We will return to use these expressions to calculate the low energy part of the tunneling spectrum.

18.7 The composite nature of the f-electron

18.7.1 A Thought experiment: a Kondo lattice of nuclear spins

In electronic materials the Kondo effect involves localized f or d electrons. However, a Kondo effect could occur equally well with a nuclear spin. This might seem absurd, yet nuclear spins do couple antiferromagnetically with conduction electrons to produce RKKY interactions that drive of nuclear antiferromagnetism. In practice the coupling is far too small to destabilize the nuclear magnetism and produce a nuclear Kondo effect, nevertheless, we learn something from the thought experiment in which the the nuclear spin coupling to electrons is is strong enough to overcome the nuclear magnetism. In this case, resonant bound-states would form with the nuclear spin lattice giving rise to *charged* heavy electrons, presumably with an expanded Fermi surface.

From this line of argument we see that while it's tempting to associate the heavy fermion in the Kondo effect with a physical f- or d- electron localized inside the local moment, from a renormalization group perspective, the heavy electron is an emergent excitation: a fermionic bound-state formed between the conduction sea and the neutral localized moments. The only memory of the underlying localized electrons is encoded in the spatial symmetry of the Kondo coupling, which of course for rare earth systems, is an f-form factor.

The composite picture of heavy electrons is useful because

- As we will see in section (18.8) it allows us to understand the formation of Fano resonant structures in Kondo lattices.
- It allows us to envisage processes in which the Kondo effect breaks-down, leading to the loss of the large Fermi surface. Such “Kondo breakdown” phenomenon are thought to be the origin of certain types of non-Fermi liquid behavior in heavy electron systems.
- It opens up the possibility of new kinds of composite structures - bosons that might pair condense - or composite fermions with different quantum numbers to electrons, such as neutral, spinless or integer spin fermions.

18.7.2 Cooper pair analogy

There is a nice analogy with superconductivity which helps to understand the both the Kondo impurity and Kondo lattice effect. In a superconductor, electron pairs behave as loose composite bosons described by the relation

$$\overline{\psi_{\uparrow}(x)\psi_{\downarrow}(x')} = -F(x - x'). \quad (18.142)$$

Here $F(x - x') = -\langle T\psi_{\uparrow}(1)\psi_{\downarrow}(2) \rangle$ is the anomalous Gor'kov Greens function which determines the Cooper pair wavefunction, extended over the coherence length $\xi \sim v_F/T_c$. We can treat the pair operator as a c-number because the pairs condense.

A similar phenomenon takes place in the Kondo effect, but here the bound-state develops between spins and electrons, forming a fermion, rather than a boson. For an isolated Kondo impurity, the analog of the coherence length in the superconductor is the “Kondo screening length” $\xi_K \sim v_F/T_K$, but in a lattice the renormalization of the heavy fermion velocity means that this screening length is of the order of a lattice spacing. In this situation, it is perhaps more useful to think in terms of a screening time $\tau_K \sim \hbar/T_K$, rather than a length, governing the electron spin-flip correlations. Both the Cooper pair and heavy electron involve

electrons that span decades of energy up to a cutoff, be it the Debye energy ω_D in superconductivity or the (much larger) bandwidth D in the Kondo effect [32, 33].

To follow this analogy in greater depth, recall that in the path integral the Kondo interaction factorizes as

$$\frac{J}{N} c^\dagger_\beta S_{\alpha\beta} c_\alpha \rightarrow \bar{V} (c^\dagger_\alpha f_\alpha) + (f^\dagger_\alpha c_\alpha) V + N \frac{\bar{V}V}{J}, \quad (18.143)$$

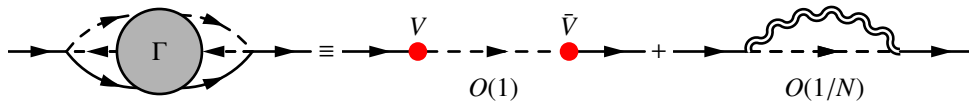
so by comparing the right and left hand side, we see that the composite operators $S_{\beta\alpha} c_\beta$ and $c^\dagger_\beta S_{\alpha\beta}$ behave as a single fermion denoted by the contractions:

$$\frac{1}{N} \sum_\beta \overline{S_{\beta\alpha} c_\beta} = \left(\frac{\bar{V}}{J}\right) f_\alpha, \quad \frac{1}{N} \sum_\beta c^\dagger_\beta \overline{S_{\alpha\beta}} = \left(\frac{V}{J}\right) f^\dagger_\alpha, \quad (18.144)$$

Composite Fermion

Physically, this means that the spins bind high energy electrons, transforming themselves into composites which then hybridize with the conduction electrons. The resulting “heavy fermions” can be thought of as moments ionized in the magnetically polar electron fluid to form mobile, negatively charged heavy electrons while leaving behind a positively charged “Kondo singlet”.

Microscopically, the many body amplitude to scatter an electron off a local moment develops a bound-state pole, which for large N we can denote by the diagrams:



The leading diagram describes a kind of “condensation” of the hybridization field; the second and higher terms describe the smaller $O(1/N)$ fluctuations around the mean-field theory.

The temporal correlations between spin-flips and conduction electrons extend over a finite time, described by the contraction

$$\frac{1}{N} \sum_\beta \overline{c_\beta(\tau) S_{\beta\alpha}(\tau')} = g(\tau - \tau') \hat{f}_\alpha(\tau'). \quad (18.145)$$

Here the spin-flip correlation function $g(\tau - \tau')$ is an analogue of the Gor'kov function, extending out to a coherence time $\tau_K \sim \hbar/T_K$. Notice that in contrast to the Cooper pair, this composite object is a fermion and thus requires a distinct operator \hat{f}_α for its expression. The Fourier (Laplace) decomposition of $g(\tau)$ describes the Spectral distribution of electrons and spin-flips inside the composite f-electron which we may calculate as follows:

$$\begin{aligned} \frac{1}{N} \sum_\beta \overline{c_\beta(\tau) S_{\beta\alpha}(\tau')} &= \frac{1}{N} \sum_\beta \overline{c_\beta(\tau) f^\dagger_\beta(\tau') f_\alpha(\tau')} \\ &= \frac{1}{N} \sum_\beta \langle T c_\beta(\tau) f^\dagger_\beta(\tau') \rangle f_\alpha(\tau') \end{aligned}$$

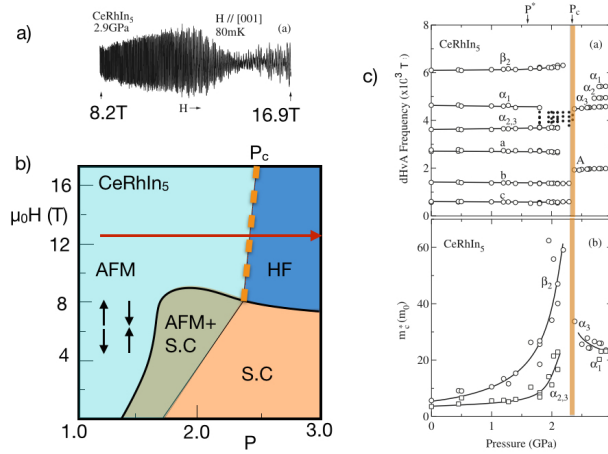
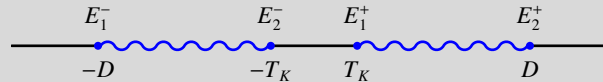


Fig. 18.12

(a) de Haas van Alphen signal [34], made as a function of pressure along the path delineated by the red arrow. (b) Schematic zero temperature pressure-field phase diagram for CeRhIn₅, showing antiferromagnetic, superconducting and heavy fermion regions of the phase diagram, adapted from [35]. (c) Showing the frequency measured in Haas van Alphen measurements on CeRhIn₅ after [34], which is a measure of the Fermi surface area of an extremal orbit. The data showing the jump in Fermi surface area at the critical pressure where antiferromagnetism disappears and a corresponding divergence in effective mass.

This function contains two branch cuts along the real-axis, corresponding to the upper and lower bands, which run from $E_1^\pm \rightarrow E_2^\pm$, where $(E_{1,2}^\pm \pm D)(E_{1,2}^\pm - \lambda) - V^2 = 0$. The low energy ends of the branch cut $|E_2^\pm| \sim |E_1^\pm| \sim V^2/D \sim T_K$ are of order the Kondo scale, whereas the high energy ends $|E_1^\pm| \sim |E_2^\pm| \sim D$ are set by the band-width.



There are thus two energy scales in this function - the bandwidth D and the Kondo temperature $T_K \sim \lambda$. The internal structure of the composite fermion is thus determined by the spectral function

$$g(\omega) = -\frac{1}{\pi} \text{Im} G_{cf}(\omega - i\delta) = -\frac{\rho V}{\omega - \lambda} \sum_{\pm} [\theta(\omega - E_1^\pm) - \theta(\omega - E_2^\pm)], \quad (18.153)$$

as shown in Fig (18.13).

In the time domain

$$g(\tau) = -\int_{-\infty}^{\infty} d\omega g(\omega) [(1 - f(\omega))\theta(\tau) - f(\omega)\theta(-\tau)] e^{-\omega\tau}. \quad (18.154)$$

For simplicity, let's examine the case where the Fermi energy is in the lower band ($\lambda > 0$). Now by

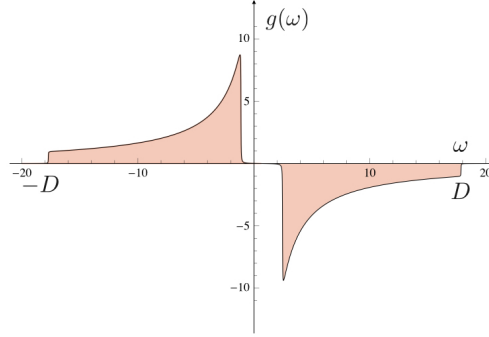


Fig. 18.13 Spectral distribution function $g(\omega)$ (18.153) describing the internal correlations of spin and electron inside a composite f-electron. See example 18.5.

(18.149) and (18.144), the bound-state amplitude V is given by the equal time Green's function,

$$\frac{V}{J} = g(0^-) = -V\rho \int_{-D}^0 \frac{d\omega}{\omega - \lambda} = \rho V \ln \frac{D}{\lambda} \quad (18.155)$$

from which we deduce

$$\frac{V}{J} = \rho V \ln \frac{D}{\lambda} \Rightarrow \lambda = D e^{-\frac{1}{J\rho}} = T_K \quad (18.156)$$

as obtained earlier from the minimization of the energy. Note that argument in the bound-state integral (18.155) depends on the inverse of the energy, right out to the band-width. If we divide the band on a logarithmic scale into n equal parts, where the ratio of the lower and upper energies is $s > 1$, we see that that each decade of energy counts equally to the bound-state amplitude

$$\begin{aligned} \frac{V}{J} &= -\rho V \int_{-D}^{-\lambda} d\epsilon \frac{1}{\epsilon} = -\rho V \left\{ \int_{-D}^{-D/s} + \int_{-D/s}^{-D/s^2} + \dots + \int_{-D/s^{n-1}}^{-\lambda} \right\} \frac{d\epsilon}{\epsilon} \\ &= \rho V \left\{ \ln s + \ln s + \dots + \ln \frac{D s^{-n+1}}{\lambda} \right\}, \end{aligned} \quad (18.157)$$

demonstrating that the low energy heavy fermion bound-state is formed from electron states that are spread out over decades of energy out to the band-width.

Finally, returning to the time dependence,

$$g(\tau) = - \int_{-D}^0 d\omega \frac{\overbrace{V\rho}^{-g(\omega)}}{\omega - \lambda} e^{-\omega\tau}, \quad (\tau < 0) \quad (18.158)$$

we see that there are two main frequency domains in

$$g(\omega) \sim \begin{cases} -\frac{1}{\omega} & (D \gg \omega \gg T_K), \\ \frac{1}{T_K} & (\omega \ll T_K). \end{cases} \quad (18.159)$$

Either by dimensional analysis, ($[\int \frac{d\omega}{\omega}] \sim [\tau^0] \sim \text{Log}[\tau]$, $[\int d\omega e^{-\omega\tau}] \sim \frac{1}{\tau}$) we then obtain

$$g(\tau) \sim \begin{cases} \rho V \ln \left(\frac{T_K \tau}{\hbar} \right) & (\hbar/D \ll \tau \ll \hbar/T_K) \\ \frac{1}{\tau} & (\tau \gg \hbar/T_K) \end{cases} \quad (18.160)$$

so that up to the Kondo time \hbar/T_K the correlations are logarithmic in time, but beyond this time-scale, they decay more rapidly with the inverse of the time.

18.8 Tunneling into Heavy Electron Fluids

The composite nature of heavy electrons allows us to understand the mechanism by which electrons tunnel into a Kondo lattice. How do electrons tunnel into a Kondo lattice? Since direct tunneling into localized magnetic orbitals is prevented by the Coulomb blockade, the naive expectation is that electrons only tunnel into the conduction sea. In fact, this is not the case, for a new tunneling process, that of “cotunneling” also permits the conduction electrons to directly interconvert into composite heavy fermions. In short, though electrons can not directly tunnel into f-states, quantum mechanics allows them to virtually hop on and then hop off the f-site, exchanging their spin, and this process gives rise to a Kondo exchange process between the tunneling tip and the Kondo lattice, given heuristically by

$$H_{cotunnel} \sim \frac{t_{tip}\mathcal{V}_0}{U} [(c^\dagger_{0\sigma'} f_{0\sigma})(f^\dagger_{0\sigma} p_{0\sigma}) + \text{H.c}] \quad (18.161)$$

where \mathcal{V}_0 and t_{tip} are the hybridization between the the f-state on the surface at position 0 and the conduction and tip electrons, respectively. Here $p_{0\sigma}$ destroys an electron in the tip and $c^\dagger_{0\sigma}$ creates an electron directly beneath it in the conduction sea of the Kondo lattice.

In the 1960s Anderson and Appelbaum [36, 37, 38], working at Bell Labs, New Jersey, recognized that magnetic ions actively participate in electron tunneling via a process we now call “cotunneling”[39, 40], in which the electron tunnelling via the localized f-state induces a spin-flip of localized moments. Cotunneling occurs when electrons tunnel into magnetic quantum dots or isolated magnetic atoms adsorbed on surfaces [39, 40, 41, 42]. One of its most notable consequences, is the formation of a “Fano” resonance[43], created via an interference between the direct and cotunneling processes[44]. This same physics occurs when electrons tunnel into Kondo lattices. The first scanning tunneling experiments into Kondo lattices were carried out in 2010 by the Séamus Davis group working at Cornell University[45] using scanning tunneling electron microscopy (STM) and has since been used to visualize hybridized heavy bands in Kondo lattice systems[46].

18.8.1 The Cotunneling Hamiltonian

Cotunneling can be understood as a result of quantum mechanical mixing between states in the tunneling tip and the localized orbitals of the Kondo lattice[47]. When a tip is introduced above site 0 on the surface of the lattice, tunneling between the f -state and the probe electrons modifies the hybridization as follows

$$\mathcal{V}_0 (c^\dagger_{0\sigma} f_{0\sigma} + \text{H.c}) \rightarrow (\mathcal{V}_0 c^\dagger_{0\sigma} + t_f p^\dagger_{0\sigma}) f_{0\sigma} + \text{H.c.}, \quad (18.162)$$

where \mathcal{V}_0 is the bare hybridization, $p^\dagger_{0\sigma}$ creates an electron at the tip of the probe and t_f is the amplitude to tunnel an f to the probe². In this way the orbital hybridizing with the f -state is modified as follows:

$$c_{0\sigma} \rightarrow c_{0\sigma} + \frac{t_f}{\mathcal{V}_0} p_{0\sigma}. \quad (18.163)$$

Now to follow the effect of this mixing on the low energy Hamiltonian, we need to carry out a Schrieffer Wolff transformation.

To follow the effect of this mixing on the Kondo lattice model, we need to carry out a Schrieffer-Wolff transformation on an Anderson model for the lattice and tunneling tip [48, 38, 40]. When we integrate out the

² Note that in this section we have adopted a caligraphic V to denote the hybridization to avoid confusion between hybridization and the bias voltage V .

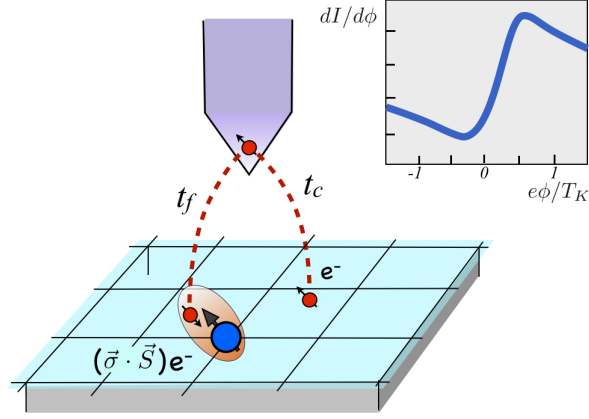


Fig. 18.14 Electron tunneling into a heavy-fermion material involves two parallel processes: direct tunneling with amplitude t_c into the conduction sea, and cotunneling with amplitude t_f into a composite combination of the conduction electron and local magnetic f -moments. These composite states are expected to develop coherence below the Kondo temperature T_K . Inset shows a typical differential conductance curve observed for tunneling into a single Kondo ion.

high energy valence fluctuations to obtain a Kondo model using a Schrieffer Wolff transformation (see section 17.6). this same replacement must be made in the Kondo interaction at site 0. The result of this procedure is then

$$\begin{aligned}
 H_K(0) &\rightarrow -J_K \left[\left(c_{0\alpha}^\dagger + \frac{t_f}{\mathcal{V}_0} p_{0\alpha}^\dagger \right) f_{0\alpha} \right] \left[f_{0\beta}^\dagger \left(c_{0\beta} + \frac{t_f}{\mathcal{V}_0} p_{0\beta} \right) \right] \\
 &= H_K(0) - \tilde{t}_f \left[(p_{0\alpha}^\dagger f_{0\alpha})(f_{0\beta}^\dagger c_{0\beta}) + \text{H.c.} \right] + O\left(\frac{\tilde{t}_f^2}{\mathcal{V}^2}\right) \\
 &\equiv H_K(0) + \tilde{t}_f \left[p_{0\alpha}^\dagger \left(\vec{\sigma}_{\alpha\beta} \cdot \vec{S}_f(0) - \frac{1}{2} \delta_{\alpha\beta} \right) c_{0\beta} + \text{H.c.} \right] + O\left(\frac{\tilde{t}_f^2}{\mathcal{V}^2}\right). \quad (18.164)
 \end{aligned}$$

where $\tilde{t}_f = Jt_f/\mathcal{V}$ and we have used the identity $f_\alpha f_\beta^\dagger = \frac{1}{2} \delta_{\alpha\beta} - \vec{S} \cdot \vec{\sigma}_{\alpha\beta}$ ³, and we have dropped terms of order \tilde{t}_f^2 . The spin-dependent part of the second term is the ‘‘cotunneling’’ term describing correlated spin-flip tunneling. When we add the cotunneling and the direct tunneling together, the complete Hamiltonian becomes

$$H = H_{KL} + \sum_{\mathbf{k}} \epsilon_{\mathbf{k}} p_{\mathbf{k}\sigma}^\dagger p_{\mathbf{k}\sigma} + H_T \quad (18.165)$$

where $p_{\mathbf{k}\sigma}^\dagger$ creates a Bloch wave of momentum \mathbf{k} in the tunneling tip,

$$H_T = t_c \hat{p}_{0\alpha}^\dagger \left[c_{0\alpha} + \frac{\tilde{t}_f}{t_c} \left(\vec{\sigma}_{\alpha\beta} \cdot \vec{S}_f(0) \right) c_{0\beta} \right] + \text{H.c.}, \quad (18.166)$$

describes the direct and co-tunneling contributions to the tunneling Hamiltonian, and $p_{0\alpha}^\dagger = \frac{1}{N_s^{1/2}} \sum_{\mathbf{k}} p_{\mathbf{k}\alpha}^\dagger$

³ When we decompose $f_\alpha f_\beta^\dagger = \hat{m}_0 \delta_{\alpha\beta} + \vec{m} \cdot \vec{\sigma}_{\alpha\beta}$, then we find $m_0 = \frac{1}{2} [f_\alpha f_\beta^\dagger \delta_{\beta\alpha}] = \frac{1}{2} (2 - n_f) = \frac{1}{2}$ while $\vec{m} = \frac{1}{2} f_\alpha f_\beta^\dagger \vec{\sigma}_{\beta\alpha} = -\frac{1}{2} f_\alpha^\dagger f_\beta \vec{\sigma}_{\beta\alpha} = -\vec{S}$.

creates an electron at the tip of the tunneling probe. In other words, to take into account the cotunneling, formally, all we have to do is to replace the field $c_{0\sigma}$ in the conduction sea by the composite $\psi_{0\sigma}$ as follows:

$$c_{0\sigma} \rightarrow \psi_{0\sigma} = \left[c_{0\sigma} + \left(\frac{\tilde{t}_f}{t_c} \right) (\vec{\sigma}_{\alpha\beta} \cdot \vec{S}_f(0)) c_{0\beta} \right]. \quad (18.167)$$

The additional composite component modifies the tunneling current, and the two components interfere with one-another to produce ‘‘Fano-lineshapes’’ in the tunneling spectra, as we now show.

18.8.2 Tunneling conductance and the ‘‘Fano Lattice’’

To calculate the tunneling conductance, we can adapt the formula obtained in (10.57),

$$\frac{dI}{d\phi}(\phi, \mathbf{x}) = g(e\phi, \mathbf{x}) = \left(\frac{Ne^2\Gamma}{\hbar} \right) A_\psi(\omega, \mathbf{x}) \Big|_{\omega=e\phi}. \quad (18.168)$$

where ϕ is the applied potential and we have adapted the formula to take account of N spin channels. $\Gamma = 2\pi|t_c|^2\rho_{tip}$ and ρ_{tip} is the density of states in the tip. The spectral function

$$A_\psi(\omega, \mathbf{x}) = \frac{1}{\pi} \text{Im} G_\psi(\mathbf{x}, \omega - i\delta) = \int dt e^{i\omega t} \langle \{ \psi_\sigma(\mathbf{x}, t), \psi^\dagger_\sigma(\mathbf{x}, 0) \} \rangle \quad (18.169)$$

is the local electron spectral function, which as usual we obtain by analytically extending the imaginary time Green’s function. To take into account the cotunneling, formally, all we have to do is to make the replacement (18.167)

$$\psi_{0\sigma} = \left[c_{0\sigma} + \left(\frac{\tilde{t}_f}{t_c} \right) (\vec{\sigma}_{\alpha\beta} \cdot \vec{S}_f(0)) c_{0\beta} \right]. \quad (18.170)$$

Lets now use the large N limit of the Kondo lattice to compute the tunneling conductance. As we saw in (18.6), the mean field theory provides a representation of the composite fermion $(\vec{\sigma}_{\alpha\beta} \cdot \vec{S}_f(j)) \hat{c}_{j\beta}$ in (18.167) as a single fermionic operator

$$\sum_\beta (\vec{\sigma}_{\alpha\beta} \cdot \vec{S}_f(j)) \hat{c}_{j\beta} \rightarrow \frac{\mathcal{V}}{J} \hat{f}_{j\alpha}, \quad (18.171)$$

where the amplitude $\frac{\mathcal{V}}{J} = -\langle \hat{f}_{j\beta}^\dagger \hat{c}_{j\beta} \rangle$. Thus in terms of composite f-electrons, we can rewrite direct and co-tunneled electron operator in (18.167) as

$$\hat{\psi}_{0\alpha} = \hat{c}_{0\alpha} + \left(\frac{\tilde{t}_f}{t_c} \right) \hat{f}_{0\alpha}, \quad (18.172)$$

where the complex amplitude for tunneling into the composite fermion state is $\tilde{t}_f = \frac{\mathcal{V}}{J} t_f$. The Green’s function for the ψ field is then

$$G_\psi(z) = \sum_{\mathbf{k}} \left(1, \frac{\tilde{t}_f}{t_c} \right) \cdot \begin{bmatrix} G_c(\mathbf{k}, z) & G_{cf}(\mathbf{k}, z) \\ G_{fc}(\mathbf{k}, z) & G_f(\mathbf{k}, z) \end{bmatrix} \cdot \begin{pmatrix} 1 \\ \tilde{t}_f/t_c \end{pmatrix} \quad (18.173)$$

where $G_c(z)$, $G_{cf}(z)$, $G_{fc}(z)$ and $G_f(z)$ are the propagators between the heavy f- and conduction electrons.

It is instructive to contrast the tunneling conductance expected in a Kondo lattice with that of a single Kondo impurity. In the case of a single Kondo impurity, the local propagators are

$$G_f(\omega - i\delta) = \dots = \frac{1}{\omega - \lambda - i\Delta} \quad (18.174)$$

$$= \sum_{\mathbf{k}} \left(1, \frac{\tilde{t}_f}{t_c}\right) \cdot \left[\begin{array}{cc} \text{---} \text{---} \text{---} & \text{---} \text{---} \text{---} \text{---} \text{---} \\ \text{---} \text{---} \text{---} \text{---} & \text{---} \text{---} \text{---} \text{---} \text{---} \end{array} \right] \cdot \begin{pmatrix} 1 \\ \tilde{t}_f/t_c \end{pmatrix} \quad (18.182)$$

where as in previous sections, the double lines denote the full conduction propagator $G_c(\mathbf{k}, z) = [(\omega - \epsilon_{\mathbf{k}}) - \mathcal{V}^2/(\omega - \lambda)]^{-1}$ while the single dashed lines denote the bare f-propagator $\frac{1}{z - \lambda}$. Writing this out in full, we have

$$\begin{aligned} G_{\psi}(z) &= \sum_{\mathbf{k}} \left(1, \frac{\tilde{t}_f}{t_c}\right) \cdot \left[\begin{array}{cc} G_c(\mathbf{k}, z) & \frac{\mathcal{V}}{z - \lambda} G_c(\mathbf{k}, z) \\ \frac{\mathcal{V}}{z - \lambda} G_c(\mathbf{k}, z) & \frac{1}{z - \lambda} + \frac{\mathcal{V}}{z - \lambda} G_c(\mathbf{k}, z) \frac{\mathcal{V}}{z - \lambda} \end{array} \right] \cdot \begin{pmatrix} 1 \\ \tilde{t}_f/t_c \end{pmatrix} \\ &= \sum_{\mathbf{k}} \left(\frac{(1 + \frac{\tilde{t}_f \mathcal{V}}{t_c (z - \lambda)})^2}{z - \epsilon_{\mathbf{k}} - \frac{\mathcal{V}^2}{z - \lambda}} + \frac{(\tilde{t}_f/t_c)^2}{z - \lambda} \right). \end{aligned} \quad (18.183)$$

In this expression we have separated out the terms that are proportional to the conduction electron propagator. Notice that the poles of this expression are at the quasiparticle energies $z = E_{\mathbf{k}\pm} = \frac{\epsilon_{\mathbf{k}} + \lambda}{2} \pm \sqrt{\left(\frac{\epsilon_{\mathbf{k}} - \lambda}{2}\right)^2 + \mathcal{V}^2}$ and the poles at $z = \lambda$ in the first and second terms actually cancel.

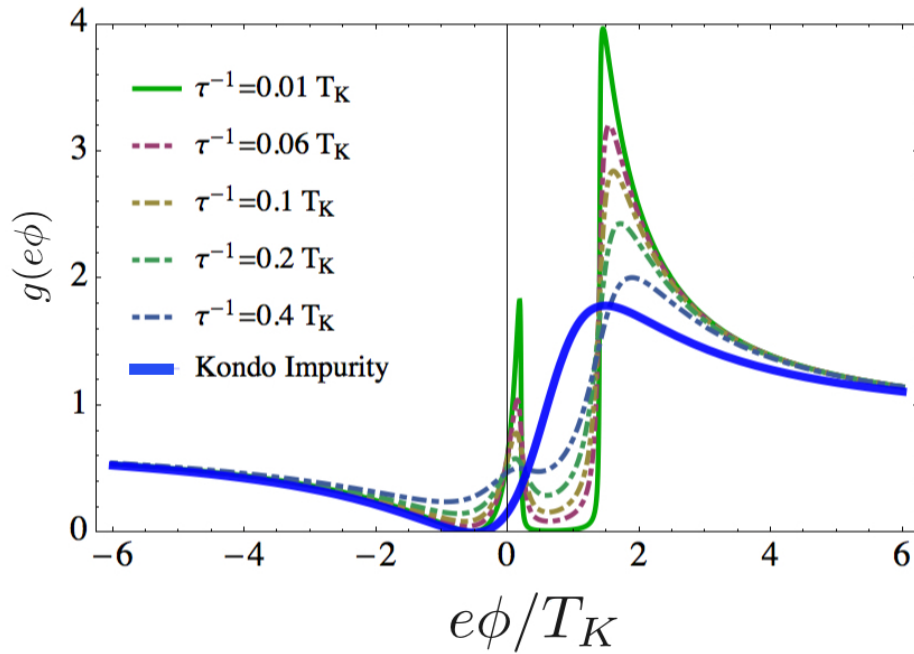


Fig. 18.15 Differential tunneling conductance $g(\phi)$ for a single Kondo impurity case (blue line) given by (18.181), a Kondo lattice (green line) given by (18.185). A typical Fano shape in the single Kondo impurity case gets replaced with a double-peaked resonance line in the Kondo lattice case. The dashed lines illustrate the effect of disorder, which destroys the coherence, closing the gap in the density of states curve. Here $\tilde{t}_f/t_c = 0.2$, $q = 1.2$, $\lambda/T_K = .6$, while $D_1 = 40T_K$, $D_2 = 80T_K$

The momentum summation in $G_{\psi}^{KL}(\omega)$ (18.182) can be carried out analytically assuming a constant conduction electron density of states ρ as follows:

$$\begin{aligned} G_{\psi}^{KL}(z) &= \rho \int_{-D_1}^{D_2} d\epsilon \left(\frac{(1 + \frac{\tilde{t}_f \mathcal{V}}{t_c z - \lambda})^2}{z - \epsilon - \frac{\mathcal{V}^2}{z - \lambda}} + \frac{(\tilde{t}_f/t_c)^2}{z - \lambda} \right) \\ &= \rho \left(1 + \frac{q\Delta}{z - \lambda}\right)^2 \ln \left[\frac{z + D_1 - \frac{\mathcal{V}^2}{z - \lambda}}{z - D_2 - \frac{\mathcal{V}^2}{z - \lambda}} \right] + \frac{2D\rho\tilde{t}_f^2/t_c^2}{z - \lambda}. \end{aligned} \quad (18.184)$$

Here $-D_1$ and D_2 are the lower and the upper conduction band edges respectively, and $2D = D_1 + D_2$ is the bandwidth. Using (18.168), the final expression for the tunneling conductance is then

$$g(e\phi) = N \left(\frac{\Gamma e^2}{\hbar} \right) \rho \frac{1}{\pi} \text{Im} \tilde{G}_{\psi}^{KL}(e\phi - i\delta), \quad (18.185)$$

where

$$\tilde{G}_{\psi}^{KL}(\omega) = \left(1 + \frac{q\Delta}{\omega - \lambda}\right)^2 \ln \left[\frac{\omega + D_1 - \frac{\mathcal{V}^2}{\omega - \lambda}}{\omega - D_2 - \frac{\mathcal{V}^2}{\omega - \lambda}} \right] + \frac{2D\rho\tilde{t}_f^2/t_c^2}{\omega - \lambda}. \quad (18.186)$$

The differential tunneling conductance predicted by this formula has two well-pronounced peaks at $e\phi \sim \lambda$ separated by a narrow hybridization gap $\Delta_g \sim 2\mathcal{V}^2/D$ in the single particle spectrum, as shown in Fig. 18.15.

In practice, experimental tunneling results will be modified by the effects of disorder. A phenomenological quasiparticle elastic relaxation rate τ^{-1} may be introduced into the theory by replacing $\omega \rightarrow \omega - i\tau^{-1}$ in (18.186). The results of this procedure are shown in Fig. 18.15. As we see, disorder removes the sharp peak structure in the tunneling conductance $g(e\phi)$ (18.185). The resulting lineshape of the tunneling conductance $dI/d\phi(e\phi)$ is an asymmetric smooth curve.

18.9 Optical Conductivity of Heavy Electrons

18.9.1 Heuristic Discussion

The optical conductivity of heavy fermion metals deserves special discussion. According to the f-sum rule (see section ??), the total integrated optical conductivity is determined by the plasma frequency (??)

$$\frac{2}{\pi} \int_0^{\infty} d\omega \sigma(\omega) = f_1 = \left(\frac{ne^2}{m} \right) \quad (18.187)$$

where n is the density of electrons. In the absence of local moments, this is the total spectral weight inside the Drude peak of the optical conductivity. But what happens to the distribution of the spectral weight when the heavy electron fluid forms? Physically we expect that while we expect this sum rule to be preserved, a new ‘‘quasiparticle’’ Drude peak will form corresponding to the heavy electron Drude peak.

$$\frac{2}{\pi} \int_0^{T_K} d\omega \sigma(\omega) = f_2 = \frac{ne^2}{m^*} = f_1 \frac{m}{m^*} \quad (18.188)$$

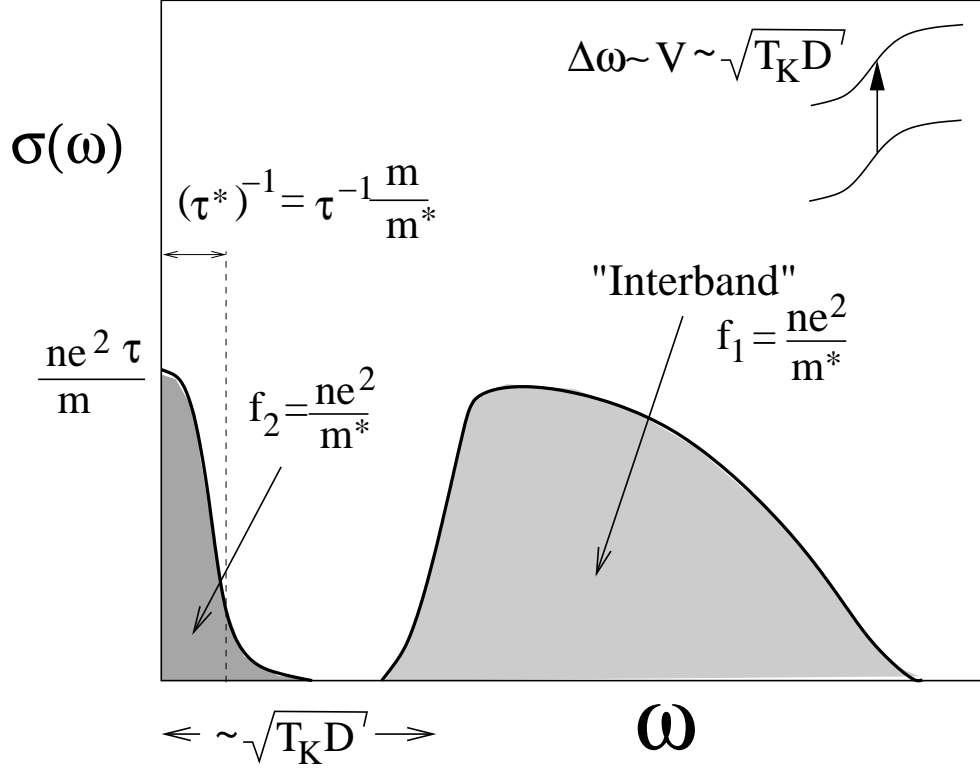


Fig. 18.16 Schematic, showing separation of the optical sum rule in a heavy fermion system into a high energy “inter-band” component of weight $f_2 \sim ne^2/m$ and a low energy Drude peak of weight $f_1 \sim ne^2/m^*$.

In other words, the spectral weight will divide into a small “heavy fermion” Drude peak, of total weight f_2 , where

$$\sigma(\omega) = \frac{ne^2}{m^*} \frac{1}{(\tau^*)^{-1} - i\omega} \quad (18.189)$$

separated off by an energy of order $V \sim \sqrt{T_K D}$ from an “inter-band” component associated with excitations between the lower and upper Kondo bands.[49, 50] This second term carries the bulk $\sim f_1$ of the spectral weight. (Fig. 18.16).

18.9.2 Calculation of the optical conductivity, including interband term

Let us now illustrate this phenomenon using the Kubo formula (??), which we rewrite here

$$\sigma^{\alpha\beta}(i\nu_n) = -\frac{1}{\nu_n} \left[\langle T j^\alpha(\nu') j^\beta(-\nu') \rangle \right]_{\nu'=0}^{\nu'=i\nu_n} \quad (18.190)$$

complete the integral over energy as a contour around the upper half plane, we will only get a finite result if this condition is satisfied. The result of this reasoning is

$$\sigma(iv_n) = \left(\frac{ne^2}{m}\right) \frac{1}{v_n} \left[2\pi iT \sum_{|\omega_r| < v_n/2} \frac{1}{iv_n + i\Gamma - (\Sigma^+ - \Sigma^-)} \right], \quad (v_n > 0) \quad (18.196)$$

where we have introduced $\Sigma^\pm = \Sigma_c(i\omega_n^\pm)$. (Notice that the contribution from the term where we replace $iv_n \rightarrow 0$ now disappears).

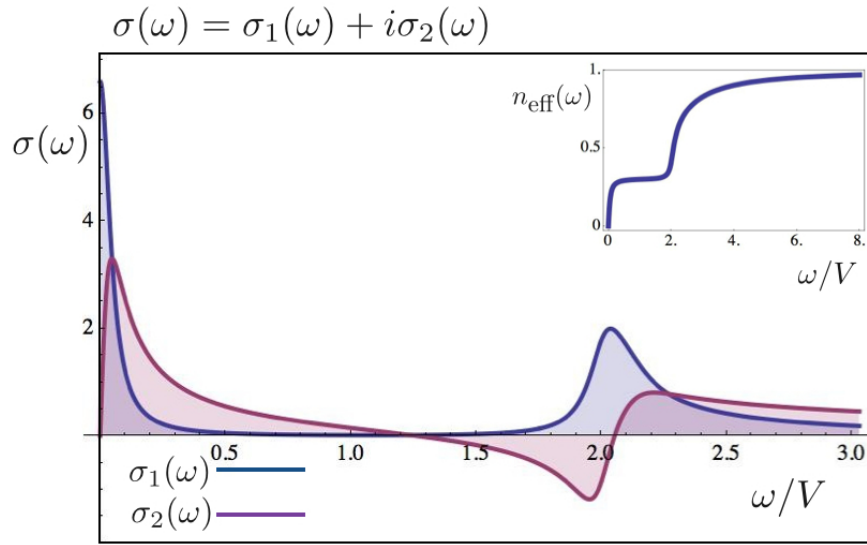


Fig. 18.17 Plot of real and imaginary parts of optical conductivity obtained from equation (18.204) using mean-field conduction electron propagators. Inset shows the integrated spectral weight $n_{eff}(\omega) = \frac{2m}{e^2} \int_0^\omega \sigma_1(x) \frac{dx}{\pi}$, showing contributions from Drude and interband parts.

Next, we take the zero temperature limit, so that $T \sum_{i\omega_r} \rightarrow \int_{-i\infty}^{i\infty} \frac{dz}{2\pi i}$ to obtain

$$\sigma(iv) = \left(\frac{ne^2}{m}\right) \frac{1}{v_n} \int_{-iv/2}^{iv/2} dz \left(\frac{1}{iv + i\Gamma - (\Sigma(z + iv/2) - \Sigma(z - iv/2))} \right), \quad (v > 0). \quad (18.197)$$

To check that we are on the right track, let us look at the low frequency limit of this expression. In this limit, we can replace

$$iv - (\Sigma(z + iv/2) - \Sigma(z - iv/2)) \rightarrow iv \left(1 - \frac{\partial \Sigma(z)}{\partial z} \right) = Z^{-1} iv, \quad (18.198)$$

where $Z = \left(1 + \frac{v^2}{x^2}\right)^{-1}$ is recognized as the quasiparticle weight, so the low frequency conductivity becomes

$$\sigma(\omega) = \left(\frac{ne^2}{m^*}\right) \frac{1}{\Gamma^* - iv} \quad (18.199)$$

where $m^* = m/Z$ is the renormalized mass and $\Gamma^* = Z\Gamma$ is the renormalized Drude width, so we have recovered the Drude peak with a overall weight reduced by the factor Z .

Let us now continue to see if we can capture the interband part of the conductivity. Fortunately, the argument of (18.145) simplifies into a two pole structure as follows

$$\begin{aligned} \frac{1}{iv + i\Gamma - (\Sigma(z + iv/2) - \Sigma(z - iv/2))} &= \frac{1}{i\tilde{\nu}} \left[1 - \frac{V^2[iv]}{(z - \lambda)^2 + \left(\frac{\nu}{2}\right)^2 + \mathcal{V}^2[iv]} \right] \\ &= \frac{1}{i\tilde{\nu}} \left[1 - \frac{V^2[iv]}{(z - z_+)(z - z_-)} \right] \end{aligned} \quad (18.200)$$

where $\tilde{\nu} = \nu + \Gamma$ and

$$z_{\pm} = \lambda \pm \sqrt{\left(\frac{iv}{2}\right)^2 - V^2[iv]}, \quad V^2[iv] = V^2 \frac{iv}{iv + i\Gamma} \quad (18.201)$$

so that when we do the integral over z , we obtain

$$\int_{-iv/2}^{iv/2} dz \left(\frac{1}{iv - (\Sigma(z + iv/2) - \Sigma(z - iv/2))} \right) = \frac{iv}{i\tilde{\nu}} \left[1 - \frac{V^2}{i\tilde{\nu}(z_+ - z_-)} \left(\ln \left[\frac{iv/2 - z_+}{-iv/2 - z_+} \right] - \ln \left[\frac{iv/2 - z_-}{-iv/2 - z_-} \right] \right) \right] \quad (18.202)$$

Inserting this into (18.197), the optical conductivity is given by

$$\sigma(iv) = \left(\frac{ne^2}{m} \right) \frac{1}{\Gamma - i(iv)} \left[1 - \frac{V^2}{i(\nu + \Gamma)(z_+ - z_-)} \left(\ln \left[\frac{iv/2 - z_+}{-iv/2 - z_+} \right] - \ln \left[\frac{iv/2 - z_-}{-iv/2 - z_-} \right] \right) \right] \quad (18.203)$$

Finally, analytically continuing $iv \rightarrow \omega + i\delta$, we obtain

$$\begin{aligned} \sigma(\omega + i\delta) &= \left(\frac{ne^2}{m} \right) \frac{1}{\Gamma - i\omega} \left[1 + \frac{V^2}{(\omega + i\Gamma)(z_+ - z_-)} \left(\ln \left[\frac{z_+ + \frac{\omega}{2}}{z_+ - \frac{\omega}{2}} \right] - \ln \left[\frac{z_- + \frac{\omega}{2}}{z_- - \frac{\omega}{2}} \right] \right) \right], \\ z_{\pm} &= \lambda \pm \sqrt{\left(\frac{\omega}{2}\right)^2 - V^2 \frac{\omega}{\omega + i\Gamma}}. \end{aligned} \quad (18.204)$$

Note that although it is tempting to combine the final logarithms into a single term, unfortunately the dangerous identity $\ln f(z) + \ln g(z) = \ln[f(z)g(z)]$ fails to preserve the branch-cut structure of the logarithms and can't be used here if one wants to preserve the full analytic structure of the conductivity. Fig (18.17) shows a plot of the optical conductivity obtained with this function. Notice the formation of the Drude peak and the direct gap of size $2V$.

These basic features- the formation of a narrow Drude peak, the presence of a hybridization gap $V \sim \sqrt{T_K D}$ that scales as the square root of the Kondo temperature have been confirmed in optical measurements on heavy electron systems[52, 53, 54, 51]. In particular, the relationship $V \sim \sqrt{T_K D}$ implies that

$$\left(\frac{V}{T_K} \right)^2 \propto \frac{D}{T_K} \sim \frac{m^*}{m} \quad (18.205)$$

Experimentally, the characteristic scale T_K can be determined from the specific heat measurements, while V can be directly inferred from optical conductivity measurements. Fig. (18.18) shows that this relationship is approximately followed by a wide range of materials.

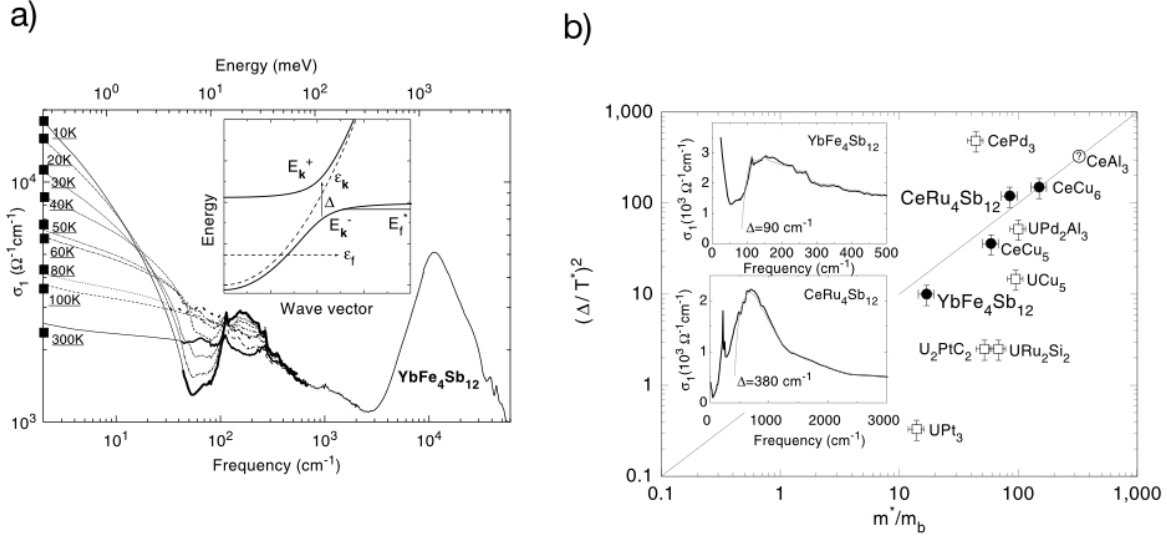


Fig. 18.18 (a) Measured optical conductivity of heavy fermion metal $\text{YbFe}_4\text{Sb}_{12}$ after [51] showing development of hybridization gap. (b) Scaling of hybridization gap with effective mass measured in a variety of heavy fermion materials after [51]

18.10 Gauge invariance and the charge of the f-electron

The large N expansion also provides a gauge theoretic interpretation of how local moments acquire charge as a kind of Anderson-Higg's mechanism[55] which locks the gauge fields of the conduction and f-electrons together. The basic idea is to regard the Kondo lattice as composed of two fluids:

- an electron fluid (c) coupled to the electromagnetic field, (Φ, \vec{A}) .
- an incompressible, initially neutral "spinon" fluid f-electrons coupled to an internal gauge field $(\lambda, \vec{\mathcal{A}})$.

When the Kondo effect develops, the coherent hybridization between the two fluids locks the internal and external gauge fields together. Specifically, the difference field develops a stiffness or mass term, described by the effective action

$$S_{\text{eff}} = \int dx^3 d\tau \left[\frac{\rho_f}{2} (\vec{\nabla}\phi_j - \vec{\mathcal{A}} + e\vec{A})^2 - \frac{\chi_f}{2} (i\partial_\tau\phi + \delta\lambda - e\Phi)^2 \right] \quad (18.206)$$

where ϕ_j is the phase of the hybridization field $V_j = |V_j|e^{i\phi_j}$, while $\chi_f \sim 1/T_K$ and ρ_f are the corresponding temporal and spatial phase stiffnesses. The quantity $\delta\lambda = \lambda - \lambda_0$ is the equilibrium value of the constraint field in the absence of an external potential. This resembles the Ginzburg Landau theory of a superconductor except it involves a *difference* field, so the corresponding "Meissner" effect causes the internal gauge field to lock to the electromagnetic field as shown in Fig. 18.19. The remarkable thing about these results is that the static saddle points with respect to $\vec{\mathcal{A}}$ and λ_j of the Free energy impose the constraints

$$\vec{\mathcal{A}}(x) - e\vec{A}(x) = 0, \quad \delta\lambda_j - e\Phi_j = 0,$$

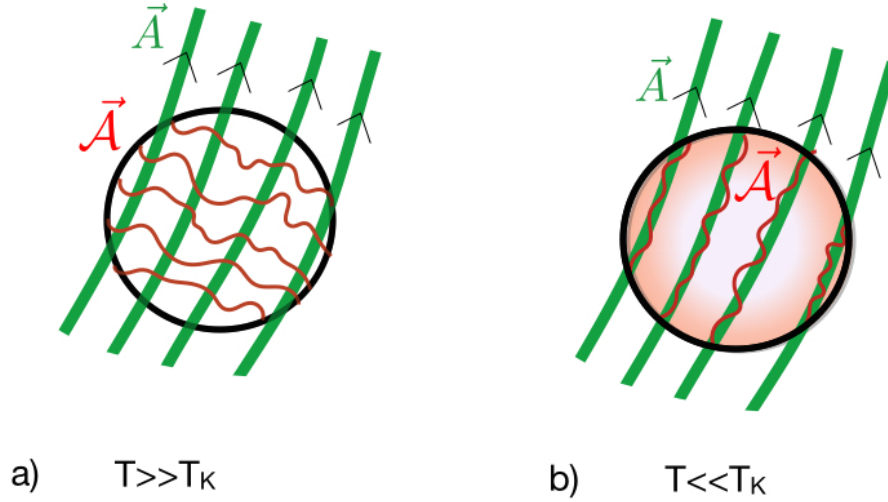


Fig. 18.19 Gauge theory picture of the Kondo lattice. a) High temperature, the internal gauge field of the f-electrons is decoupled from the electromagnetic field. b) At low temperature $T \ll T_K$, the internal field locks together with the electromagnetic field.

$$\Rightarrow \vec{\mathcal{A}}(x) = e\vec{A}(x), \quad \delta\lambda_j = e\Phi_j. \quad (18.207)$$

causing the internal and external fields to lock together. It is this process that causes the f-electrons to become charged. The system is not a superconductor because the sum of the two fields is still massless and propagates through the Kondo lattice as a physical electromagnetic field (albeit with a renormalized plasma frequency). This locking of the two fields has an important consequence for our interpretation of the constraint term, which becomes

$$\delta\lambda_j(n_f(j) - Q) \rightarrow -|e|\Phi_j(n_f(j) - Q). \quad (18.208)$$

where we have explicitly written $e = -|e|$. In other words, we must not only consider the emergent f-electrons as particles of charge $e = -|e|$, but we must regard the constraint term $|e|\Phi_j Q$ as a coupling of the external potential to a background positive charge. In this way, we see that the local moment has “ionized” into a mobile negative electron plus a localized positive charge which we may associate with the Kondo singlet.

To see how this works, it is helpful to consider a Kondo lattice model with an additional nearest-neighbour antiferromagnetic Heisenberg interaction, described by

$$H = H_c + H_K + H_M \quad (18.209)$$

where

$$H_c = \sum_{ij,\sigma} \left(t_{ij} e^{-ie \int_j^i \vec{A} \cdot d\vec{x}} + (e\Phi_i - \mu)\delta_{ij} \right) c_{i\sigma}^\dagger c_{j\sigma}, \quad (18.210)$$

describes the conduction band while

$$\begin{aligned} H_K &= -\frac{J}{N} \sum_{\alpha\beta} (c_{j\alpha}^\dagger f_{j\alpha})(f_{j\beta}^\dagger c_{j\beta}), \\ H_H &= -\frac{J_H}{N} \sum_{(i,j)} (f_{i\alpha}^\dagger f_{j\alpha})(f_{j\beta}^\dagger f_{i\beta}), \end{aligned} \quad (18.211)$$

describe the on-site Kondo coupling (H_K) and the super-exchange between neighboring spin sites (H_H). A scalar and a vector potential (Φ, \vec{A}) have been introduced into H_c using the ‘‘Peierls substitution’’ to include the vector potential as a phase factor in the hopping. For uniform vector and scalar potentials H_c can be rewritten as $H_c = \sum(\epsilon_{\vec{k}-e\vec{A}} + e\Phi) c_{\vec{k}\sigma}^\dagger c_{\vec{k}\sigma}$, where the dispersion $\epsilon_{\vec{k}} = \sum_{\vec{R}} t(\vec{R})e^{-i\vec{k}\cdot\vec{R}} - \mu$ is the kinetic energy of the conduction electrons.

The internal gauge fields appear when we formulate the problem as a path integral. When we factorize the Kondo interaction, we can always use the radial gauge to absorb the phase of the hybridization into the f-electron field. But in once we’ve fixed the gauge of the f-electrons, then when we factorize the Heisenberg interaction:

$$H_H \rightarrow H_H = \sum_{(i,j)} \left(|\chi_{ij}| e^{-i \int_j^i \vec{\mathcal{A}} \cdot d\vec{x}} f_{i\alpha}^\dagger f_{j\alpha} + \text{H.c.} \right) + \frac{N|\chi_{ij}|^2}{J_H}.$$

the phase of the bond variables gives rise to a dynamical vector potential \mathcal{A} . This kind of decoupling was first introduced to describe spin liquids in the context of the RVB model of high temperature superconductivity[56, 57]. Without the hybridization, the bond-variables describe the motion of ‘‘spinons’’ in a neutral spin fluid. If the χ_{ij} are uniform, the dispersion of the spinons is given by $j_{\mathbf{k}} = \sum_{\mathbf{R}} \chi(\mathbf{R})e^{-i\mathbf{k}\cdot\mathbf{R}} + \lambda$. The main difference between the internal field (λ, \mathcal{A}) and the electro-magnetic field, is that the internal field has no field energy $\frac{1}{2\mu_0}[B^2 + (E/c)^2]$ so the saddle point conditions which normally generate Gauss’ and Ampères law are simply

$$-\frac{\delta S}{\delta \lambda} = n_f - Q = 0, \quad -\frac{\delta S}{\delta \vec{\mathcal{A}}} = j = 0, \quad (18.212)$$

enforcing the incompressible nature of the spin fluid.

When $V_j = 0$, there are two independent gauge symmetries for the conduction and spin fluid, but once the hybridization becomes finite, a single gauge invariance applies equally to both c and f electrons,

$$\begin{aligned} c_j &\rightarrow c_j e^{-i\alpha}, & f_j &\rightarrow f_j e^{-i\alpha} \\ (e\Phi, e\vec{A}) &\rightarrow (e\Phi + i\partial_\tau \alpha, e\vec{A} + \vec{\nabla}\alpha) \\ (\lambda, \vec{\mathcal{A}}) &\rightarrow (\lambda + i\partial_\tau \alpha, \vec{\mathcal{A}} + \vec{\nabla}\alpha) \end{aligned} \quad (18.213)$$

The emergence of a single gauge transformation for all fermions indicates that once the Kondo effect develops, the composite f-electrons become charged. Moreover, only the difference fields $e\vec{A} - \vec{\mathcal{A}}$ and $e\Phi - \lambda$ are gauge invariant, and the long-wavelength action, which is gauge invariant can thus only be a functional of the difference of these two quantities.

Lets look at this in more detail. In the absence of the hybridization, the energy of the conduction electrons is $\epsilon_{\mathbf{k}-e\vec{A}}$. Adding an external field \vec{A} simply shifts all the momenta of the quasiparticles by $-e\vec{A}$ and since we sum over all momenta to get the total free energy or action, the action remains unchanged. However, once the hybridization is switched on, the energy of the quasiparticles becomes

$$E_{\mathbf{k}}^\pm = \frac{1}{2}(\epsilon_{\mathbf{k}-e\vec{A}} + j_{\mathbf{k}-\vec{\mathcal{A}}}) \pm \sqrt{\left(\frac{(\epsilon_{\mathbf{k}-e\vec{A}} - j_{\mathbf{k}-\vec{\mathcal{A}}})}{2}\right)^2 + V^2} \quad (18.214)$$

Since the vector potential only couples to the conduction electrons, its introduction is not equivalent to a simple shift of momentum, so the energy now depends on \vec{A} as if we have a superconductor! Suppose we differentiate the Free energy twice with respect to \vec{A} , then we get

$$\begin{aligned} \rho_f^{(1)} \delta_{ab} &= \frac{1}{e^2} \frac{\partial^2 F}{\partial A_a \partial A_b} = - \left(\nabla_{ab}^2 \epsilon_{\mathbf{k}} \text{ [diagram: double loop with wavy lines] } + \nabla_a \epsilon_{\mathbf{k}} \text{ [diagram: double loop with wavy lines] } \nabla_b \epsilon_{\mathbf{k}} \right) \\ &= T \sum_{\kappa=(\mathbf{k}, i\omega_r)} \left[\nabla_{ab}^2 \epsilon_{\mathbf{k}} G_c(\kappa) + \nabla_a \epsilon_{\mathbf{k}} \nabla_b \epsilon_{\mathbf{k}} G_c(\kappa)^2 \right] \end{aligned} \quad (18.215)$$

where the double and single vertices reflect the double and second derivatives of the energy with respect to momentum. (The minus sign on the first line appears because the diagrammatic expansion of the Free energy is $-1 \times$ the sum of linked cluster diagrams). Were the spinon fluid dispersionless, so that $\mathbf{j}_{\mathbf{k}} = \text{constant}$, this expression would be a perfect differential $T \sum_{\mathbf{k}} \nabla_a (\nabla_b G_c(\mathbf{k})) = 0$ and vanish, but otherwise, his stiffness becomes finite. At first sight this looks like a superconductor.

However, if we change the internal and external vector potentials by the same amount, i.e $e\vec{A} = \vec{\mathcal{A}}$, then this is equivalent to uniformly shifting the momenta, and in this case, the effective action is unchanged. The effective action must therefore be a function of $e\vec{A} - \vec{\mathcal{A}}$, vanishing when the two fields are equal. In other words, the Anderson-Higg's mass of the Kondo lattice is associated with the difference of the internal and external fields with a long-wavelength effective action of the form

$$S_{\text{eff}} = \int dx^3 d\tau \left[\frac{\rho_f}{2} (\mathcal{A} - e\vec{A})^2 - \frac{\chi_f}{2} (\lambda - e\Phi)^2 \right]. \quad (18.216)$$

The above expression holds in the radial gauge. If we return to the original ‘‘cartesian gauge’’, restoring the complex $V_j = |V_j| e^{i\phi}$, then we must replace $\lambda_j \rightarrow \lambda_j + i\partial_\tau \phi$ and $\vec{\mathcal{A}} \rightarrow \vec{\mathcal{A}} - \nabla \phi$, giving rise to a more general expression,

$$S_{\text{eff}} = \int dx^3 d\tau \left[\frac{\rho_f}{2} (\vec{\nabla} \phi_j - \vec{\mathcal{A}} + e\vec{A})^2 - \frac{\chi_f}{2} (i\partial_\tau \phi + \delta\lambda - e\Phi)^2 \right], \quad (18.217)$$

as discussed earlier. Thus the acquisition of charge by the f-electrons can be regarded as a consequence of the stiffness that develops in the phase of the hybridization. An similar phase stiffness also occurs in the ‘‘Chiral Gross Neveu’’ model, a 1+1 dimensional, relativistic version of the Kondo model[21].

From this discussion, we see that the very same stiffness is shared by both the internal and external vector potential, in particular, the coupled stiffness

$$\begin{aligned} \rho_f^{(2)} \delta_{ab} &= -\frac{1}{e} \frac{\partial^2 F}{\partial A_a \partial A_b} = \nabla_a \mathbf{j}_{\mathbf{k}} \text{ [diagram: loop with wavy lines and red dots] } \nabla_b \epsilon_{\mathbf{k}}, \\ &= -T \sum_{\kappa=(\mathbf{k}, i\omega_r)} \left[\nabla_a \mathbf{j}_{\mathbf{k}} G_{fc}(\kappa) \nabla_b \epsilon_{\mathbf{k}} G_{cf}(\kappa) \right] \end{aligned} \quad (18.218)$$

where the vertices reflect the current operators $\nabla_{\mathbf{k}} \mathbf{j}_{\mathbf{k}}$ and $\nabla_{\mathbf{k}} \epsilon_{\mathbf{k}}$ of the f- and c- fields respectively, is also equal to $\rho_f^{(1)}$.

To prove the equivalence of $\rho_f^{(1)} = \rho_f^{(2)}$, we use the fact that when we uniformly shift the momenta of all particles, physical quantities must not change. This is a restatement of gauge invariance, because a uniform

$$H = \sum_{\mathbf{k}, \sigma \in [1, N]} \epsilon_{\mathbf{k}} c_{\mathbf{k}\sigma}^{\dagger} c_{\mathbf{k}\sigma} + \sum_{\mathbf{k}\sigma \in [1, N]} [V_{\mathbf{k}} c_{\mathbf{k}\sigma}^{\dagger} X_{0\sigma} + V_{\mathbf{k}}^* X_{\sigma 0} c_{\mathbf{k}\sigma}] + E_f \sum_{\sigma=1, N} X_{\sigma\sigma}. \quad (18.222)$$

Infinite U Anderson Impurity Model.

Here the $\hat{X}_{\alpha\beta} = |\alpha\rangle\langle\beta|$ are ‘‘Hubbard operators’’ linking the the restricted set of atomic states

$$|\alpha\rangle = \begin{cases} |f^0\rangle, & (\alpha = 0), \\ |f^1 : \sigma\rangle, & (\alpha \in \{\sigma\} \in [1, \dots N]), \end{cases} \quad (18.223)$$

which respectively denote the empty ($\alpha = 0$) and N magnetic states ($\alpha \in [1, N]$) of an ion. For instance, in a mixed valent cerium atom, the N magnetic states refer to the $2j + 1 = 6$ magnetic configurations of the $j = 5/2$ Ce^{3+} ion. If we denote $P = X_{00}$ as the projector onto the empty state, then the Hubbard operators

$$X_{\sigma 0} = |f^1 : \sigma\rangle\langle f^0| \equiv f_{\sigma}^{\dagger} P_0 \quad X_{0\sigma} \equiv |f^0\rangle\langle f^1 : \sigma| = P_0 f_{\sigma}, \quad (18.224)$$

are projected fermion operators which respectively describe the addition or removal of an f-electron from the singly occupied (f^1) state. By contrast, the operators

$$X_{\sigma\sigma'} = |f^1 : \sigma\rangle\langle f^1 : \sigma'|, \quad (\sigma, \sigma' \in [1, N]) \quad (18.225)$$

are spin operators with a commuting (bosonic) algebra⁴. Hubbard operators pose two difficulties:

- they do not satisfy a canonical commutation (or anticommutation) algebra, so that Wick’s theorem is not obeyed.
- The no-double occupancy condition $n_f \leq 1$ is a non-holomorphic inequality, not naturally encompassed in a field theory.

A solution to this problem, devised independently by Stuart Barnes, working at Trinity College Dublin and Piers Coleman, the author, while a graduate student at Princeton University, is to factorize the Hubbard operators in terms of canonical operators by introducing an auxilliary or ‘‘slave boson’’ field b^{\dagger} [26, 27, 29] which creates the empty f^0 configuration, so that

$$\begin{aligned} |f^0\rangle &= b^{\dagger}|0\rangle, \\ |f^1 : \sigma\rangle &= f_{\sigma}^{\dagger}|0\rangle, \end{aligned} \quad (18.227)$$

describes the restricted Hilbert space. The corresponding Hubbard operators are then

$$\begin{aligned} X_{\sigma 0} &= f_{\sigma}^{\dagger} b, & X_{0\sigma} &= b^{\dagger} f_{\sigma} \\ X_{00} &= b^{\dagger} b, & X_{\sigma\sigma'} &= f_{\sigma}^{\dagger} f_{\sigma'} \end{aligned} \quad (18.228)$$

Slave Boson formulation of Hubbard operators

⁴ Notice that the proper traceless spin operator is given by

$$S_{\alpha\beta} = X_{\alpha\beta} - \frac{1}{N} \delta_{\alpha\beta} X_{\alpha\alpha} \quad (18.226)$$

This representation faithfully reproduces the super-algebra of Hubbard operators

$$[X_{\alpha\beta}, X_{\gamma\delta}]_{\pm} = X_{\alpha\delta}\delta_{\beta\gamma} \pm X_{\gamma\beta}\delta_{\alpha\delta}, \quad (18.229)$$

(where the “+” sign is used when both Hubbard operators are fermionic). Moreover, each operator commutes with the conserved charge

$$Q = b^{\dagger}b + n_f \quad (18.230)$$

measuring the number of bosons and fermions at each site, $[X_{\alpha\beta}, Q] = 0$ so the non-holomorphic constraint $n_f \leq 1$ is now replaced by the holomorphic constraint $Q = 1$. We can identify Q as a kind of Casimir of the supergroup defined by the Hubbard operators, permitting us to generalize its representations to any $Q \leq N$. This permits one to take a large N limit following the same scheme as in the Kondo lattice, namely keeping the ration $q = Q/N$ fixed as $N \rightarrow \infty$, so that Q becomes an extensive variable. Finally, in a many-site lattice, the above replacements are made at each site, adding a site label j to each operator, so that $X_{\sigma 0}(j) = f^{\dagger}_{j\sigma}b_j$, thus the the infinite U Anderson lattice model becomes

$$H = \sum_{\mathbf{k}, \sigma \in [1, N]} \epsilon_{\mathbf{k}} c^{\dagger}_{\mathbf{k}\sigma} c_{\mathbf{k}\sigma} + \sum_{\mathbf{k}\sigma \in [1, N]} [V_{\mathbf{k}} c^{\dagger}_{\mathbf{k}\sigma} (b^{\dagger} f_{\sigma}) + V_{\mathbf{k}}^* (f_{\sigma}^{\dagger} b) c_{\mathbf{k}\sigma}] + E_f n_f + \lambda(n_f + n_b - Q). \quad (18.231)$$

Infinite U Anderson Model: Slave boson Formulation

Notice that

- The reformulation of the infinite U constraint using slave bosons introduces a local constraint, leading to a gauge theory of interacting particles.
- The slave boson describes the deviation of the valence from the maximum value $n_f = Q$, and as such is a field that keeps track of valence fluctuations.
- In the mean field we can explore solutions in which the slave boson condenses. In the Anderson model, this leads to the renormalization of the hybridization,

$$V_{\mathbf{k}} \rightarrow \tilde{V}_{\mathbf{k}} = V_{\mathbf{k}} \langle b_j \rangle \quad (18.232)$$

giving a natural account of the narrowing of the resonance width that results from the Kondo effect.

- The constraint also has the effect of renormalizing the position of the f-level

$$E_f \rightarrow \tilde{E}_f = E_f + \lambda \quad (18.233)$$

It is this effect that leads to the formation of the Kondo resonance near the Fermi energy, even when the bare f-energy $E_f < 0$ is far below (or above) the Fermi energy.

18.11.1 Path integrals with Slave Bosons

Now we have formulated the Hubbard operators in terms of cononical fields, using the coherent state representations developed in chapter 15 we can immediately formulate the infinite U Anderson model as a path integral. The result of this procedure, is to reincorporate valence fluctuatiios into the Kondo lattice. Consider

the infinite U Anderson lattice model, written as

$$H = \sum_{\mathbf{k}, \sigma \in [1, N]} \epsilon_{\mathbf{k}} c_{\mathbf{k}\sigma}^\dagger c_{\mathbf{k}\sigma} + \sum_{j\sigma} \frac{V_0}{\sqrt{N}} \left[c_{j\sigma}^\dagger (b_j^\dagger f_{j\sigma}) + \text{H.c.} \right] + \sum_j E_f n_f(j) \quad (18.234)$$

where for pedagogy, we assume an s-wave, momentum independent hybridization of strength V_0 . Here we have taken the liberty of rescaling the hybridization with respect to the spin degeneracy, anticipating that as N becomes large, $\langle b \rangle \sim O(\sqrt{N})$, so that each term in the Hamiltonian is extensive in N , permitting a controlled large N expansion. If we now represent the fields as coherent states, we can immediately write down a path integral for the partition function:

$$\begin{aligned} Z &= \int \mathcal{D}[\bar{b}, b, \lambda] \int \mathcal{D}[\bar{\psi}, \psi] \exp[-S] \\ S &= \int_0^\beta d\tau \left[\sum_{\mathbf{k}\sigma} c_{\mathbf{k}\sigma}^\dagger (\partial_\tau + \epsilon_{\mathbf{k}}) c_{\mathbf{k}\sigma} + \sum_{j\sigma} f_{j\sigma}^\dagger (\partial_\tau + E_f + \lambda_j) f_{j\sigma} + \sum_j b_j^\dagger (\partial_\tau + \lambda_j) b_j \right. \\ &\quad \left. + \sum_{j\sigma} \frac{V_0}{\sqrt{N}} \left[c_{j\sigma}^\dagger (b_j^\dagger f_{j\sigma}) + (f_{j\sigma}^\dagger b_j) c_{j\sigma} \right] - \sum_j \lambda_j Q \right]. \end{aligned} \quad (18.235)$$

Infinite U Anderson Lattice Model: Slave Boson Formulation

Here following our earlier convention, we use the dagger notation to represent Hermitian conjugates of both operators and their c-number expectation values inside the path integral. We have also introduced the Lagrange multiplier field λ_j at each site, coupled to $(n_{fj} + n_{bj} - Q)$, so that by integrating over the Lagrange multiplier fields λ_j along the imaginary axis we impose the constraint. By comparing this expression with the corresponding one for the Kondo Lattice (18.55), we recognize that the slave boson field plays the same role as the hybridization field used to factorize the Coqblin Schrieffer Hamiltonian, but with a number of differences:

- The bare f-level position E_f appears explicitly in the Lagrangian, shifted by the amount λ_j . This shift is responsible for the formation of the Kondo resonance. In the Kondo regime, we expect the renormalized f-level position $\lambda_j + E_f \sim T_K \sim 0$ to be of order the Kondo temperature, so that $\lambda_j \sim -E_f = |E_f|$.
- The slave boson carries gauge charge, and couples to the constraint field λ_j .
- The slave boson field, has its own dynamics, represented by the slave boson action $b_j^\dagger (\partial_\tau + \lambda_j) b_j$, associated with charge fluctuations at a scale $\omega \sim \lambda_j \sim |E_f|$ in the Kondo regime.

As in the Kondo lattice the presence of local gauge symmetries associated with the local conservation of Q (see 18.237) allows us to choose a gauge in which the slave boson field is purely real. Let $r_j = |b_j|$ be the magnitude of the slave boson field at site j , then under the transformations

$$\begin{aligned} b_j &\rightarrow r_j e^{i\phi_j}, \\ f_{j\sigma} &\rightarrow e^{i\phi_j} f_{j\sigma} \end{aligned} \quad (18.236)$$

the action at site j transforms as

$$S_A(j) = \int_0^\beta d\tau \left[f_{j\sigma}^\dagger (\partial_\tau + E_f + \lambda_j) f_{j\sigma} + b_j^\dagger (\partial_\tau + \lambda_j) b_j + \left[\frac{V_0}{\sqrt{N}} (c_{j\sigma}^\dagger b_j^\dagger f_{j\sigma} + \text{H.c.}) - \lambda_j Q \right] \right]$$

$$\xrightarrow{b_j \rightarrow e^{i\phi_j} b_j, f_j \rightarrow e^{i\phi_j} f_j} \int_0^\beta d\tau \left[f_{j\sigma}^\dagger (\partial_\tau + E_f + \lambda_j + i\dot{\phi}_j) f_{j\sigma} + r_j (\partial_\tau + \lambda_j + i\dot{\phi}_j) r_j + \frac{V_0 r_j}{\sqrt{N}} (c_{j\sigma}^\dagger f_{j\sigma} + \text{H.c.}) - \lambda_j Q \right]. \quad (18.237)$$

If we now shift the constraint field to absorb the phase velocity terms $\dot{\phi}_j$, we obtain

$$\begin{aligned} S_A(J) &\xrightarrow{\lambda_j \rightarrow \lambda_j - i\dot{\phi}_j} \int_0^\beta d\tau \left[f_{j\sigma}^\dagger (\partial_\tau + E_f + \lambda_j) f_{j\sigma} + \frac{V_0 r_j}{\sqrt{N}} (c_{j\sigma}^\dagger f_{j\sigma} + \text{H.c.}) + \lambda_j (r_j^2 - Q) \right] + \overbrace{\int_0^\beta d\tau \left(\frac{1}{2} \partial_\tau r_j^2 + iQ\dot{\phi}_j \right)}^{2\pi i \times \text{integer}} \\ &\equiv \int_0^\beta d\tau \left[f_{j\sigma}^\dagger (\partial_\tau + E_f + \lambda_j) f_{j\sigma} + \frac{V_0 r_j}{\sqrt{N}} (c_{j\sigma}^\dagger f_{j\sigma} + \text{H.c.}) + \lambda_j (r_j^2 - Q) \right]. \end{aligned} \quad (18.238)$$

where the final remainder term is a perfect differential which vanishes (up to an integer multiple of $2\pi i$) under periodic boundary conditions. The resulting action is then

$$S = \int_0^\beta d\tau \left\{ \sum_{\mathbf{k}\sigma} c_{\mathbf{k}\sigma}^\dagger (\partial_\tau + \epsilon_{\mathbf{k}}) c_{\mathbf{k}\sigma} + \sum_{j\sigma} \left(f_{j\sigma}^\dagger (\partial_\tau + E_f + \lambda_j) f_{j\sigma} + \frac{V_0 r_j}{\sqrt{N}} [c_{j\sigma}^\dagger f_{j\sigma} + \text{H.c.}] \right) + \sum_j \lambda_j (r_j^2 - Q) \right\}. \quad (18.239)$$

Infinite U Anderson lattice: radial gauge.

Notice how the dynamics of the slave boson field have been absorbed into the constraint field. The resulting action is remarkably like that of the Kondo lattice. Indeed, if we make the change of variables

$$\begin{aligned} \lambda_j &\rightarrow \lambda_j - E_f \\ \frac{V_0 r_j}{\sqrt{N}} &= |\tilde{V}_j|, \end{aligned} \quad (18.240)$$

then the constraint term becomes

$$\begin{aligned} \lambda_j (r_j^2 - Q) &\rightarrow (\lambda_j - E_f) \left(N \frac{|\tilde{V}_j|^2}{V_0^2} - Q \right) \\ &= N \frac{|\tilde{V}_j|^2}{J} + N \sum_j \left(\frac{|V_j|^2}{V_0^2} \lambda_j + E_f q \right) \end{aligned} \quad (18.241)$$

where $q = Q/N$ and

$$J = \frac{V_0^2}{-E_f} = \frac{V_0^2}{|E_f|}, \quad (18.242)$$

is recognized as the Schrieffer Wolff expression for the Kondo coupling constant in the infinite U limit, assuming that $E_f = -|E_f| < 0$. The resulting Lagrangian is

$$\begin{aligned} L_{AL} &= \sum_{\mathbf{k}\sigma} c_{\mathbf{k}\sigma}^\dagger (\partial_\tau + \epsilon_{\mathbf{k}}) c_{\mathbf{k}\sigma} + \sum_{j\sigma} \left(f_{j\sigma}^\dagger (\partial_\tau + \lambda_j) f_{j\sigma} + |\tilde{V}_j| [c_{j\sigma}^\dagger f_{j\sigma} + \text{H.c.}] \right) + \sum_j N \frac{|\tilde{V}_j|^2}{J} - \lambda_j Q \\ &\quad + N \sum_j \left(\frac{|V_j|^2}{V_0^2} \lambda_j + E_f q \right). \end{aligned} \quad (18.243)$$

In this way we have rederived the Coqblin Schrieffer transformation. The Kondo and infinite U models differ only through the last term which couples the constraint field to the hybridization field,

$$L_{AL} = L_{KL} + N \sum_j \lambda_j \left(\frac{|\tilde{V}_j|^2}{V_0^2} \right) + E_f q, \quad (q = Q/N). \quad (18.244)$$

Remarkably, this small term, which counts the charge content of the slave boson field, contains all the high frequency dynamics of the valence fluctuations that are absent in the Kondo model.

Notice also that if we differentiate the corresponding action with respect to λ_j , setting $\langle \delta S / \delta \lambda_j \rangle = 0$ we obtain

$$|\tilde{V}_j| = \frac{V_0}{\sqrt{N}} \sqrt{Q - \langle n_f \rangle} \quad (18.245)$$

showing that as the valence approaches Q , the hybridization renormalizes to zero. In this way, the slave boson approach includes the wavefunction (Gutzwiller) renormalization[?] of the hybridization.

Example 18.6: By adding the additional coupling term $N(|\tilde{V}|^2/V_0^2)\lambda + E_f Q$ to the mean-field impurity energy obtained in (18.107), show that

- a) the mean-field energy for the infinite U Anderson model can be written

$$\Delta E_A = N \text{Im} \left[\xi \ln \left[\frac{\xi}{eD} \right] + \frac{(\xi - E_{fc})^2}{2\Delta_0} \right]$$

where $E_{fc} = E_f + i\Delta_0 q$ and $\xi = \lambda + i\tilde{\Delta}$ with $\Delta_0 = \pi\rho V_0^2$ and $\tilde{\Delta} = \pi\rho|\tilde{V}|^2$

- b) The mean field equations can be written

$$\xi + \frac{\Delta_0}{\pi} \ln \left(\frac{\xi}{D} \right) = E_f + i\Delta_0 q = E_{fc} \quad (18.246)$$

- c) How can one rewrite the mean-field equations in a cut-off invariant fashion?

Solution:

- a) From (18.107), the Kondo impurity energy is given by

$$\begin{aligned} \Delta E_K &= \frac{N}{\pi} \text{Im} \left[\xi \ln \left[\frac{\xi}{eT_K e^{i\pi q}} \right] \right] \\ &= \frac{N}{\pi} \text{Im} \left[\xi \ln \left[\frac{\xi}{eD} \right] - \frac{(E_f + i\Delta_0 q)\xi}{\Delta_0} \right] \\ &= \frac{N}{\pi} \text{Im} \left[\xi \ln \left[\frac{\xi}{eD} \right] - \frac{E_{fc}\xi}{\Delta_0} \right], \end{aligned} \quad (18.247)$$

where in the second line, we have replaced $T_K = D e^{-1/J\rho} \rightarrow D \exp[\pi E_f / \Delta_0]$. Now by (18.244), the correction required to derive the infinite U Anderson ground-state energy is

$$\begin{aligned} \Delta E_A &= \Delta E_K + N \left(\frac{|\tilde{V}|^2 \lambda}{V_0^2} + E_f q \right) = \Delta E_K + N \text{Im} \left[\frac{(E_f + i\Delta_0 q)^2}{2\Delta_0} + \frac{(\lambda + i\tilde{\Delta})^2}{2\Delta_0} \right] \\ &= \Delta E_K + N \text{Im} \left[\frac{E_{fc}^2}{2\Delta_0} + \frac{\xi^2}{2\Delta_0} \right] \end{aligned} \quad (18.248)$$

Combining (18.247) and (18.248) we obtain

$$\Delta E_A = \text{Im} \left[\frac{\xi}{\pi} \ln \left[\frac{\xi}{eD} \right] + \frac{(E_{fc} - \xi)^2}{2\Delta_0} \right] \quad (18.249)$$

b) Taking variations of ΔE_A with respect to $d\xi = d\lambda + id\tilde{\Delta}$ then gives

$$\xi + \frac{\Delta_0}{\pi} \ln\left(\frac{\xi}{D}\right) = E_f + i\Delta_0 q \quad (18.250)$$

c) If we introduce the invariant f-level position

$$E_f^* = E_f + \frac{\Delta_0}{\pi} \ln\left(\frac{D}{\Delta}\right) \quad (18.251)$$

then the mean-field equation beomes

$$\xi + \frac{\Delta_0}{\pi} \ln\left(\frac{\xi}{\Delta}\right) = E_f^* + i\Delta_0 q. \quad (18.252)$$

We see that:

(i) models with the same value of E_f^* , i.e

$$E_f(D) = E_f^* - \frac{\Delta_0}{\pi} \ln\left(\frac{\xi}{\Delta}\right) \quad (18.253)$$

lie on a scaling trajectory. In other words, as the cutoff reduces, the f-level position renormalizes upwards. This is the large- N version of ‘‘Haldane Scaling’’[?].

(ii) When $|E_f^*|/\Delta_0$ is large, we can write

$$\xi = \Delta \exp\left[\frac{\pi E_{fc}^*}{\Delta_0} = T_K e^{iq}\right] \quad (18.254)$$

where $T_K = \Delta \exp\left[\frac{-\pi|E_f^*|}{\Delta_0}\right]$, corresponding to the Kondo limit of the model.

18.12 Kondo and Topological Kondo Insulators

Let us now formulate

18.13 Summary

In this lecture we have presented Doniach’s argument that the enhancement of the Kondo temperature over and above the characteristic RKKY magnetic interaction energy between spins leads to the formation of a heavy electron ground-state. This enhancement is thought to be generated by the large spin degeneracies of rare earth, or actinide ions. A simple mean-field theory of the Kondo model and Kondo lattice, which ignores the RKKY interactions, provides a unified picture of heavy electron formation and the Kondo effect, in terms of the formation of a composite quasiparticle between high energy conduction band electrons and local moments. This basic physical effect is local in space, but non-local in time. Certain analogies can be struck between Cooper pair formation, and the formation of the heavy electron bound-state, in particular, the charge on the f-electron can be seen as a direct consequence of the temporal phase stiffness of the Kondo bound-state. This bound-state hybridizes with conduction electrons- producing a single isolated resonance in a Kondo impurity, and an entire renormalized Fermi surface in the Kondo lattice.

Exercises

Exercise 18.1 1 Directly confirm the Read-Newn's gauge transformation (??).

- 2 Directly calculate the "phase stiffness" $\rho_\phi = -\frac{d^2 F}{d\lambda^2}$ of the large N Kondo model and show that at $T = 0$,

$$\rho_\phi = \frac{N}{\pi} \left(\frac{\sin(\pi q)}{T_K} \right).$$

Exercise 18.2 1 Introduce a simple relaxation time into the conduction electron propagator, writing

$$G(\vec{k}, i\omega_n)^{-1} = i\omega_n + i\text{sgn}(\omega_n)/2\tau + \frac{V^2}{i\omega_n - \lambda} \quad (18.255)$$

Show that the poles of this Greens function occur at

$$\omega = E_k \pm \frac{i}{2\tau^*}$$

where

$$\tau^* = \frac{m^*}{m} \tau$$

is the renormalized elastic scattering time.

- 2 The Kubo formula for the optical conductivity of an isotropic one-band system is

$$\sigma(\nu) = -\frac{Ne^2}{3} \sum_k v_k^2 \frac{\Pi(\nu)}{i\nu}$$

where we have used the N fold spin degeneracy, and $\Pi(\nu)$ is the analytic extension of

$$\Pi(i\nu_n) = T \sum_m G(\vec{k}, i\omega_m) \left[G(\vec{k}, i\omega_m + i\nu_n) - G(\vec{k}, i\omega_m) \right]$$

where in our case, $G(\vec{k}, i\omega_n)$ is the conduction electron propagator. Using (18.255), and approximating the momentum sum by an integral over energy, show that the low frequency conductivity of the large N Kondo lattice is given by

$$\sigma(\nu) = \frac{ne^2}{m^*} \frac{1}{(\tau^*)^{-1} - i\nu}.$$

- 3 Consider the infinite U Hubbard model.

$$H = -t \sum_{(i,j),\sigma} \left(X_{\sigma 0}(i) X_{0\sigma}(j) + \text{H.c.} \right) - \mu \sum_{j,\sigma} X_{\sigma\sigma}. \quad (18.256)$$

Infinite U Hubbard Model

describing the hopping of electrons between sites with an infinite U constraint that maintains $n_f \leq 1$.

- 1 Reformulate the infinite U Hubbard model using the slave boson approach and show that in the radial gauge the action becomes

$$S = \int_0^\beta d\tau \left[\sum_j f_{j\sigma}^\dagger \partial_\tau f_{j\sigma} + H \right] \quad (18.257)$$

where

$$H = -t \sum_{(i,j),\sigma} r_i r_j \left[f_{i\sigma}^\dagger f_{j\sigma} + \text{H.c.} \right] + \sum_{j,\sigma} \left[\lambda_j (n_f(j) + r_j^2 - Q) - \mu n_f(j) \right] \quad (18.258)$$

where r_j is the amplitude of the Slave boson field.

- 2 Calculate the mean-field equations for the infinite U Hubbard model.
- 3 Show that the effective mass of the electrons diverges as $n_f \rightarrow Q$.

References

- [1] E. Bucher, J. P. Maita, G. W. Hull, R. C. Fulton, and A. S. Cooper, *Electronic properties of beryllides of the rare earth and some actinides*, Phys. Rev. B, vol. 11, pp. 440, 1975.
- [2] F. Steglich, J. Aarts, C. D. Bredl, W. Leike, D. E. Meshida W. Franz, and H. Schäfer, *Superconductivity in the Presence of Strong Pauli Paramagnetism: CeCu₂Si₂*, Phys. Rev. Lett., vol. 43, pp. 1892, 1976.
- [3] K. Andres, J. Graebner, and H. R. Ott, *4f-Virtual-Bound-State Formation in CeAl₃ at Low Temperatures*, Phys. Rev. Lett., vol. 35, pp. 1779, 1975.
- [4] M. A. Ruderman and C. Kittel, *Indirect Exchange Coupling of Nuclear Magnetic Moments by Conduction Electrons*, Phys. Rev., vol. 96, pp. 99–102, 1954.
- [5] A. Menth, E. Buehler, and T. H. Geballe, *Magnetic and Semiconducting Properties of SmB₆*, Phys. Rev. Lett., vol. 22, pp. 295, 1969.
- [6] M B Maple and D Wohlleben, *Nonmagnetic 4f shell in the high-pressure phase of SmS*, Physical review letters, vol. 27, no. 8, pp. 511, 1971.
- [7] NF Mott, *Rare-earth compounds with mixed valencies*, Philosophical Magazine, vol. 30, no. 2, pp. 403–416, 1974.
- [8] S DONIACH, *Kondo lattice and weak antiferromagnetism*, Physica, July 1977, 91 B+ C, 231-234, 1977.
- [9] Tadao Kasuya, *A Theory of Metallic Ferro- and Antiferromagnetism on Zener's Model*, Progress of Theoretical Physics, vol. 16, no. 1, pp. 45–57, July 1956.
- [10] Y. Onuki and T. Komatsubara, *Heavy fermion state CeCu₆*, J. Mag. Mat., vol. 63-64, pp. 281, 1987.
- [11] Richard M. Martin, *Fermi-Surface Sum Rule and its Consequences for Periodic Kondo and Mixed-Valence Systems*, Phys. Rev. Lett., vol. 48, pp. 362–365, Feb 1982.
- [12] M. Oshikawa, *Topological Approach to Luttinger's Theorem and the Fermi Surface of a Kondo Lattice*, Phys. Rev. Lett., vol. 84, pp. 3370, 2000.
- [13] L. Taillefer, R. Newbury, G. G. Lonzarich, Z. Fisk, and J. L. Smith, *Direct observation of heavy quasiparticles in UPt₃ via the dHvA effect*, J. Magn. Magn. Matter., vol. 63-64, pp. 372., 1987.
- [14] L. Taillefer and G. G. Lonzarich, *Heavy-fermion quasiparticles in UPt₃*, Phys. Rev. Lett., vol. 60, pp. 1570–1573, Apr 1988.
- [15] H. Shishido, R. Settai, H. Harima, and Y. Onuki, *A Drastic Change of the Fermi Surface at a Critical Pressure in CeRhIn 5: dHvA Study under Pressure*, Journal of the Physical Society of Japan, vol. 74, pp. 1103, 2005.
- [16] B. Coqblin and J. R. Schrieffer, *Exchange Interaction in Alloys with Cerium Impurities*, Phys. Rev., vol. 185, pp. 847, 1969.
- [17] Hiroaki Ikeda and Kazumasa Miyake, *A theory of anisotropic semiconductor of heavy fermions*, Journal of the Physical Society of Japan, vol. 65, no. 6, pp. 1769–1781, 1996.
- [18] M. Mekata, S. Ito, N. Sato, T. Satoh, and N. Sato, *Spin fluctuations in dense Kondo alloys*, Journal of Magnetism and Magnetic Materials, vol. 54, pp. 433, 1986.

- [19] Urano C., Nohara M., Kondo S., Sakai F. Takagi H., Shiraki T, and Okubo T., , Phys. Rev. Lett., vol. 85, pp. 1052, 2000.
- [20] Anderson P. W., Valence Fluctuations in Solids, North Holland, Amsterdam, 1981.
- [21] E. Witten, Chiral symmetry, the $1/N$ expansion and the $SU(N)$ Thirring model, Nucl. Phys. B, vol. 145, pp. 110, 1978.
- [22] P. Coleman, *$1/N$ expansion for the Kondo lattice*, Phys. Rev., vol. 28, pp. 5255, 1983.
- [23] N. Read and D.M. Newns, *On the solution of the Coqblin-Schreiffer Hamiltonian by the large- N expansion technique*, J. Phys. C, vol. 16, pp. 3274, 1983.
- [24] C. Lacroix and M. Cyrot, Phase diagram of the kondo lattice, Phys. Rev. B, vol. 20, pp. 1969–1976, Sep 1979.
- [25] S. Charavarty, *Unpublished Preprint*, Proc. Am. Phys. Soc. (March), 1982.
- [26] P. Coleman, *New approach to the mixed-valence problem* , Phys. Rev. B, vol. 29, pp. 3035, 1984.
- [27] N. Read and D. M. Newns, *A new functional integral formalism for the degenerate Anderson model*, J. Phys. C, vol. 29, pp. L1055, 1983.
- [28] A. Auerbach and K. Levin, *Kondo bosons and the Kondo lattice: microscopic basis for the heavy Fermi liquid*, Phys. Rev. Lett., vol. 57, pp. 877, 1986.
- [29] S. E. Barnes, *New method for the Anderson model*, J. Phys., vol. F 6, pp. 1375, 1976.
- [30] A. J. Millis, P. A., and Lee, *Large-orbital-degeneracy expansion for the lattice Anderson model*, Phys. Rev. B, vol. 35, no. 7, pp. 3394–3414, 1987.
- [31] P. Coleman, *Mixed valence as an almost broken symmetry*, Phys. Rev. B, vol. 35, pp. 5072, 1987.
- [32] Martin C. Gutzwiller, *Effect of Correlation on the Ferromagnetism of Transition Metals*, Phys. Rev. Lett., vol. 10, no. 5, pp. 159–162, 1963, The Hubbard model was written down independently by Gutzwiller in eqn 11 of this paper.
- [33] S. Burdin, A. Georges, and D. R. Grempel, *Coherence Scale of the Kondo Lattice* , Phys. Rev. Lett, vol. 85, pp. 1048, 2000.
- [34] T. A. Costi and N. Manini, *Low-Energy Scales and Temperature-Dependent Photoemission of Heavy Fermions*, Journal of Low Temperature Physics, vol. 126, pp. 835–866, 2002.
- [35] Hiroaki Shishido, Rikio Settai, Hisatomo Harima, and Yoshichika Ōnuki, *A Drastic Change of the Fermi Surface at a Critical Pressure in CeRhIn 5: dHvA Study under Pressure*, Journal of the Physical Society of Japan, vol. 74, no. 4, pp. 1103–1106, Apr. 2005.
- [36] Tuson Park, F Ronning, H Q Yuan, M B Salamon, R Movshovich, J L Sarrao, and J D Thompson, *Hidden magnetism and quantum criticality in the heavy fermion superconductor CeRhIn5*, Nature, vol. 440, no. 7080, pp. 65–68, Mar. 2006.
- [37] AFG Wyatt, Phys. Rev. Lett. 13, 401 (1964): *Anomalous Densities of States in Normal Tantalum and Niobium*, Physical review letters, 1964.
- [38] J Appelbaum, "sd" Exchange Model of Zero-Bias Tunneling Anomalies, Physical Review Letters, 1966.
- [39] P W Anderson, *Localized magnetic states and Fermi-surface anomalies in tunneling*, Physical Review Letters, 1966.
- [40] D V Averin and Y V Nazarov, *Virtual electron diffusion during quantum tunneling of the electric charge*, Physical review letters, vol. 65, no. 19, pp. 2446–2449, 1990.
- [41] M Pustilnik and L Glazman, *Kondo Effect in Real Quantum Dots*, Physical Review Letters, 2001.
- [42] D Goldhaber-Gordon, H Shtrikman, and D Mahalu, *Kondo effect in a single-electron transistor*, Nature, vol. 391, no. 6663, pp. 156–159, 1998.

-
- [43] M I Katsnelson, A I Lichtenstein, and H Van Kempen, Real-space imaging of an orbital Kondo resonance on the Cr (001) surface, *Nature*, vol. 415, no. 6871, pp. 507–509, 2002.
- [44] U Fano, Effects of Configuration Interaction on Intensities and Phase Shifts, *Phys. Rev.*, vol. 124, no. 6, pp. 1866–1878, 1961.
- [45] V Madhavan, Tunneling into a Single Magnetic Atom: Spectroscopic Evidence of the Kondo Resonance, *Science (New York, NY)*, vol. 280, no. 5363, pp. 567–569, Apr. 1998.
- [46] AR Schmidt, MH Hamidian, P Wahl, and F Meier, Imaging the Fano lattice to 'hidden order' transition in URu₂Si₂, *Nature*, 2010.
- [47] Pegor Aynajian, Eduardo H da Silva Neto, András Gyenis, Ryan E Baumbach, J D Thompson, Zachary Fisk, Eric D Bauer, and Ali Yazdani, Visualizing heavy fermions emerging in a quantum critical Kondo lattice, *Nature*, vol. 486, no. 7402, pp. 201–206, June 2012.
- [48] Marianna Maltseva, M Dzero, and Piers Coleman, Electron Cotunneling into a Kondo Lattice, *Physical Review Letters*, vol. 103, no. 20, Nov. 2009.
- [49] J. R. Schrieffer and P. Wolff, *Relation between the Anderson and Kondo Hamiltonians*, *Phys. Rev.*, vol. 149, pp. 491, 1966.
- [50] A. J. Millis, *Effect of a nonzero temperature on quantum critical points in itinerant fermion systems*, *Phys. Rev. B*, vol. 48, pp. 7183, 1993.
- [51] L. Degiorgi, F. Anders, and G. Gruner, *Charge excitations in heavy electron metals*, *European Physical Journal B*, vol. 19, pp. 167, 2001.
- [52] S. V. Dordevic, D. N. Basov, N. R. Dilley, E. D. Bauer, and M. B. Maple, Hybridization Gap in Heavy Fermion Compounds, *Phys. Rev. Lett.*, vol. 86, pp. 684, 2001.
- [53] B. Bucher, Z. Schlesinger, D. Mandrus, Z. Fisk, J. Sarrao, J. F. DiTusa, C. Oglesby, G. Aeppli, and E. Bucher, *Charge dynamics of Ce-based compounds: Connection between the mixed valent and Kondo-insulator states*, *Phys. Rev. B*, vol. 53, pp. R2948–R2951, Feb 1996.
- [54] W. P. Beyerman, G. Gruner, Y. Dlicheouch, and M. B. Maple, *Frequency-dependent transport properties of UPt₃*, *Phys. Rev. B*, vol. 37, pp. 10353, 1988.
- [55] S. Donovan, A. Schwartz, and G. Grüner, *Observation of an Optical Pseudogap in UPt₃*, *Phys. Rev. Lett.*, vol. 79, pp. 1401–1404, Aug 1997.
- [56] Piers Coleman, J B Marston, and A J Schofield, Transport anomalies in a simplified model for a heavy electron quantum critical point, *Phys. Rev. B*, vol. 72, no. cond-mat/0507003, pp. 245111. 15 p, June 2005.
- [57] P. W. Anderson, *The Resonating Valence Bond State in La₂CuO₄ and Superconductivity*, *Science*, vol. 235, pp. 1196, 1987.
- [58] L. B. Ioffe and A. I. Larkin, Gapless fermions and gauge fields in dielectrics, *Phys. Rev. B*, vol. 39, pp. 8988–8999, May 1989.